(19) Europäisches Patentamt
European Patent Office
Office européen des brevets

(11) **EP 2 696 771 B1**

(12) **EUROPEAN PATENT SPECIFICATION**

(45) Date of publication and mention of the grant of the patent:
12.09.2018 Bulletin 2018/37

(21) Application number: **12715304.7**

(22) Date of filing: **13.04.2012**

(51) Int Cl.:
A61B 8/08 *(2006.01)* ***A61B 8/06*** *(2006.01)*

(86) International application number:
PCT/US2012/033584

(87) International publication number:
WO 2012/142455 (18.10.2012 Gazette 2012/42)

(54) VASCULAR CHARACTERIZATION USING ULTRASOUND IMAGING

VASKULÄRE CHARAKTERISIERUNG MIT ULTRASCHALLBILDGEBUNG

CARACTÉRISATION VASCULAIRE UTILISANT L'IMAGERIE ULTRASONORE

(84) Designated Contracting States:
AL AT BE BG CH CY CZ DE DK EE ES FI FR GB GR HR HU IE IS IT LI LT LU LV MC MK MT NL NO PL PT RO RS SE SI SK SM TR

(30) Priority: **14.04.2011 US 201161475550 P**

(43) Date of publication of application:
19.02.2014 Bulletin 2014/08

(73) Proprietor: **Regents Of The University Of Minnesota**
St. Paul, Minnesota 55114-8658 (US)

(72) Inventors:
- **EBBINI, Emad S.**
  Edina
  Minnesota 55435 (US)
- **LIU, Dalong**
  Issaquah
  Washington 98029 (US)
- **WAN, Yayun**
  Birmingham
  Alabama 35244 (US)
- **CASPER, Andrew J.**
  Eau Claire
  Wisconsin 54701 (US)

(74) Representative: **Latzel, Klaus**
Latzel-IP
Traunstrasse 3
81825 München (DE)

(56) References cited:
WO-A2-2008/053457 **US-A1- 2012 083 692**

- **TRAHEY G E ET AL: "Angle independent ultrasonic blood flow detection by frame-to-frame correlation of B-mode images", ULTRASONICS, IPC SCIENCE AND TECHNOLOGY PRESS LTD. GUILDFORD, GB, vol. 26, no. 5, 1 September 1988 (1988-09-01), pages 271-276, XP025824234, ISSN: 0041-624X, DOI: 10.1016/0041-624X(88)90016-9 [retrieved on 1988-09-01]**
- **GRONNINGSAETER A ET AL: "Vessel wall detection and blood noise reduction in intravascular ultrasound imaging", IEEE TRANSACTIONS ON ULTRASONICS, FERROELECTRICS AND FREQUENCY CONTROL, IEEE, US, vol. 43, no. 3, 1 May 1996 (1996-05-01), pages 359-369, XP011437389, ISSN: 0885-3010, DOI: 10.1109/58.489392**
- **E.S. EBBINI: "Phase-coupled two-dimensional speckle tracking algorithm", IEEE TRANSACTIONS ON ULTRASONICS, FERROELECTRICS AND FREQUENCY CONTROL, vol. 53, no. 5, 1 May 2006 (2006-05-01), pages 972-990, XP055054547, ISSN: 0885-3010, DOI: 10.1109/TUFFC.2006.1632687**

EP 2 696 771 B1

Description

[0001] The disclosure herein relates generally to ultrasound imaging. More particularly, the disclosure herein pertains to ultrasound imaging methods and systems for use in, e.g., diagnostic and/or therapy applications (e.g., imaging of blood vessels and/or regions proximate thereto, etc.).

[0002] Vascular imaging is gaining increased attention not only as a way to detect cardiovascular diseases, but also for the evaluation of response to new anti-atherosclerotic therapies (see, Ainsworth, et al., "3D ultrasound measurement of change in carotid plaque volume - A tool for rapid evaluation of new therapies," Stroke, vol. 36, no. 9, pp. 1904-1909, SEP 2005). Intravascular ultrasound (IVUS) has been shown to provide an effective tool in measuring the progression or regression of atherosclerotic disease in response to therapies. However, IVUS is invasive, potentially risky, and more expensive than noninvasive imaging with ultrasound.

[0003] Advanced imaging modes on ultrasound scanners have led to increased interest in imaging important quantities like wall shear rate (WSR) using Doppler (see, Blake, et al., "A method to estimate wall shear rate with a clinical ultrasound scanner," Ultrasound in Medicine and Biology, vol. 34, no. 5, pp. 760-764, MAY 2008) and tissue/wall motion (see, Tsou et al., "Role of ultrasonic shear rate estimation errors in assessing inflammatory response and vascular risk," Ultrasound in Medicine and Biology, vol. 34, no. 6, pp. 963-972, JUN 2008; Karimi et al., "Estimation of Nonlinear Mechanical Properties of Vascular Tissues via Elastography," Cardiovascular Engineering, vol. 8, no. 4, pp. 191-202, DEC 2008; and Weitzel, et al., "High-Resolution Ultrasound Elasticity Imaging to Evaluate Dialysis Fistula Stenosis," Seminars In Dialysis, vol. 22, no. 1, pp. 84-89, JAN-FEB 2009) using speckle tracking.

[0004] Recently, there has been increased interest in imaging flow in conjunction with computational fluid dynamic (CFD) modeling the evaluation of large artery hemodynamics (see, Steinman et al., "Flow imaging and computing: Large artery hemodynamics," ANNALS OF BIOMEDICAL ENGINEERING, vol. 33, no. 12, pp. 1704-1709, DEC 2005; Figueroa, et al., "A computational framework for fluid-solid-growth modeling in cardiovascular simulations," Computer Methods in Applied Mechanics and Engineering, vol. 198, no. 45- 46, pp. 3583 - 3602, 2009; and Taylor et al., "Open problems in computational vascular biomechanics: Hemodynamics and arterial wall mechanics," Computer Methods in Applied Mechanics and Engineering, vol. 198, no. 45-46, pp. 3514 - 3523, 2009). In this context, modeling fluid-solid interfaces has been defined as a challenge area in vascular mechanics.

[0005] Gronninsaeter et al describe in IEEE TRANSACTIONS ON ULTRASOUND ELECTRONICS, FERROELECTRICS AND FREQUENCY CONTROL, vol. 43, no. 3, 1 May 1996, pages 359-369 a method of differentiation of blood noise from vessel structure, as present in the general part of the independent claims. It does not disclose the characterizing part of the independent claims. In particular, GRONNINGSAETER is not concerned with adaptive tracking of a vessel wall by modifying a speckle region. WO 2008/053457 A2 describes a method that combines enhancing and mitigating techniques for speckle tracking, for obtaining a series of images of the movement of a target, such as tissue over time.

[0006] The present invention is defined by the claims 1 and 9 relating to an imaging method and a system for vascular imaging, respectively. Further preferred embodiments are described in the dependent claims and in the subsequent paragraphs.

[0007] At least one embodiment of this disclosure relates to ultrasound imaging capable of simultaneously imaging both wall tissue motion (e.g., perivascular tissue) and deformation, together with fluid flow. For example, in one embodiment of this disclosure, imaging vascular mechanics using ultrasound is accomplished utilizing speckle tracking (e.g., a 2D phase coupled speckle tracking method suitable for subsample displacement estimation in both axial and lateral directions with minimum interpolation) in conjunction with an imaging mode (e.g., M2D mode imaging) that provides sufficient frame rates for vector displacement tracking in both tissue and fluid simultaneously. For example, M2D imaging may be implemented on a clinical scanner equipped with a research interface for controlling the imaging sequence and streamlining the RF data for performing 2D speckle tracking in a region of interest (e.g., around a blood vessel). Combining 2D speckle tracking with sufficiently high frame rate imaging allows for fine displacement tracking in both lateral and axial directions. Vector displacement fields resulting from such processing are well suited for strain and shear strain calculations with minimum filtering and using relatively small tracking windows (i.e., speckle regions) to maximize resolution. Flow and tissue motion strain fields (e.g., in a tissue/flow application, such as *in vivo* in the carotid of a patient) may be evaluated (e.g., to identify vascular characteristics or for one or more other purposes, e.g., for use in therapy).

[0008] One exemplary embodiment of an imaging method may include providing ultrasound pulse-echo data of a region in which at least one portion of a blood vessel is located (e.g., wherein the pulse-echo data comprises pulse-echo data at a frame rate such that measured displacement of the vessel wall defining the at least one portion of the blood vessel and measured average blood flow through the at least one portion of the blood vessel have a quasi-periodic profile over time to allow motion tracking of both the vessel wall and the blood flow simultaneously) and generating strain and shear strain image data for the region in which the at least one portion of the vessel is located using speckle tracking. For example, the speckle tracking may include using multi-dimensional correlation of pulse-echo data of one or more speckle regions undergoing deformation in the region in which the at least one portion of a blood vessel is located (e.g.,

wherein the multi-dimensional correlation comprises determining a cross-correlation peak for the sampled pulse-echo data based on phase and magnitude gradients of the cross-correlated pulse-echo data). Further, the method may include identifying at least one vascular characteristic of the region in which at least one portion of a blood vessel is located based on the strain and shear strain image data (e.g., wherein the at least one vascular characteristic comprises at least one of a flow characteristic associated with flow through the blood vessel, a structural characteristic associated with the blood vessel, and a hemodynamic characteristic associated with the blood vessel).

[0009] Another exemplary imaging method may include providing ultrasound pulse-echo data of a region in which at least one portion of a blood vessel is located and using speckle tracking of one or more speckle regions of the region in which at least one portion of the blood vessel is located to track motion of both the vessel wall defining the at least one portion of the blood vessel and the blood flow through the at least one portion of the blood vessel. The pulse-echo data is provided at a frame rate such that displacement of the vessel wall defining the at least one portion of the blood vessel and blood flow through the at least one portion of the blood vessel are measurable simultaneously within a same periodic cycle (e.g., corresponding to a cardiac pulse cycle). Further, the method may include identifying at least one vascular characteristic of the region in which at least one portion of a blood vessel is located based on the simultaneously measured displacement of the vessel wall and average blood flow. Such an imaging method may also include generating strain and shear strain image data for the region in which the at least one portion of the vessel is located using the speckle tracking, wherein the speckle tracking comprises using multi-dimensional correlation of sampled pulse-echo data of the one or more speckle regions undergoing deformation in the region in which the at least one portion of a blood vessel is located (e.g., the multi-dimensional correlation may include determining a cross-correlation peak for the sampled pulse-echo data based on phase and magnitude gradients of the cross-correlated sampled pulse-echo data).

[0010] In one or more embodiments of methods described herein, identifying at least one vascular characteristic may include identifying one or more vessel wall boundaries; and still speckle tracking of such methods may include modifying a characteristic of at least one of the one or more speckle regions being tracked (e.g., location, size, shape, etc.) based on the one or more vessel wall boundaries identified such that the at least one speckle region is entirely within or outside of the vessel wall.

[0011] Further, in one or more embodiments of methods described herein, identifying at least one vascular characteristic may include identifying vessel wall boundaries around the entire blood vessel (e.g., wall boundaries in the entire cross-section view taken along the axis of the vessel); may include measuring tissue property within the one or more vessel wall boundaries (e.g., stiffness or compliance); may include identifying one or more portions of a plaque architecture adjacent the one or more vessel wall boundaries (e.g., such that therapy may be focused on a portion of such a structure; such as the base thereof); and/or may include calculating one or more hemodynamic measurements based on both the motion tracking motion of the vessel wall and the blood flow simultaneously.

[0012] Still further, in one or more embodiments of methods described herein, using multi-dimensional correlation of sampled pulse-echo data of one or more speckle regions may include using two-dimensional correlation of sampled pulse-echo data of one or more speckle regions (e.g., to track wall displacement or blood flow), and even three-dimensional correlation.

[0013] Yet further, in one or more embodiments of methods described herein, the method may further include delivering therapy to a patient based on the identification of the at least one vascular characteristic of the region in which at least one portion of a blood vessel is located (e.g., using ultrasonic energy to deliver therapy based on the identification of the at least one vascular characteristic of the region in which at least one portion of a blood vessel is located). For example, at least one transducer configured to transmit and receive ultrasonic energy may be provided, wherein the at least one transducer is used to obtain the pulse-echo data (e.g., for image data generation) and to generate ultrasonic energy to deliver therapy.

[0014] In one or more other embodiments of methods described herein, generating strain and shear strain image data for the region in which the at least one portion of the vessel is located using two-dimensional speckle tracking may include generating at least one of axial strain and axial shear strain image data and/or lateral strain and lateral shear strain image data. Further, in such methods, providing ultrasound pulse-echo data of a region in which at least one portion of a blood vessel is located may include using coded excitation.

[0015] In yet one or more other embodiments of methods described herein, the method may include applying a dereverberation filter to the pulse-echo data from one or more speckle regions in the blood to remove echo components in the pulse-echo data due to reflection at the vessel wall when performing speckle tracking of the pulse-echo data from the one or more speckle regions in the blood.

[0016] The imaging method according to the invention includes providing ultrasound pulse-echo data of a region in which at least one portion of a blood vessel is located; using speckle tracking of one or more speckle regions of the region in which the at least one portion of the blood vessel is located to track motion of at least one of the vessel wall defining the at least one portion of the blood vessel and the blood flow through the at least one portion of the blood vessel; identifying one or more vessel wall boundaries based on the speckle tracking of the one or more speckle regions; and modifying at least one characteristic of at least one of the one or more speckle regions being tracked based on the

one or more vessel wall boundaries identified such that the at least one speckle region is entirely within or outside of the vessel wall (e.g., the at least one of the one or more speckle regions being tracked may be modified by at least one of location, size, or shape based on the one or more vessel wall boundaries identified such that the at least one speckle region is entirely within or outside of the vessel wall).

[0017] In another exemplary imaging method, the method may include providing ultrasound pulse-echo data of a region in which at least one portion of a blood vessel is located; using speckle tracking of one or more speckle regions of the region in which at least one portion of the blood vessel is located to track motion of at least blood flow through the at least one portion of the blood vessel; and removing echo components in the pulse-echo data due to reflection at the vessel wall when performing speckle tracking of the pulse-echo data from the one or more speckle regions in the blood (e.g., removing echo components in the pulse-echo data due to reflection at the vessel wall may include using a time-varying inverse filter to reduce the components in the pulse-echo data due to reflection at the vessel wall).

[0018] One exemplary embodiment of a system for vascular imaging may include one or more ultrasound transducers (e.g., wherein the one or more transducers are configured to deliver ultrasound energy to a vascular region resulting in pulse-echo data therefrom) and processing apparatus configured (e.g., operative by execution of one programs, routines, or instructions to cause the performance of one or more functions) to control the capture of pulse-echo data at a frame rate such that measured displacement of a vessel wall defining at least one portion of a blood vessel in the vascular region and measured average blood flow through the at least one portion of the blood vessel have a quasi-periodic profile over time to allow motion tracking of both the vessel wall and the blood flow simultaneously; to generate strain and shear strain image data for the region in which the at least one portion of the vessel is located using speckle tracking (e.g., wherein the speckle tracking may include using multi-dimensional correlation of pulse-echo data of one or more speckle regions undergoing deformation in the region in which the at least one portion of a blood vessel is located; the multi-dimensional correlation may include determining a cross-correlation peak for the sampled pulse-echo data based on phase and magnitude gradients of the cross-correlated pulse-echo data); and to identify at least one vascular characteristic of the vascular region in which at least one portion of a blood vessel is located based on the strain and shear strain image data (e.g., wherein the at least one vascular characteristic comprises at least one of a flow characteristic associated with flow through the blood vessel, a structural characteristic associated with the blood vessel, and a hemodynamic characteristic associated with the blood vessel).

[0019] Another exemplary system for vascular imaging may include one or more ultrasound transducers (e.g., wherein the one or more transducers are configured to deliver ultrasound energy to a vascular region resulting in pulse-echo data therefrom) and processing apparatus configured (e.g., operative by execution of one programs, routines, or instructions to cause the performance of one or more functions) to control the capture of pulse-echo data of the vascular region in which at least one portion of a blood vessel is located and use speckle tracking of one or more speckle regions of the vascular region in which at least one portion of the blood vessel is located to track motion of both the vessel wall defining the at least one portion of the blood vessel and the blood flow through the at least one portion of the blood vessel. The pulse-echo data may be captured at a frame rate such that displacement of the vessel wall defining the at least one portion of the blood vessel and blood flow through the at least one portion of the blood vessel are measurable simultaneously within a same periodic cycle corresponding to a cardiac pulse cycle. Further, the processing apparatus may be configured to identify at least one vascular characteristic of the vascular region in which the at least one portion of the blood vessel is located based on the simultaneously measured displacement of the vessel wall and average blood flow. In one embodiment of such a system, the processing apparatus may further be operable to generate strain and shear strain image data for the region in which the at least one portion of the vessel is located using the speckle tracking (e.g., wherein the speckle tracking may include using multi-dimensional correlation of sampled pulse-echo data of the one or more speckle regions undergoing deformation in the region in which the at least one portion of a blood vessel is located; and further wherein the multi-dimensional correlation may include determining a cross-correlation peak for the sampled pulse-echo data based on phase and magnitude gradients of the cross-correlated sampled pulse-echo data).

[0020] According to the invention, the processing apparatus is operable to identify one or more vessel wall boundaries, and still further, the processing apparatus is be operable, when using the speckle tracking, to modify a characteristic of at least one of the one or more speckle regions being tracked (e.g., the location, size, shape, etc.) based on the one or more vessel wall boundaries identified such that the at least one speckle region is entirely within or outside of the vessel wall.

[0021] Further, in one or more embodiments of the exemplary systems, the processing apparatus may be operable to identify vessel wall boundaries around the entire blood vessel; the processing apparatus may be operable to measure tissue property within the one or more vessel wall boundaries; the processing apparatus may be operable to identify one or more portions of a plaque architecture adjacent the one or more vessel wall boundaries; and/or the processing apparatus may be operable to calculate one or more hemodynamic measurements based on both the motion tracking motion of the vessel wall and the blood flow simultaneously.

[0022] Still further, in one or more embodiments of the exemplary systems provided herein, the processing apparatus may be operable to use two-dimensional correlation of sampled pulse-echo data of one or more speckle regions (e.g.,

to track speckle regions), and even three-dimensional correlation.

[0023] Yet further, in one or more embodiments of the exemplary systems provided herein, the system may further include a therapy apparatus to deliver therapy to a patient based on the identification of the at least one vascular characteristic of the region in which at least one portion of a blood vessel is located (e.g., a device operable to use ultrasonic energy to deliver therapy based on the identification of the at least one vascular characteristic of the region in which at least one portion of a blood vessel is located). For example, the therapy apparatus may include at least one transducer configured to transmit and receive ultrasonic energy, wherein the at least one transducer is operable to provide ultrasonic energy to deliver therapy based on the identification of the at least one vascular characteristic of the region in which at least one portion of a blood vessel is located and the at least one transducer is operable for use in obtaining the pulse-echo data to generate image data.

[0024] Still further, in one or more embodiments of the exemplary systems provided herein, the processing apparatus may be operable to generate strain and shear strain image data for the region in which the at least one portion of the vessel is located using two-dimensional speckle tracking, wherein using two-dimensional speckle tracking comprises generating at least one of axial strain and axial shear strain image data and/or lateral strain and lateral shear strain image data. Further, for example, the processing apparatus may be operable to control providing ultrasound pulse-echo data of a region in which at least one portion of a blood vessel is located using coded excitation.

[0025] Still further, in another of the one or more embodiments of the exemplary systems provided herein, the processing apparatus may be operable to apply a dereverberation filter to the pulse-echo data from one or more speckle regions in the blood to remove echo components in the pulse-echo data due to reflection at the vessel wall when performing speckle tracking of the pulse-echo data from the one or more speckle regions in the blood.

[0026] Another exemplary system for vascular imaging may include one or more ultrasound transducers (e.g., wherein the one or more transducers are configured to deliver ultrasound energy to a vascular region resulting in pulse-echo data therefrom) and processing apparatus configured to control capture of ultrasound pulse-echo data of the vascular region in which at least one portion of a blood vessel is located; use speckle tracking of one or more speckle regions of the vascular region in which the at least one portion of the blood vessel is located to track motion of at least one of the vessel wall defining the at least one portion of the blood vessel and the blood flow through the at least one portion of the blood vessel; identify one or more vessel wall boundaries based on the speckle tracking of the one or more speckle regions; and modify a characteristic of at least one of the one or more speckle regions being tracked based on the one or more vessel wall boundaries identified such that the at least one speckle region is entirely within or outside of the vessel wall. For example, the processing apparatus may be operable to modify at least one of location, size, or shape of the at least one speckle region based on the one or more vessel wall boundaries identified such that the at least one speckle region is entirely within or outside of the vessel wall.

[0027] In yet another exemplary system for vascular imaging, the system may include one or more ultrasound transducers (e.g., wherein the one or more transducers are configured to deliver ultrasound energy to a vascular region resulting in pulse-echo data therefrom) and processing apparatus configured to control capture of ultrasound pulse-echo data of the vascular region in which at least one portion of a blood vessel is located; use speckle tracking of one or more speckle regions of the region in which at least one portion of the blood vessel is located to track motion of at least blood flow through the at least one portion of the blood vessel; and remove echo components in the pulse-echo data due to reflection at the vessel wall when performing speckle tracking of the pulse-echo data from the one or more speckle regions in the blood (e.g., using a time-varying inverse filter to reduce the components in the pulse-echo data due to reflection at the vessel wall).

[0028] Still further, another exemplary system for vascular imaging may include one or more ultrasound transducers (e.g., wherein the one or more transducers are configured to deliver ultrasound energy to a vascular region resulting in pulse-echo data therefrom); apparatus for controlling the capture of pulse-echo data at a frame rate such that measured displacement of a vessel wall defining at least one portion of a blood vessel in the vascular region and measured average blood flow through the at least one portion of the blood vessel have a quasi-periodic profile over time to allow motion tracking of both the vessel wall and the blood flow simultaneously; apparatus for generating strain and shear strain image data for the region in which the at least one portion of the vessel is located using speckle tracking (e.g., wherein the speckle tracking may include using multi-dimensional correlation of pulse-echo data of one or more speckle regions undergoing deformation in the region in which the at least one portion of a blood vessel is located, and further wherein the multi-dimensional correlation may include determining a cross-correlation peak for the sampled pulse-echo data based on phase and magnitude gradients of the cross-correlated pulse-echo data); and apparatus for identifying at least one vascular characteristic of the vascular region in which at least one portion of a blood vessel is located based on the strain and shear strain image data (e.g., wherein the at least one vascular characteristic comprises at least one of a flow characteristic associated with flow through the blood vessel, a structural characteristic associated with the blood vessel, and a hemodynamic characteristic associated with the blood vessel). Further, for example, the system may include therapy apparatus for delivering therapy to a patient based on the identification of the at least one vascular characteristic of the region in which at least one portion of a blood vessel is located (e.g., ultrasound therapy apparatus).

[0029] The above summary is not intended to describe each embodiment or every implementation of the present disclosure. A more complete understanding will become apparent and appreciated by referring to the following detailed description and claims taken in conjunction with the accompanying drawings.

BRIEF DESCRIPTION OF THE DRAWINGS

[0030]

FIG. 1 is a block diagram depicting an exemplary ultrasound imaging system, with an optional therapy system.

FIG. 2 is a flow chart depicting an exemplary ultrasound imaging method.

FIG. 3 is a block diagram of one exemplary embodiment of an imaging system shown generally in Figure 1.

FIG. 4 is a block diagram of one exemplary GPU implementation of an imaging system such as shown in Figure 3.

FIG. 5A-5D provides exemplary graphs showing channel diameter and average flow velocity over time for image data captured at various frame rates.

FIGS. 6A-6B shown graphs including contours of certain parameters of cross-correlations used to describe one exemplary embodiment of speckle tracking that may be used in an imaging method and/or system shown generally in Figures 1-2.

FIG. 7 provides an exemplary image of a blood vessel for use in describing one or more methods and/or systems shown generally in Figures 1-2 as they relate to vascular diagnostics or vascular therapy.

FIGS. 8A-8B show axial stain and axial shear strain images of flow channel walls relating to examples carried out and described at least in part herein.

FIGS. 9A-9B show lateral stain and lateral shear strain images of flow channel walls relating to examples carried out and described at least in part herein.

FIG. 10 shows a graph of channel diameter computed from tracked channel wall displacements over time and average flow velocity obtained from tracked fluid displacements over time within a flow channel relating to an example carried out and described at least in part herein.

FIG. 11 shows graphs of total displacement vector waveforms with a channel at different time instances relating to an example carried out and described at least in part herein.

FIGS. 12A-12B show axial stain and axial shear strain images of carotid artery longitudinal vessel walls relating to examples carried out and described at least in part herein.

FIGS. 13A-13B show lateral stain and lateral shear strain images of carotid artery longitudinal vessel walls relating to examples carried out and described at least in part herein.

FIGS. 14A-14B show axial stain and axial shear strain images of carotid artery cross-sectional vessel walls relating to examples carried out and described at least in part herein.

FIGS. 15A-15B show lateral stain and lateral shear strain images of carotid artery cross-sectional vessel walls relating to examples carried out and described at least in part herein.

FIGS. 16A-16B show lateral and axial displacements relating to dereverberation filtering examples.

FIGS. 17A-17B show spatio-temporal maps relating to dereverberation filtering examples.

FIGS. 18A-18B show spatio-temporal maps relating to dereverberation filtering examples.

FIGS. 19A-19D show graphs relating to dereverberation filtering results of examples presented herein.

DETAILED DESCRIPTION OF EXEMPLARY EMBODIMENTS

[0031] In the following detailed description of illustrative embodiments, reference is made to the accompanying figures of the drawing which form a part hereof, and in which are shown, by way of illustration, specific embodiments which may be practiced. It is to be understood that other embodiments may be utilized and structural changes may be made without departing from (e.g., still falling within) the scope of the disclosure presented hereby.

[0032] Exemplary methods, apparatus, and systems shall be described with reference to Figures 1-19. It will be apparent to one skilled in the art that elements or processes (e.g., including steps thereof) from one embodiment may be used in combination with elements or processes of the other embodiments, and that the possible embodiments of such methods, apparatus, and systems using combinations of features set forth herein is not limited to the specific embodiments shown in the Figures and/or described herein. Further, it will be recognized that the embodiments described herein may include many elements that are not necessarily shown to scale. Still further, it will be recognized that timing of the processes and the size and shape of various elements herein may be modified but still fall within the scope of the present disclosure, although certain timings, one or more shapes and/or sizes, or types of elements, may be advantageous over others.

[0033] FIG. 1 shows an exemplary ultrasound imaging system 10 including processing apparatus (block 12) and one or more ultrasound transducers, such as a transducer array that provides for transmission of pulses and reception of echoes (block 22). The processing apparatus (block 12) may be operably coupled to the one or more transducers (block 22) to facilitate imaging of an object of interest (e.g., capture of pulse-echo data) using the one or more transducers (block 22). Further, the processing apparatus (block 12) includes data storage (block 14). Data storage (block 14) allows for access to processing programs or routines (block 16) and one or more other types of data (block 18) that may be employed to carry out the exemplary imaging methods (e.g., one which is shown generally in the block diagram of FIG. 2).

[0034] For example, processing programs or routines (block 16) may include programs or routines for performing computational mathematics, matrix mathematics, compression algorithms (e.g., data compression algorithms), calibration algorithms, image construction algorithms, inversion algorithms, signal processing algorithms, standardization algorithms, comparison algorithms, vector mathematics, or any other processing required to implement one or more embodiments as described herein (e.g., provide imaging, carry out speckle tracking, generate strain images, etc.). Exemplary mathematical formulations/equations that may be used in the systems and methods described herein are more specifically described herein with reference to FIGS. 3-19.

[0035] Data (block 18) may include, for example, sampled pulse-echo information (e.g., sampled or collected using the one or more transducers (block 22)), data representative of measurements (e.g., vascular characteristics), results from one or more processing programs or routines employed according to the disclosure herein (e.g., reconstructed strain images of an object of interest, such as a blood vessel or regions around same), or any other data that may be necessary for carrying out the one or more processes or methods described herein.

[0036] In one or more embodiments, the system 10 may be implemented using one or more computer programs executed on programmable computers, such as computers that include, for example, processing capabilities (e.g., computer processing units (CPUs), graphical processing units (GPUs)), data storage (e.g., volatile or non-volatile memory and/or storage elements), input devices, and output devices. Program code and/or logic described herein may be applied to input data to perform functionality described herein and generate desired output information (e.g., strain images, vascular characteristics, etc.). The output information may be applied, or otherwise used, as input to, or by, one or more other devices and/or processes as described herein (e.g., one or more therapy apparatus (block 20) such as a drug therapy apparatus, an ultrasound therapy apparatus, etc.).

[0037] The program(s) or routine(s) used to implement the processes described herein may be provided using any programmable language, e.g., a high level procedural and/or object orientated programming language that is suitable for communicating with a computer system. Any such programs may, for example, be stored on any suitable device, e.g., a storage media, readable by a general or special purpose program, computer or a processor apparatus for configuring and operating the computer (e.g., processor(s)) when the suitable device is read for performing the procedures described herein. In other words, at least in one embodiment, the system 10 may be implemented using a computer readable storage medium, configured with a computer program, where the storage medium so configured causes the computer to operate in a specific and predefined manner to perform functions described herein.

[0038] Likewise, the imaging system 10 may be configured at a remote site (e.g., an application server) that allows access by one or more users via a remote computer apparatus (e.g., via a web browser), and allows a user to employ the functionality according to the present disclosure (e.g., user accesses a graphical user interface associated with one or more programs to process data).

[0039] The processing apparatus (block 12), may be, for example, any fixed or mobile computer system (e.g., a personal computer or minicomputer, for example, with a CPU, GPU, etc.). The exact configuration of the computing apparatus is not limiting and essentially any device capable of providing suitable computing capabilities and control capabilities (e.g., control the imaging set up configuration and acquire data, such as pulse-echo data) may be used.

Further, various peripheral devices, such as a computer display, mouse, keyboard, memory, printer, scanner, etc. are contemplated to be used in combination with the processing apparatus (block 12), such as for visualization of imaging results (e.g., display of strain images, display of therapy delivery in real time such as with use of high intensity focused ultrasound, etc.).

[0040] Further, in one or more embodiments, the output (e.g., an image, image data, an image data file, a digital file, a file in user-readable format, etc.) may be analyzed by a user, used by another machine that provides output based thereon, etc.

[0041] As described herein, a digital file may be any medium (e.g., volatile or non-volatile memory, a CD-ROM, a punch card, magnetic recordable tape, etc.) containing digital bits (e.g., encoded in binary, trinary, etc.) that may be readable and/or writeable by processing apparatus (block 14) described herein.

[0042] Also, as described herein, a file in user-readable format may be any representation of data (e.g., ASCII text, binary numbers, hexadecimal numbers, decimal numbers, audio, graphical) presentable on any medium (e.g., paper, a display, sound waves, etc.) readable and/or understandable by a user.

[0043] Generally, the methods and systems as described herein may utilize algorithms implementing computational mathematics (e.g., matrix inversions, substitutions, Fourier transform techniques, etc.) to reconstruct the images described herein (e.g., from pulse-echo data).

[0044] In view of the above, it will be readily apparent that the functionality as described in one or more embodiments according to the present disclosure may be implemented in any manner as would be known to one skilled in the art. As such, the computer language, the computer system, or any other software/hardware which is to be used to implement the processes described herein shall not be limiting on the scope of the systems, processes or programs (e.g., the functionality provided by such systems, processes or programs) described herein.

[0045] One will recognize that a graphical user interface may be used in conjunction with the embodiments described herein. The user interface may provide various features allowing for user input thereto, change of input, importation or exportation of files, or any other features that may be generally suitable for use with the processes described herein. For example, the user interface may allow default values to be used or may require entry of certain values, limits, threshold values, or other pertinent information.

[0046] The methods described in this disclosure, including those attributed to the systems, or various constituent components, may be implemented, at least in part, in hardware, software, firmware, or any combination thereof. For example, various aspects of the techniques may be implemented within one or more processors, including one or more microprocessors, DSPs, ASICs, FPGAs, or any other equivalent integrated or discrete logic circuitry, as well as any combinations of such components, image processing devices, or other devices. The term "processor" or "processing circuitry" may generally refer to any of the foregoing logic circuitry, alone or in combination with other logic circuitry, or any other equivalent circuitry.

[0047] Such hardware, software, and/or firmware may be implemented within the same device or within separate devices to support the various operations and functions described in this disclosure. In addition, any of the described components may be implemented together or separately as discrete but interoperable logic devices. Depiction of different features, e.g., using block diagrams, etc., is intended to highlight different functional aspects and does not necessarily imply that such features must be realized by separate hardware or software components. Rather, functionality may be performed by separate hardware or software components, or integrated within common or separate hardware or software components.

[0048] When implemented in software, the functionality ascribed to the systems, devices and methods described in this disclosure may be embodied as instructions on a computer-readable medium such as RAM, ROM, NVRAM, EEPROM, FLASH memory, magnetic data storage media, optical data storage media, or the like. The instructions may be executed by one or more processors to support one or more aspects of the functionality described in this disclosure.

[0049] The imaging system 10 may further be used with, or may form a part of an optional therapy apparatus (block 20). For example, the therapy apparatus (block 20) may use the results of ultrasound imaging to provide one or more therapies. In one or more embodiments, the therapy apparatus (block 20) may be a non-invasive or invasive therapy apparatus such as a drug delivery apparatus or system (delivery of a drug to a particular location), a surgical apparatus or system (e.g., delivery of a stent to a particular position), an ablation apparatus or system (e.g., a high frequency or high intensity focused ultrasound therapy apparatus or system), etc.

[0050] In one or more embodiments, the therapy apparatus (block 20) may be a separate system or apparatus that receives an output from the imaging system (e.g., image information) and delivers one or more therapies. In other embodiments, the therapy apparatus (block 20) may be integrated with the imaging system to perform the one or more therapies (e.g., a high intensity focused ultrasound system that uses dual mode ultrasound transducer(s); for diagnostics such as imaging, as well as for treatment, such as ablation). For example, in one or more embodiments, the therapy apparatus (block 20) may include one or more portions of a system such as described in PCT International Publication No. WO2009/002492 entitled "Image Guided Plaque Ablation," published 31 December 2008. For example, the ultrasound imaging described herein may be used for reducing vascular plaque non-invasively. For example, the ultrasound

imaging described herein may be used to identify flow and vascular characteristics needed to non-invasively perform ablation of plaque as described in PCT International Publication No. WO2009/002492.

[0051] For example, the therapy system may be a system for non-invasively elevating the temperature of tissue by ultrasound energy waves including: at least one ultrasound delivery device adapted to deliver ultrasound energy waves to a focal point of targeted tissue; a temperature monitoring device for monitoring the temperature of targeted tissue at the focal point; and a controller for steering and controlling the ultrasound delivery device to deliver ultrasound energy waves at a focal point to elevate the temperature of targeted tissue to a desired temperature.

[0052] Further, for example, the therapy system may use one or more imaging systems described herein to produce an image of at least a portion of a mammalian body, e.g., such that the location of at least one vascular plaque in said image can be determined and to ascertain the location of the base of said vascular plaque. For example, ultrasound delivery device may ascertain one or more target locations at the base of the plaque. Still further one or more embodiments of the imaging system provided herein may be used in a method for elevating the temperature at a target location by an energy wave using an ultrasound therapy system (e.g., which may be the same ultrasound system (ultrasound transducers thereof) used for imaging). For example, the method may include delivering a beam of ultrasound energy waves from a source to the target location; monitoring the temperature of the target location; and stopping the delivering of the beam of ultrasound energy waves if a desired temperature at the target location has been reached.

[0053] Further, a method of preparing a plan for non-invasively elevating the temperature of tissue in a vessel wall leading to regression of vascular plaques may include imaging at least a portion of a body to produce an image (e.g., using ultrasound imaging as described herein to image a vascular region); determining the location of at least one vascular plaque in said image; ascertaining the location of the base of said vascular plaque and one or more target locations at the base of the plaque (e.g., using the ultrasound generated image); and/or determining the parameters for delivering ultrasound energy waves from a source to a focal point for elevating the temperature of targeted tissue in the vessel wall to a desired temperature, sufficient for reducing or destroying vaso vasorum.

[0054] Further, for example, the ultrasound imaging described herein may be used to identify flow and vascular characteristics needed to perform invasive treatments of plaque (e.g., stent delivery, cardiac surgery, etc.)

[0055] Still further, in one or more embodiments, the therapy apparatus (block 20) may include one or more portions of a system such as described in U.S. Provisional Patent Application No. 61/353,096, entitled "Dual Mode Ultrasound Transducer (DMUT) System for Monitoring and Control of Lesion Formation Dynamics" filed 9 June 2010. For example, the ultrasound imaging described herein may be performed with the same or similar transducer arrays described therein which can be used for both imaging (e.g., to monitor a therapy procedure), as well as for delivering therapy (e.g., to deliver high intensity focused ultrasound energy). For example, therapy may be delivered using the ultrasound transducer array, while the imaging modes using the same transducer array may be used to guide the therapeutic beam, assess thermal and mechanical tissue response to estimate doses of therapy (e.g., initial dose of therapy), monitor and characterize tissue response during therapy, and assess the state of the treated tissue at the completion of each exposure to the therapeutic ultrasound energy (e.g., real time monitoring between periods of therapy delivery).

[0056] For example, ultrasound imaging as described herein may be used to identify one or more vascular characteristics. An exemplary diagram of a blood vessel 50 is shown in Figure 7 to facilitate discussion of the use of imaging described herein. The blood vessel 50 shown in Figure 7 includes a vessel wall 52 having a plaque structure 54 formed on the interior of the vessel wall 52. The plaque architecture of the structure 54 may include, for example, a plaque base 56, a lipid core 58, and a fibrous or calcified cap 60. Blood 62 flows through the blood vessel 50 defined by the vessel wall 52.

[0057] One or more embodiments of methods and/or systems described herein may be used to identify one or more vascular characteristics, e.g., flow characteristics associated with the flow through the blood vessel 50, structural characteristics associated with the blood vessel 50, and/or hemodynamic characteristics. For example, flow characteristics may include flow velocity, volume flow, wall shear stress, wall shear rate, etc.

[0058] For example, structural characteristics may include determining boundaries of the vessel wall (e.g., outer and inner boundaries, such as in a coordinate system), thickness of the vessel wall, measurement of tissue properties within the vessel wall (e.g., stiffness of tissue, such as, for example, it relates to a diseased state), differentiation of plaque from vessel wall, differentiation of the various components of plaque (e.g., differentiation of base from lipid core, differentiation of base from fibrous cap, differentiation of lipid core from fibrous cap, etc.), etc. For example, in one or more embodiments, upon differentiation of the base from the fibrous cap of the plaque architecture, treatment may be provided to ablate the base to reduce further plaque buildup or growth or provide treatment according to PCT International Publication No. WO2009/002492.

[0059] Still further, for example, hemodynamic characteristics may include calculated hemodynamic measurements, such as, for example, arterial pressure, cardiac output, arterial compliance, pulse wave velocity, etc. At least in one embodiment, such hemodynamic measurements may be determined based on parameters relating to both tracking of the blood flow and tracking of vessel wall motion or displacement. As such, to obtain an accurate hemodynamic determination, the parameters or measurements relating to both tracking of the blood flow and tracking of vessel wall motion

or displacement must be determined simultaneously, or within a periodic cycle in which both can be determined (e.g., determined effectively). For example, compliance of the vessel may be based on both volume flow which relates to tracking of blood flow and pressure within the vessel which can be determined by tracking vessel displacement.

[0060] For example, accurate estimation of the vessel diameter and estimation of the lateral flow within the lumen with high frame rate imaging will allow for useful measurement of the pulse wave velocity (PWV) noninvasively. For example, the time waveforms shown in, for example, Figures 5C-5D can be plotted in phase space (volume flow, Q_A, vs. vessel area, A). Volume flow can be calculated from the flow data, while the area can be obtained from the vessel wall movement. This measurement must be made during the reflection-free part of the heart cycle in the form of a slope measurement of the form PWV=dQ/dA. With the adequately sampled time waveforms (e.g., using M2D mode imaging), the task of estimating the vessel wall motion and the flow within the vessel can be accomplished.

[0061] In other words, both lateral flow velocity and wall motion can be estimated simultaneously thus providing pressure (through vessel diameter) and flow (through vector velocity)). Such measurements can provide the basis for hemodynamic computations that may be used in the assessment of vessel wall compliance, an important indicator of the health of the vessel as described herein. Further, as described herein, axial and lateral displacement fields are well-behaved and allow for strain and shear strain calculations in both tissue and blood. Together with anatomical image information, these velocity/strain fields may provide input for computational fluid dynamic models, which may allow for inverse calculations suitable for the assessment of the health of the vasculature and surrounding tissue (e.g. detection and staging of atherosclerosis).

[0062] In one or more embodiments, the ultrasound-enabled quantitative imaging system may be used for assessment of the disease state in atherosclerotic blood vessels. For example, the imaging may be used for the direct estimation of the strain fields in the vicinity of the vessel walls. Such methods may mitigate the deleterious effects of local deformations that could result in loss of correlation, and which may render the correlation-based speckle tracking approach useless in the vicinity of the vessel wall. Such deformations, depending on severity, could result in erroneous estimate in the velocity (and therefore strain) estimation or may even result in loss of accuracy.

[0063] A three-pronged approach to the problem of restoring the true velocity/strain estimates may include: 1) A two-step algorithm for direct estimation of the velocity/strain components using a deformed model of the 2D RF data in the vicinity of the wall, 2) A reconstructive approach employing a forward computational fluid dynamics (CFD) model as a regularization filter, and 3) A quantitative inverse reconstruction of the tissue mechanical properties using ultrasound-based velocity/strain fields as observations. As described herein, simultaneous imaging of tissue motion and flow with subsample accuracy in both axial and lateral directions may be implemented. For example, such imaging may include using a phase-coupled 2D speckle tracking approach, which employs the true 2D complex cross correlation to find sub-pixel displacements in both axial and lateral directions. Further, a modified imaging sequence on a Sonix RP scanner to allow high frame rate 2D data collection in a limited field of view covering the region of interest (M2D-mode) may be used. Together with the robust 2D speckle tracking method, M2D imaging allows for capturing the full dynamics of the flow and wall/tissue motion, even when the flow is primarily in the lateral direction (with respect to the imaging beam). The fine vector displacement estimates in both axial and lateral directions are shown to allow for smooth and contiguous strain and shear strain calculations with minimal filtering. The simultaneous imaging of the vector flow field and the wall/tissue motion and the corresponding strains at high spatial and temporal sampling may provide a tool in modeling the fluid-solid interactions between the blood and blood vessel. Such an image-based modeling of the vessel response may allow for the prediction of the disease state and possible evolution of the disease state.

[0064] Furthermore, the integration between the observation model and inverse reconstruction of the tissue properties in the vicinity of the vessel wall may allow for quantitative assessment of the plaque composition (e.g. lipid content or calcification). This may provide a reliable noninvasive model for selecting treatment options based on probability of rupture and other risk factors.

[0065] In other words, the imaging described herein may be used in conjunction with computational fluid dynamic (CFD) modeling the evaluation of large artery hemodynamics. CFD has been shown to produce useful prediction of time-varying, 3D flow fields in large arteries with complex geometries. In this context, modeling fluid-solid interfaces has been defined as a challenge area in vascular mechanics. Imaging methods as described herein capable of capturing both perivascular (and wall) tissue motion and deformations, together with fluid flow may be used to address this issue. Advances in MRI and other imaging modalities have led to increased interest in image-based, patient-specific CFD modeling to monitor disease progression. MRI has excellent soft tissue contrast that may allow the accurate capture of the tissue (solid) model. Although this may be an advantage over diagnostic ultrasound, which does not offer the same level of definition for tissue boundaries and discrimination between tissue types, this limitation may be mitigated, however, by the recent improvements in 3D image acquisition, both freehand and motorized. Therefore, diagnostic ultrasound scanners may provide an attractive alternative for image-based CFD modeling. Based on 3D ultrasound and improved 2D velocity/strain imaging using M2D mode, processes for providing quantitative tissue property images in the vicinity of the vessel wall for the characterization of the disease state may be implemented. The imaging methods described herein address the limitations of existing correlation-based methods for velocity/strain estimation to restore the lost or

artifact-ridden estimates in the vicinity of the wall. Further, the integration of our velocity/strain estimation as an observation model in a dynamic, forward/inverse CFD-based model for the reconstruction of the field/tissue property values consistent with the Navier-Stokes equations may be accomplished. For example, the following may be developed: a two-step algorithm for direct strain estimation at the vessel wall using M2D-mode data; a regularized approach for the reconstruction of displacement/strain maps utilizing a forward CFD model obtained from 3D Ultrasound (e.g., the forward model may provide a reconstruction filter to regularize the velocity/strain estimation obtained using the speckle tracking algorithm); and/or an inverse method for the reconstruction of the mechanical properties in the vicinity of the vessel wall based on strain maps obtained using M2D-mode data.

[0066] The one or more ultrasound transducers (block 22) may be any apparatus (e.g., transmitting, receiving components, etc.) capable of delivering ultrasound pulses and sampling/collecting ultrasound echo energy contemplated to be used in ultrasound imaging systems and in combination with processing apparatus (block 12) of the system 10. As used herein, such transducers may include a transmitting portion, e.g., to deliver pulse energy, and a receiving portion, e.g., to sample/collect echo or reflected energy, which may or may not be the same portion. During the ultrasound imaging of a target (e.g., a blood vessel, such as a carotid artery, coronary artery, etc.), the one or more transducers (block 22) may be positioned relative to the target so as to be capable of delivering energy to the target resulting in reflected energy (also known as the resultant pulse-echo or echo energy) and also sampling the echo energy.

[0067] The one or more transducers (block 22) may include multiple transducers position separately from one another or may be a transducer array. In one or more embodiments, various arrays may have one or more benefits over others. For example, in one or more embodiments, the transducer array may be a segmented concave transducer with multiple sub-apertures to insonify the vessel from multiple angles. This will allow for better definition of the vessel boundaries from more directions. At least one sub-aperture may be used in linear array or phased array mode for initial B-mode and strain imaging of the vessel. The driver of the transducer may be designed to drive the multiple sub-apertures with independent codes. Each sub-aperture may be a one-dimensional or two-dimensional array. Coded excitation may help improve both the data rates (e.g., provide higher frame rates) and echo quality (e.g., by reducing reverberations within the lumen). The receiver may be a multichannel receiver with beamforming and/or pulse compression for coded excitation.

[0068] For example, various arrays and operation thereof, are described in Ebbini, et al., "Dual-Mode Ultrasound Phased Arrays for Image-Guided Surgery," Ultrasound Imaging, vol. 28, pp. 65-82 (2006); Ballard, et al., "Adaptive Transthoracic Refocusing of Dual-Mode Ultrasound Arrays," IEEE Transactions on Biomedical Engineering, vol. 57, no. 1, pp. 93-102 (Jan. 2010); and Wan et al., "Imaging with Concave Large-Aperture Therapeutic Ultrasound Arrays Using Conventional Synthetic-Aperture Beamforming," IEEE Transactions on Ultrasound, Ferroelectrics, and Frequency Control, vol. 55, no. 8, pp. 1705-1718 (August 2008).

[0069] A flow chart of an exemplary ultrasound imaging method 30 for vascular imaging is depicted in FIG. 2. One will recognize that one or more of the blocks of functionality described herein may be carried out using one or more programs or routines, and/or any other components of an imaging system (e.g., the imaging system 10 of FIG. 1) and/or therapy system (e.g., the therapy system 20 of FIG. 1).

[0070] Generally, the method 30 provides for the capture of pulse-echo data at a sampled frame rate (block 32). In one embodiment, ultrasound pulse-echo data is provided of a region in which at least one portion of a blood vessel is located. For example, the pulse-echo data may be pulse-echo data sampled at a frame rate such that measured displacement of the vessel wall defining the at least one portion of the blood vessel and measured average blood flow through the at least one portion of the blood vessel have a quasi-periodic profile over time to allow motion tracking of both the vessel wall and the blood flow simultaneously. Further, the method includes applying speckle tracking (block 34) to the pulse-echo data to allow, for example, the generation of strain and shear strain image data.

[0071] As set forth herein with respect to the system shown in Figure 1, one or more vascular characteristics, e.g., flow characteristics associated with the flow through the blood vessel 50, structural characteristics associated with the blood vessel 50, and/or hemodynamic characteristics, may be identified (block 36) based on the tracking of motion in the vessel wall and flow. In one embodiment, due the simultaneous capture of displacement fields in both the flow and vessel wall, e.g., during a periodic cycle, such as a cardiac cycle, one or more vascular characteristics which depend on measurements resulting from or relating to both such types of displacements (e.g., such as hemodynamics) may be determined.

[0072] Still further, as shown in Figure 2, optionally the method 30 may include delivering therapy based on one or more vascular characteristics (block 38). For example, as described with respect to the system of Figure 1, delivery of therapy may take one or more different forms (e.g., drug, ablation, surgical, or any other invasive or non-invasive treatment).

[0073] In one or more embodiments, the method may include M2D mode imaging designed to maximize the lateral extent of the imaged region at sufficiently high frame rates to capture the full dynamics of the vessel wall and the flow within the vessel. M2D mode produces 2D beamformed RF echo data from a selected region of the field of view (FoV) of a given probe. The region may be contiguous or comprised of more than one disjoint subsegments. As an example, on the SonixRP scanner (Ultrasonix, BC, Canada), an arbitrary set of A-lines within the FoV can be used to form the

M2D mode image with frame mode approximately M_B/M_{M2D} higher than B-mode imaging, where M_B *and* M_{M2D} indicate the number of A-lines used to form B-mode and M2D-mode images, respectively.

[0074] As shown in Figure 4, M2D mode imaging may be enabled by creating a powerful pipelined execution/flow program architecture capable of employing a variety of computational resources for real-time implementation. In addition, the program architecture may allow the user to invoke additional computational resources available on the computer (or generally on the Internet) to achieve other computational tasks. The results from these computations can be integrated seamlessly with the program. For example, the beamformed RF echo data may be transferred in real time through a Gigabit interface to allow real-time 2D axial strain computations using GPU (or FPGA) using ID speckle tracking. However, the beamformed RF data is available for additional processing using, for example, a pre-installed MATLAB engine. The MATLAB results can be imported back seamlessly to the M2D mode imaging program with minimum latency (e.g., after the completion of the MATLAB calculations). This capability may allow us to perform real-time 2D speckle tracking to enable strain and shear strain in the vicinity of the vessel wall, e.g., heavy-duty MATLAB-based calculations are performed on a small RoI allowing for their incorporation in real time. In at least one embodiment, true 2D speckle tracking approaches may be implemented in real time as is currently the case with 1D speckle tracking. In this way, a pipelined program execution architecture may be implemented to support M2D imaging which allows us to reap the benefits of powerful computational tools for the analysis of the vessel walls in quasi real-time.

[0075] The high frame rate M2D mode preserves the correlation to produce well-behaved 2D displacement/velocity profiles to allow for robust strain computation. High quality 2D (+time) strain and shear strain fields produce views of the vessel wall boundaries on both sides of the vessel in the axial view. Further, they may also produce better definition of the wall in the lateral direction in the cross-sectional view. This may allow for measurements of wall thickening, an early sign of atherosclerosis.

[0076] Still further, the high quality 2D (+time; i.e., over time) strain and shear strain will allow for tissue property measurements within the vessel wall, e.g. stiffness. Such tissue property measurements will allow for the characterization of the disease state and, given the high resolution, the plaque architecture (e.g., base, lipid core, and fibrous or calcified cap). Therapy or treatments may be delivered based on such information or such information may be used during the delivery of such therapy (e.g., high intensity focused ultrasound treatments that target the base of the plaque without damage to the cap or even the lipid core, continual determination of the response of tissue to therapy, such as between doses of high intensity focused ultrasound, etc.).

[0077] The pulse-echo data may be provided using any imaging system (e.g., the imaging system 10 of FIG. 1), although one or more imaging systems may be advantageous over others. In one or more embodiments, the data acquisition may be performed by an imaging system 100 such as shown in Figures 3 and 4. For example, as shown in Figure 3, the imaging system 100 may be used to acquire and perform real-time processing of such acquired data. The imaging system 100 may include an ultrasound scanner 102 (e.g., a Sonix RP (Ultrasonix, Canada)) loaded with a program used for high frame rate pulse-echo data collection. The ultrasound scanner may include features such as chirp generation, waveform generation, data collection, and data transfer capabilities.

[0078] As shown in the exemplary embodiment, collected data may be streamlined to a controller PC 104 through, for example, Gigabit Ethernet for real-time data processing. The data processing computer 104 can handle the intensive computations required by high-resolution (both spatial and temporal) speckle tracking and separable 2-D post-filtering by utilizing a many-core graphics processing unit 106 (e.g., GPU; nVIDIA, Santa Clara, CA). The ultrasound scanner 102 may operate in B mode for image guidance (e.g., producing a B-mode image) and in M2D mode for high-frame-rate data collection. The M2D mode achieves high-frame-rate imaging by limiting the number of scan lines to the region of interest (ROI), as defined by the user. M2D data may be used for speckle tracking. For example, in one embodiment, M2D-mode acquisition with 10 A lines per frame at 1000 fps may be performed. For example, a linear array probe (e.g., LA14-5/38) may be used for data collection at a frame rate of 1000 fps in M2D mode by limiting the number of scan lines to 10 and the imaging range to 40 mm. In one or more embodiments with coded excitation, M2D-mode may collect data at frame rates from 2000 to 5000 frames per second or more.

[0079] In the embodiment shown in Figure 3, high intensity focused ultrasound (HIFU) is also possible (e.g., for generating ultrasound for treatment or subtherapeutic mechanical and/or thermal effects). As such, a Virtex2Pro (Xilinx, CA) field-programmable gate array (FPGA) board 108 is dedicated for HIFU source and synchronized frame trigger generation. This implementation allows an interference-free data collection by briefly silencing the HIFU generator while pulse-echo imaging is active.

[0080] Speckle tracking used for imaging herein relies on accurate estimation of incremental frame-to-frame time shifts, which are typically much smaller than RF-echo sampling period. In one embodiment, a 2-D complex correlation of two subsequent frames of pulse-echo data is carried out. The real-time data processing engine 110 is based on a GPU 106 with a large number of cores (e.g., a GTX285 GPU with 240 processing cores and designed to take full advantage of its highly parallel architecture). Implementation of real-time processing is supplemented with Integrated Performance Primitives (Intel) and Matlab tools 112, 114. Further, a research interface system 120 is provided for operator control.

[0081] Figure 4 shows an exemplary block diagram of a GPU-based implementation 130 for an imaging system, such as shown in Figure 3. In one embodiment, for each processing stage, fine-grained partition is performed for the algorithm in a data-independent manner so that all 240 processors are working efficiently on individual blocks of data.

[0082] For example, Figure 4 shows one exemplary embodiment of a real-time signal processing chain of beamformed ultrasound data for strain imaging (e.g., shown for 1D, but which can be generalized to 2D or 3D). The real-time speckle tracking is performed in the axial direction, but axial strain and axial shear strain can be performed in real-time as a first step to identify the vessel boundaries (e.g., this has been tested in vivo on vessels of various diameters (~1 mm in rat) and (~4 mm in swine)). The 2D strain calculations can be performed in a region-of-interest (RoI) around the identified blood vessel. Axial and lateral strains and corresponding shear strains can be calculated in real-time following this step. Furthermore, direct estimation of strains and shear strains in the immediate vicinity of the vessel wall may be provided. For both 1D and 2D versions of the strain calculations, additional processing in the time direction will further define the vessel boundaries and the internal boundaries of the wall. For example, in the context of imaging atherosclerosis, this may yield the internal composition of the plaque.

[0083] As shown in Figure 4, on the CPU side, data can be come from Network Stack (e.g., experimental mode, where data is streamlined from SonixRP scanner) or Data File (e.g., review mode). The processed result can be visualized with a designed UI system (OpenGL based) or exposed to other commercial software for further analysis (e.g., Matlab). The result can be also used in feedback control for real-time temperature control.

[0084] On the GPU side, Figures 4 shows a GPU-based implementation of the algorithm described in (see, e.g., Simon, et al., "Two-Dimensional Temperature Estimation Using Diagnostic Ultrasound," IEEE Transactions on Ultrasonics, Ferroelectronics, and Frequency Control, vol. 45, no. 4, pp. 1088-1099, JULY 1998). The various blocks shown in Figure 4 have at least the following functionality: Hilbert transform: computes the analytic signal of the RF echo using an FIR Hilbert Transformer; Cross correlation/Phase projection/Accumulate: implements 1D version of speckle tracking; 2D Separable Filter: allows temperature estimation (e.g., thermal strain computation); Bilinear Interpolation: provides hardware accelerated interpolation for data visualization; and Local Storage: provides data management in GPU domain.

[0085] In other words, in one or more embodiments, a system for vascular imaging is provided herein that includes one or more ultrasound transducers (e.g., wherein the one or more transducers are configured to deliver ultrasound energy to a vascular region resulting in pulse-echo data therefrom) and processing apparatus (e.g., including one or more programs executable by one or more processors of the system to perform one or more functions thereof and as described herein, such as control of data frame acquisition, speckle tracking, visualization, image generation, characteristic identification, etc.).

[0086] In other words, the processing apparatus (e.g., GPU, CPU, etc.) may be configured (e.g., operate under control of one or more programs) to, for example, control the capture of pulse-echo data at a frame rate such that measured displacement of a vessel wall defining at least one portion of a blood vessel in the vascular region and measured average blood flow through the at least one portion of the blood vessel have a quasi-periodic profile over time to allow motion tracking of both the vessel wall and the blood flow simultaneously; generate strain and shear strain image data for the region in which the at least one portion of the vessel is located using speckle tracking; and identify at least one vascular characteristic of the vascular region in which at least one portion of a blood vessel is located based on the strain and shear strain image data (e.g., wherein the at least one vascular characteristic comprises at least one of a flow characteristic associated with flow through the blood vessel, a structural characteristic associated with the blood vessel, and a hemodynamic characteristic associated with the blood vessel).

[0087] According to the invention, the processing apparatus is configured to use speckle tracking of one or more speckle regions of the vascular region in which at least one portion of the blood vessel is located to track motion of both the vessel wall defining the at least one portion of the blood vessel and the blood flow through the at least one portion of the blood vessel (e.g., wherein the pulse-echo data is captured at a frame rate such that displacement of the vessel wall defining the at least one portion of the blood vessel and blood flow through the at least one portion of the blood vessel are measurable simultaneously within a same periodic cycle corresponding to a cardiac pulse cycle and/or identify at least one vascular characteristic of the vascular region in which the at least one portion of the blood vessel is located based on the simultaneously measured displacement of the vessel wall and average blood flow. The processing apparatus is further operable (e.g., by executing one or more programs) to generate strain and shear strain image data for the region in which the at least one portion of the vessel is located using the speckle tracking (e.g., wherein the speckle tracking includes using multi-dimensional correlation of sampled pulse-echo data of the one or more speckle regions undergoing deformation in the region in which the at least one portion of a blood vessel is located, wherein the multi-dimensional correlation comprises determining a cross-correlation peak for the sampled pulse-echo data based on phase and magnitude gradients of the cross-correlated sampled pulse-echo data).

[0088] As shown in Figures 5A-5D, in one or more embodiments, the frame rate at which pulse echo data is acquired should be at least greater than 100 fps, and even greater than 200 fps. In at least one embodiment, the frame rate is greater than 300 fps. The frame rate should be sufficiently high for reliable motion tracking in both tissue and blood synchronously (e.g., such that measurements relating to the same are relevant to the same time frame or periodic cycle).

For example, in one embodiment, the M2D mode allows for providing a high frame rate while maintaining the correlation at high levels to produce smooth and contiguous displacement /velocity fields (e.g., displacement of tissue, motion of blood flow) to allow for robust strain and shear strain determinations.

[0089] The frame rate for acquiring pulse-echo data should be adequate to provide displacement fields in both flow and tissue that are well-behaved. In one embodiment, such well-behaved displacement can be identified by the measurements of channel diameter related to tracking of tissue displacement (e.g., vessel wall displacement or motion) and average flow velocity related to the tracking of flow through the vessel (e.g., tracking of blood flow through the blood vessel) over time. As such, Figures 5A-5D show graphs of both the tracking of flow in a vessel (e.g., represented by the change of average flow velocity shown in solid lines) as well as the tracking of vessel tissue displacement (e.g., represented by change in channel diameter over time shown by dashed lines) for multiple frame rates. Figure 5A shows determinations for a frame rate of 40 fps; Figure 5B shows determinations for a frame rate of 81 fps; Figure 5C shows determinations for a frame rate of 162 fps; and Figure 5D shows determinations for a frame rate of 325 fps.

[0090] It is clear from Figures 5A and 5B, that such low frame rates (e.g., less than 100 fps) do not produce measured displacement of the vessel wall defining a blood vessel and measured average blood flow through the blood vessel which are well behaved. In other words, measurements of flow and tissue displacement (e.g., vessel wall displacement) could not be accurately measured simultaneously. For example, as clearly shown in Figures 5A and 5B, the blood flow is shown to be rather random throughout a periodic cycle of the displacement of the vessel wall represented by the channel diameter information (e.g., from peak to peak of the vessel wall displacement). In other words, such blood flow data is ridden with artifacts making an accurate flow determination difficult during the cycle. Even the vessel wall displacement information appears to include some artifacts.

[0091] However, discernible from Figures 5C and 5D, at higher frame rates (e.g., greater than 100 fps) the measured displacement of the vessel wall defining a blood vessel and measured average blood flow through the blood vessel are well behaved such that measurements of flow and tissue displacement (e.g., vessel wall displacement) could be accurately measured synchronously (e.g., corresponding to the same time). For example, as clearly shown in Figures 5C and 5D, the blood flow is shown to be much less random throughout a periodic cycle of the displacement of the vessel wall represented by the channel diameter information (e.g., from peak to peak of the vessel wall displacement). In other words, the measured displacement of the vessel wall defining a blood vessel and measured average blood flow through the blood vessel have a quasi-periodic profile over time which allows motion tracking of both the vessel wall and the blood flow simultaneously. Note the strong peaks for both the channel diameter and average flow velocity within the same periodic cycle (e.g., corresponding to the cardiac cycle).

[0092] As used herein, the term quasi-periodic profile is meant to reflect a profile that is substantially consistent over periodic cycles in the form of a regularized pattern, even though there will be some variation on a frame to frame basis, e.g., periodic cycles corresponding to cardiac cycles. For example, such a quasi-periodic profile for flow velocity may include strong peaks during each cycle indicating maximum flow followed by flow measurements that indicate little or no flow during the remainder of the cycle. Further, for example, such a quasi-periodic profile for channel diameter may include strong peaks during each cycle indicating maximum displacement of the vessel wall followed by measurements that indicate a relaxation of the vessel to a normal state during the remainder of the cycle. Such a frame rate that results in a quasi-periodic profile allows for tracking of flow and vessel displacement simultaneously, or in other words, synchronously with each other (e.g., in phase with each other).

[0093] The frame rate may vary depending on various factors. For example, the frame rate may be based on the vessel structure (e.g., carotid artery versus peripheral vein), timing of the periodic flow through the vessel (e.g., pulse cycle length), motion of the vessel structure (e.g., time for vessel to relax to normal); depth of the target vessel (e.g., deeper vessels may be imaged at lower frame rates), use of coded excitation (e.g., coded excitation may allow for increased frame rates), and the f-number of imaging focus (e.g., higher f-numbers may result in reduced lateral resolution), etc.

[0094] Still further, in one or more embodiments, higher frame rates may be accomplished when coded excitation ultrasound is used. Such coded excitation ultrasound is described, for example, in the literature and will not be discussed in detail herein. For example, one or more illustrative examples of coded excitation ultrasound which may be used in combination with the imaging method and/or systems described herein are provided in Shen et al., "A New Coded-Excitation Ultrasound Imaging System---Part I: Basic Principles," IEEE Transactions on Ultrasonics, Ferroelectrics, and Frequency Control, vol. 43, no. 1, pp. 131 -140, Jan. 1996); Shen et al., "A New Coded-Excitation Ultrasound Imaging System---Part II: Operator Design," IEEE Transactions on Ultrasonics, Ferroelectrics, and Frequency Control, vol. 43, no. 1, pp. 141 -148, Jan. 1996); and Shen et al., "Filter-Based Coded-Excitation System for High-Speed Ultrasound Imaging," IEEE Transactions on Medical Imaging, vol. 17, no. 6, pp. 923-934, Dec. 1 998).

[0095] In one or more embodiments, the frame rate may be greater than 100 fps, greater than 200 fps, greater than 300 fps, greater than 500 fps, greater than 1000 fps, and even greater than 5000 fps. In other embodiments, the frame rate may be less than 5000 fps, less than 4000 fps, less than 3000 fps, less than 2000 fps, less than 1000 fps, less than 600 fps, less than 500 fps, less than 400 fps, less than 300 fps, or less than 200 fps. In at least one embodiment, the

frame rate is within the range of 100 fps to 5000 fps.

[0096] As shown in the imaging method 30 in Figure 2, speckle tracking is applied to the pulse-echo data (block 34). For example, strain and shear strain image data for the region in which at least one portion of the vessel is located may be generated using speckle tracking. In one or more embodiments, the speckle tracking may include using multi-dimensional correlation of sampled pulse-echo data of one or more speckle regions (e.g., windows) undergoing deformation in the region in which the at least one portion of a blood vessel is located. The multi-dimensional correlation may include determining a cross-correlation peak for the sampled pulse-echo data based on phase and magnitude gradients of the cross-correlated sampled pulse-echo data.

[0097] Such generation of strain and shear strain image data allows for the identification of at least one vascular characteristic of the region in which at least one portion of a blood vessel is located (block 36) (e.g., a flow characteristic associated with flow through the blood vessel, a structural characteristic associated with the blood vessel, a hemodynamic characteristic associated with the blood vessel, etc.). One or more types of strain and shear strain image data may be used and/or visualized to identify such vascular characteristics.

[0098] Strain calculations include performing band-limited gradient calculations on the 2D (or 3D) displacement fields obtained using speckle tracking (in 2D or 3D). Real-time speckle tracking on full image sizes (i.e., for every pixel of the RF echo data) may be achievable in the axial direction. 2D and 3D speckle tracking may be achieved in real time in a region of interest around the blood vessel. The strains and shear strains can be overlaid on B-mode or other ultrasound imaging formats. For example, information regarding such calculations are also found in Liu et al., "Real-Time 2-D Temperature Imaging Using Ultrasound," IEEE Transactions on Biomedical Engineering, vol. 57, no. 1, pp. 12-16 (Jan. 2010).

[0099] For example, generation of strain and shear strain image data for the region in which the at least one portion of the vessel is located using speckle tracking may include generation of at least one of axial strain and/or axial shear strain image data (e.g., axial relating to the axis through the vessel being imaged). Further, such generation of strain and shear strain image data may include generation of lateral strain and/or lateral shear strain image data. Such data may be visualized, for example, in both longitudinal views (e.g., along the blood vessel) or cross-section views (e.g., orthogonal to the axis of the blood vessel), as further provided herein.

[0100] For example, one or more types of strain and shear strain image data may be used and/or visualized to identify one or more vessel wall boundaries, including the vessel wall boundaries around the entire blood vessel (e.g., such boundaries may be visualized in cross-section and/or measured about the entire blood vessel). One or more other vascular characteristics may be identified, measured or calculated therefrom, such as tissue property within the one or more vessel wall boundaries, one or more portions of a plaque architecture adjacent the one or more vessel wall boundaries, and/or one or more hemodynamic measurements based on both the motion tracking of the vessel wall and the blood flow simultaneously.

[0101] Certain types of strain and shear strain image data may be more beneficial for imaging one or more portions of the blood vessel and flow therethrough than others. For example, axial strain image data may be beneficial in identifying a first set of opposing wall boundaries (e.g., on opposite sides of the vessel) while the axial shear strain image data may be beneficial in identifying a second set of opposing wall boundaries (e.g., on opposite sides of the vessel) such that the boundaries of the entire vessel (e.g., discernible in cross-section) can be identified. Further, the same is generally the case for lateral strain and lateral shear strain. Further, for example, the lateral shear strain may be beneficial in providing wall shear stress data (e.g., used for identification of possible plaque formation).

[0102] Further, for example, shear strain images further define the vessel walls, not only the proximal and distal walls, but also the side walls, which are hard to see on conventional ultrasound. (2D/3D+Time) calculations may also be used to refine the detection of the wall boundaries as a function of time during the heart cycle.

[0103] The speckle tracking applied to the pulse-echo data (block 34) may include using any multi-dimensional correlation of sampled pulse-echo data of one or more speckle regions (i.e., windows being tracked). For example, two-dimensional correlation of sampled pulse-echo data of one or more speckle regions may be used, as well as other multi-dimensional correlation techniques.

[0104] In one embodiment, for example, speckle tracking is performed as described in E. S. Ebbini, "Phase-coupled two-dimensional speckle tracking algorithm," IEEE Trans. Ultrason., Ferroelect., Freq. Contr., vol. 53, no. 5, pp. 972-990, May 2006 (hereinafter "Ebbini 2006''). For example, in general, such speckle tracking includes coarsely searching the magnitude of the sampled pulse-echo data in a lateral and axial direction to locate a vicinity of the cross-correlation peak within the cross-correlated sampled pulse-echo data; determining, within the vicinity of the cross-correlation peak, at least two opposing gradient vectors in proximity to the cross-correlation peak; determining, within the vicinity of the cross-correlation peak, a zero-phase line of the cross-correlated sampled pulse-echo data; and using the at least two opposing gradient vectors in proximity to the cross-correlation peak and the zero-phase line to estimate the cross-correlation peak.

[0105] More specifically, as described in Ebbini (2006), a two-dimensional (2-D) speckle tracking method for displacement estimation based on the gradients of the magnitude and phase of 2-D complex correlation in a search region is provided. This approach couples the phase and magnitude gradients near the correlation peak to determine its coordi-

nates with subsample accuracy in both axial and lateral directions. This is achieved with a minimum level of lateral interpolation determined from the angles between the magnitude and phase gradient vectors on the sampled (laterally interpolated) 2-D cross-correlation grid. One result behind this algorithm is that the magnitude gradient vectors' final approach to the true peak is orthogonal to the zero-phase contour. This leads to a 2-D robust projection on the zero-phase contour that results in subsample accuracy at interpolation levels well below those needed. Further, the approach includes a robust fast search algorithm that allows the localization of the true peak without the need for exhaustive search.

[0106] In other words, the speckle tracking uses the phase of the 2-D complex cross correlation for robust and efficient estimation of displacement from speckle data. This speckle tracking method finds the true peak of the 2-D complex cross correlation as a constrained optimization problem. The objective of this optimization problem is to find the coordinates of the axial and lateral lags at the true peak of the 2-D complex cross correlation subject to the zero-phase constraint. The basis for this formulation is shown mathematically from the inverse of the Fourier transform of the 2-D cross spectrum near the true correlation peak. This geometric approach finds both the axial and lateral displacement estimates with subsample accuracy. The method is based on the fact that the gradient vectors of the magnitude of the 2-D cross correlation approach the true peak along the orthogonal to the zero-phase contour. Knowing that the zero-phase contour also passes through the true peak, it is possible to locate this peak simply by finding the point on this contour at which the magnitude gradient vectors are orthogonal, provided these vectors originate from a grid point that is sufficiently close to the peak. One feature of this algorithm is that interpolation of the complex cross correlation is used at a minimum level that allows for a valid projection to be made. Therefore, the algorithm is computationally efficient in terms of determining the level of interpolation needed for subsample accuracy from the properties of the underlying 2-D, cross-correlation function, not from the desired lateral resolution.

[0107] The following is a mathematical basis for correlation-based 2-D speckle tracking and relates it to a 2-D cross spectrum approach. Thereafter, two implementations of a phase-coupled 2-D speckle tracking algorithm are then provided.

[0108] Let $s(x, z, t_0)$ be the analytic ultrasonic signal received from a 2-D region (e.g., speckle region or window) at time t_0 with spatial coordinates x and z representing the lateral and axial directions, respectively. The received signal model assumes a linear space-invariant imaging system with rectangular sampling (e.g., linear array). After undergoing translation d_x and d_z (respectively in the x and z directions), the received signal at time, t_1, $s(x, z, t_1) = s(x - d_x, z - d_z, t_0)$ has a 2-D Fourier transform:

$$S(k_x, k_z, t_1) = S(k_x, k_z, t_0) e^{-j(k_x d_x + k_z d_y)}, \qquad (1)$$

where k_x and k_z are the spatial frequency variables (in rad/m) in the x and z directions, respectively. The 2-D cross spectrum is given by:

$$\begin{aligned} \Gamma_{12}(k_x, k_z) &= S(k_x, k_z, t_1) S^*(k_x, k_z, t_0) \\ &= |S(k_x, k_z, t_0)|^2 \, e^{-j(k_x d_x + k_z d_z)}. \end{aligned} \qquad (2)$$

[0109] Motivated by this equation, one investigator developed an algorithm based on the 2-D cross spectrum for estimation of fine displacement in both the axial and lateral directions. An iterative weighted least squares approach to estimate the slopes of the axial and lateral frequency components has been proposed. However, a more efficient solution to this problem can be obtained by finding the true peak of the 2-D cross-correlation function, given by (3) and (4),

$$\gamma_{12}(l_x, l_z) = \frac{1}{4\pi^2}\int_{-\infty}^{\infty}\int_{-\infty}^{\infty}\Gamma_{12}(k_x, k_z)e^{j(k_x l_x + k_z l_z)}dk_x dk_z$$
$$= \frac{1}{4\pi^2}\int_{-\infty}^{\infty}\int_{-\infty}^{\infty}|S(k_x, k_z, t_0)|^2$$
$$\times e^{j[k_x(l_x - d_x) + k_z(l_z - d_z)]}dk_x dk_z \quad (3)$$
$$= \gamma_{11}(l_x - d_x, l_y - d_z), \quad (4)$$

where l_x and l_z are the lags in the *x* and z directions, respectively. This function peaks at lag values equal to the shift values in both the axial and lateral directions. This result drives all correlation-based, 2-D displacement tracking methods. However, with the use of sampled correlation functions due to the discrete nature of the RF data collection, the true correlation peak must be found with subsample accuracy. This is especially true for the lateral displacement estimation in which the sampling interval (spacing between A-lines) is on the order of 10 times the axial sampling interval.

[0110] Insight into this problem can be obtained by evaluating the cross-correlation function in the vicinity of the true peak where $k_x(l_x$ - dx) ≈ 0 and $k_z(l_z - d_z) \approx 0$, from (3):

$$\gamma_{12}(l_x, l_z) \approx \frac{1}{4\pi^2}\int_{-\infty}^{\infty}\int_{-\infty}^{\infty}|S(k_x, k_z, t_0)|^2(1 + j[k_x(l_x - d_x)$$
$$+ k_z(l_z - d_z)])dk_x dk_z$$
$$= \gamma_{11}(0, 0) + j[M_{xz}(l_x - d_x) + M_{zx}(l_z - d_z)], \quad (5)$$

where:

$$M_{xz} = \frac{1}{4\pi^2}\int_{-\infty}^{\infty}\int_{-\infty}^{\infty}|S(k_x, k_z, t_0)|^2 k_x dk_x dk_z, \quad (6)$$

$$M_{zx} = \frac{1}{4\pi^2}\int_{-\infty}^{\infty}\int_{-\infty}^{\infty}|S(k_x, k_z, t_0)|^2 k_z dk_x dk_z. \quad (7)$$

[0111] The factor M_{xz} is related to the mean lateral frequency of the 2-D auto spectrum. Similarly, the factor M_{zx} is related to the mean axial frequency of the 2-D auto spectrum. Due to the fact that the axial component in many coherent imaging systems has a carrier and that the complex envelope is used, $|M_{zx}| \gg 0$. This modulation property does not exist for the lateral factor M_{xz}, and its magnitude is generally small. It is important to note, however, that in a speckle environment, $|M_{xz}| \neq 0$ (typically $|M_{zx}| \gg |M_{xz}|$). The result in (5) can be seen as a generalization of a 1-D speckle tracking case in which the slope of the phase curve is equal to the center frequency of the (analytic) echo signal [8]. In fact, expressing (4) in vector form (and including the quadratic phase term in the Taylor series expansion of the exponential), we get:

$$\gamma_{12}(\mathbf{l}) = \frac{1}{4\pi^2}\int_{-\infty}^{\infty}\int_{-\infty}^{\infty}\Gamma_{12}(\mathbf{k})e^{j\mathbf{k}'\mathbf{dx}}d\mathbf{k}$$

$$= \frac{1}{4\pi^2}\int_{-\infty}^{\infty}\int_{-\infty}^{\infty}|S(\mathbf{k},t_0)|^2 e^{j\mathbf{k}'(\mathbf{l}-\mathbf{dx})}d\mathbf{k} \quad (8)$$

$$\approx \frac{1}{4\pi^2}\int_{-\infty}^{\infty}\int_{-\infty}^{\infty}|S(\mathbf{k},t_0)|^2(1+j\mathbf{k}'(\mathbf{l}-\mathbf{dx}) - \frac{1}{2}(\mathbf{k}'(\mathbf{l}-\mathbf{dx}))^2)d\mathbf{k}$$

$$= \gamma_{11}(0,0) - \frac{1}{2}(\mathbf{l}-\mathbf{dx})'\begin{bmatrix}W_{xx} & W_{xz}\\ W_{zx} & W_{zz}\end{bmatrix}(\mathbf{l}-\mathbf{dx}) + j\left[M_{xz}\ M_{zx}\right](\mathbf{l}-\mathbf{dx}), \quad (9)$$

where the elements W_{xx}, W_{xz}, W_{zx}, W_{zz} are given by:

$$W_{xx} = \frac{1}{4\pi^2}\int_{-\infty}^{\infty}\int_{-\infty}^{\infty}|S(k_x,k_z,t_0)|^2 k_x^2 dk_x dk_z, \quad (10)$$

$$W_{zz} = \frac{1}{4\pi^2}\int_{-\infty}^{\infty}\int_{-\infty}^{\infty}|S(k_x,k_z,t_0)|^2 k_z^2 dk_x dk_z, \quad (11)$$

$$W_{zx} = W_{zx} = \frac{1}{4\pi^2}\int_{-\infty}^{\infty}\int_{-\infty}^{\infty}|S(k_x,k_z,t_0)|^2 k_z k_x dk_x dk_z. \quad (12)$$

[0112] Note that *Wxx* is related to the lateral frequency bandwidth of the imaging system. It is easy to see that $\gamma_{12}(d_x, d_z) = \gamma_{11}(0, 0) > \gamma_{12}(l_x, l_z)\ \forall (l_x, l_z) \neq (d_x, d_z)$. Also note that $\gamma_{12}(d_x, d_z)$ is real, which implies that the true peak of the 2-D cross correlation must lie on the zerophase contour defined by:

$$\angle\gamma_{12}(l_x,l_y) \approx M_{xz}(l_x-d_x) + M_{zx}(l_z-d_z), = \left[M_{xz}\ M_{zx}\right](\mathbf{l}-\mathbf{dx}) = \mathbf{m}'(\mathbf{l}-\mathbf{dx}). \quad (13)$$

[0113] However, based on the above approximation, the magnitude of the 2-D cross correlation is given by:

$$|\gamma_{12}(\mathbf{l})| = \sqrt{(\gamma_{11}(0,0) - (\mathbf{l}-\mathbf{dx})'\mathbf{W}(\mathbf{l}-\mathbf{dx}))^2 + (\mathbf{m}'(\mathbf{l}-\mathbf{dx}))^2}, \quad (14)$$

for which the transpose of the gradient vector can be evaluated as shown in (15), which indicates that the gradient is identically zero at the true peak (l = dx) as expected.

$$\frac{\partial|\gamma_{12}(\mathbf{l})|}{\partial \mathbf{l}} = \frac{-2\left(\gamma(0,0) - (\mathbf{l}-\mathbf{dx})'\mathbf{W}(\mathbf{l}-\mathbf{dx})\right)(\mathbf{l}-\mathbf{dx})'\mathbf{W} + (\mathbf{m}'(\mathbf{l}-\mathbf{dx}))\,\mathbf{m}'}{\sqrt{(\gamma_{11}(0,0) - (\mathbf{l}-\mathbf{dx})'\mathbf{W}(\mathbf{l}-\mathbf{dx}))^2 + (\mathbf{m}'(\mathbf{l}-\mathbf{dx}))^2}} \quad (15)$$

[0114] Furthermore, the magnitude of the magnitude gradient near l = dx is proportional to the distance from the true peak, i.e., the closer the grid point to the true peak, the smaller the magnitude of the gradient. In addition, if the grid point is such that l - dx is orthogonal to m (m'(l - dx) = 0), then the magnitude gradient is orthogonal to m, and the true peak can be obtained by finding the intersection of the line along the magnitude gradient with the tangent to the zero phase contour. Of course, this is only valid when the grid point is sufficiently close to the true peak. This can be determined from the magnitude of the magnitude gradient on the grid. This result provides us with insight for approach to determine the true peak of the 2-D cross-correlation function from a grid of computed values around the peak. Specifically, by comparing the slope of the minimum magnitude gradient with the slope of the phase contour in the vicinity of the peak, one can determine whether the true peak is sufficiently close to the grid points to make a valid approximation.

[0115] This leads to algorithms as described herein for finding the true peak that are both robust and numerically efficient in the sense that interpolation is used at a minimum level to ensure the conditions of a valid projection onto the zero-phase contour. The formulation described herein also provides the basis for an optimization procedure of finding a point on a quadratic surface (magnitude of the 2-D cross correlation) subject to the zero-phase condition. This problem can be solved using the Lagrange multiplier method as described herein.

[0116] The above result can be easily extended to the case of affine transformation [13]:

$$s(\mathbf{x}_1, t_1) = s(\mathbf{x}_0(\mathbf{x}_1), t_0), \quad (16)$$

where:

$$\mathbf{x}_0 = \mathbf{T}\mathbf{x}_1 - \mathbf{dx} \quad (17)$$

$$\begin{bmatrix} x_1 \\ z_1 \end{bmatrix} = \begin{bmatrix} 1+e_{xx} & e_{xz} \\ e_{zx} & 1+e_{zz} \end{bmatrix} \begin{bmatrix} x_0 \\ z_0 \end{bmatrix} - \begin{bmatrix} dx \\ dz \end{bmatrix}, \quad (18)$$

which accounts for translation (dx), strain (e_{xx} and e_{zz}), and shear strain (e_{xz} and e_{zx}). In this case, we use the Fourier transform of the received signal at time t_1 in vector form:

$$S(\mathbf{k}, t_1) = S(\mathbf{T}'^{-1}\mathbf{k}, t_0) e^{j(\mathbf{k}'\mathbf{T}^{-1}\mathbf{dx})}/|\mathbf{T}|, \quad (19)$$

where T' is the transpose of T and |·| is the determinant of a matrix. Note that (19) is just a generalization of the scaled property of the Fourier transform in 1-D, which has previously been used in the analysis of decorrelation of ultrasonic echoes in the presence of strains. It is also consistent with the 2-D/3-D formulation shown in [5], which analyzes the combined effects of deformation and waveform warping on the variance of the displacement estimate.

[0117] It suggests that both axial and lateral strains can affect the displacement estimates based on phase matching alone. It also may provide an opportunity to directly (or iteratively) estimate the strains on the tissue region interrogated

by the window. We note here that, in cases in which the strain parameters, e_{xx}, e_{zz}, e_{xz}, and e_{zx}, have non-negligible values, the zero-phase contour does not necessarily go through the true peak of the magnitude of the 2-D cross correlation. To illustrate this point, (19) can be written explicitly in terms of the shift and strain parameters as shown in (20), which shows that the scaling of the Fourier transform in the k_x and k_z coordinates is coupled through the shear strain parameters. Amplitude scaling leads to decorrelation effects previously reported for 1-D tracking. Furthermore, the estimated shift from the zero-phase contour is also coupled, i.e., a shift in the x direction contributes to the estimated shift in the z direction and vice versa (through the shear strain parameters). The simple result given by (5) is only approximately valid for infinitesimal strains within the tracking window. Fortunately, (20) provides a method to detect when the strain effects within the window are significant enough to affect the phase estimation.

$$S(k_x,k_z,t_1)=\frac{1}{|\mathbf{T}|}S\left(\frac{(1+e_{zz})k_x-e_{zx}k_z}{|\mathbf{T}|},\frac{-e_{xz}k_x+(1+e_{xx})k_z}{|\mathbf{T}|},t_0\right)\cdot \cdot e^{-j\left(\frac{((1+e_{zz})dx-e_{xz}dz)k_x+((1+e_{xx})dz-e_{zx}dx)k_z}{|\mathbf{T}|}\right)} \tag{20}$$

[0118] In the speckle tracking method, one is interested in the use of phase-coupled approach in finding the true peak of the 2-D cross-correlation function when the tissue is undergoing displacement and/or infinitesimal strains. This can be considered a first step in estimating the displacement vectors needed in applications such as, for example, vector velocity estimation and elastography. Such applications may require displacement tracking based on the peak of the 2-D cross correlation as a common step, but they may differ in the deformation model parameters used. This can be done by implementing a post-processing step that extracts the deformation parameters from the shift estimation results obtained from finding the true peak of the 2-D cross correlation. Such post-processing depends on the specific problem to be determined.

An Exemplary Phase-Coupled 2-D, Speckle Tracking Algorithm

[0119] The steps of the exemplary speckle tracking algorithm are guided by the properties of the 2-D correlation of the speckle region undergoing motion and/or deformation. The magnitude of the 2-D correlation with the complex envelope has a well behaved peak with extent in axial and lateral directions proportional to the speckle cell size. The main idea is to use a fast search algorithm to find a correlation-based match within a search window (i.e., correlation values above a threshold). If the current search point is far from the correlation peak, a fast search can be used with axial and lateral steps on the order of one-half the extent of the correlation cell size in the axial and lateral directions. This allows the search to coarsely cover large regions without missing the true peak (if it exists). Once a match is found, the magnitude gradient of the cross correlation is used to find the peak cross correlation on the sampling grid (determined by the RF sampling frequency and spacing between the A-lines in the image). This is done by following a gradient ascent trajectory, which requires two to three correlation values to be computed for every point along the trajectory. Gradient search for the peak is very robust and efficient from any direction if search point is within the width of the correlation peak in the axial and lateral directions, e.g., within 3 dB from the peak. Once the grid-based correlation peak is found, a 3 X 3 correlation grid is calculated (centered at the peak). In the immediate vicinity of the correlation peak, the true peak can be determined from the magnitude gradient vectors and the zero-phase contour passing the true peak. From the 3 X 3 grid in the original sampling coordinates, a fine estimate of the true correlation peak is produced by coupling the phase of the 2-D cross correlation to the amplitude (gradients) in a way that will allow us to use (13).

[0120] Two exemplary approaches for obtaining the fine estimates are described in the following subsections.

A. Two-Dimensional Projection on the Zero-Phase Contour

[0121] This method interpolates the 3 X 3 grid near the true peak in the lateral lag direction by a sufficiently large factor (i.e., as small as possible) in order to estimate a magnitude gradient vector orthogonal to the zero-phase contour. The intersection of the magnitude gradient and the zerophase contour is the estimated true peak of the 2-D cross correlation.

[0122] The steps of this algorithm are outlined as follows.

[0123] Step 0: From the 2-D autocorrelation function at t_0, estimate the search step size L_z and L_x in the axial and lateral directions, directly. Typically, $L_z > L_x$ due to the finer sampling in the axial direction.

[0124] Step 1: Perform any fast search algorithm to find the vicinity of correlation peak (above a threshold) using L_x and L_z in a defined search region.

[0125] Step 2: Without any interpolation, compute the local magnitude gradient and move along the gradient ascent trajectory. This step stops when the peak point on the uninterpolated grid is reached.

[0126] Step 3: Once the maximum point on the uninterpolated grid is reached, compute cross-correlation values on 3 X 3 grid centered at the maximum. Interpolate the 3 X 3 grid laterally by a small factor (e.g., 8) and find the line equations for the two gradient vectors closest to the true peak, but pointing in opposite lateral directions. If this condition is not satisfied with the current interpolation factor, increase interpolation by two and repeat the test. If maximum interpolation factor is reached (e.g., 128) and correlation at the interpolated peak is below a threshold (e.g., 0.75) displacement estimate is declared invalid and assigned a value of NaN. Otherwise, proceed to Step 4.

[0127] Step 4: Find the line equations for the zero-phase line of the correlation function on the interpolated grid. The estimated true correlation peak is the point of intersection between the zero-phase line and the orthogonal line that passes through the point of intersection of the two maximum-slope lines from the magnitude gradient.

[0128] For illustration purposes, the search trajectory in Fig. 6A is based on L_x = 1 and L_z = 5 (from Step 0). Fig. 6A shows contours of the 2-D cross correlation with the search path shown [starting from (0,0) lag as indicated by the arrow]. The * indicates correlation lags tested by the fast-search algorithm and the • indicates lags tested by the gradient-ascent algorithm (L_x = 1 and L_z = 5). Note that the true correlation peak has a well behaved set of contours that distinguish it from several false peaks in the search region shown. Furthermore, the 0.7 contour extends by approximately 4 lateral lags and 10 axial lags (which justifies the choice of L_x and L_z). Step 1 begins at lag (0,0) and tests the cross-correlation coefficient. If below the set threshold (0.65 in this case), it moves to the next point as indicated by the arrow (-1 lateral and -5 axial). If still below threshold, it tests correlation values along each pixel on the (predefined) trajectory. In this case, the predefined search trajectory is along rectangular counterclockwise loops (dimensions $2 L_x * i + 1 \times 2 * L_z * i + 1$ where i = 0, 1, ..., Imax is the loop number). The parameter I_{max} defines the extent of the allowed search region to find a valid peak (I_{max} = 6 for the search region shown in Fig. 6A).

[0129] In this search example, the eight lags on the first loop are tested, and no candidate peak is found (i.e., no correlation value > 0.65). The algorithm jumps from the last point in the first loop (-1 lateral and 0 axial) to the first point in the second loop (-2 lateral and -10 axial) and moves counter clockwise along the lateral lag direction. This step stops once the threshold test is successful, i.e., correlation value at the current correlation lag above the chosen threshold. In Fig. 6A, this step stops at lateral lag 0 and axial lag -10 after a threshold of 0.65 was reached. Step 2 also is illustrated with the help of Fig. 6A. The • signs at (0,-10), (1,-10)(1,-11), (1,-12), (2,-12), (2,-13), (2,-14) are the grid points tested by the gradient ascent. The neighboring points of (2,-14) also are tested before declaring this point as the maximum point on the correlation grid.

[0130] The final two steps of the algorithm may be illustrated with the help of Fig. 6B which shows the magnitude and phase contours of the interpolated 2-D cross correlation near the true peak. Further, Figure 6B shows magnitude and phase contours of the 2-D cross correlation on the laterally-interpolated 3 X 3 grid in the vicinity of the correlation peak (between lags -13 and -15 axially and 1 and 3 laterally). The arrows represent the magnitude gradient vectors on the interpolated grid. Lateral interpolation by a factor of 16 is used in this case (with the interpolated grid points indicated by the arrow bases). The phase contours are labeled with phase values in radians and appear to be almost straight with a small tilt. The true peak is indicated by the open circle on the zero-phase line. The dash-dotted lines are the directions of the magnitude gradient vectors closest to the peak and the tangent and the orthogonal to the zero-phase line. In addition, one can see the magnitude gradient vectors pointing in the (general) direction of the true peak. An interpolation factor of 16 was used for this case between lateral lags 1 and 3 and axial lags -13 and -15 (i.e., centered at 2 lateral and -14 axial from Step 2). Four (thick dash-dotted) lines are drawn along the two closest magnitude gradient vectors, the tangent to the zero-phase line, and the orthogonal to the zero-phase passing through the point of intersection of the maximum-slope lines. The true correlation peak, indicated by the open circle, is the point of intersection of the latter with the zero-phase line.

[0131] The final step in the projection on zero-phase algorithm is an approximation of the magnitude gradient vector orthogonal to the zero-phase contour at the true peak. The approximation error depends on the level of interpolation used and can be controlled by using a lateral interpolation factor just enough to ensure that at least one of the two magnitude-gradient vectors used in the final approximation is not substantially parallel to the zero-phase contour near the true peak. In general, this condition is needed only when the axial shift is practically equal to integer multiple of the axial sampling interval. For example, in Fig. 6B one can see the magnitude gradient vectors at axial lag -14 approaching from the right are almost parallel to the zero-phase line. The interpolation factor of 16 used here was just enough to produce a valid projection. A valid projection is one in which the two magnitude gradient vectors closest to the peak intersect the tangent of the zero-phase line at points in which the tangent approximates the phase contour well. The key point here, however, is that the interpolation can be performed adaptively, thus minimizing any unnecessary calculations in the displacement estimation algorithm. In addition to the computational advantage of this approach, one can reduce or eliminate the error due to interpolation.

[0132] It should be noted that one or more different steps may be implemented in the method, and the specific steps provided herein are not take to be limiting on the disclosure. For example, the exemplary search algorithm may be implemented using one or more other digital signal processing approaches. Further, for example, for template matching, one can use the autocorrelation sequence in the vicinity of the (0,0) lag. A related issue is the declaration of an invalid

estimate based on the correlation threshold in Step 3 and assigning a value of NaN. This can be thought of as a flag to be used in subsequent processing if necessary. For example, one may use an adaptive window size to maximize the composite signal-to-noise ratio (SNR). Alternatively, one may use an explicit deformation model similar to that described by (19).

[0133] Further, the present disclosure is not limited to use of 2D speckle tracking. For example, other multi-dimensional tracking methods, such as 3D speckle tracking methods may also be applicable in one or more embodiments herein.

B. Surface Polynomial Fit with Phase Constraints

[0134] The 2-D phase projection approach described above can be thought of as an efficient method for implementation of an optimization procedure for finding the true peak of the complex 2-D cross correlation. The peak finding problem can be cast as finding the coefficients of a polynomial fit to the surface of the magnitude of the 2-D cross correlation in the vicinity of the true peak. The nominal and interpolated contour plots shown in Figures 6A and 6B are obtained from actual imaging data and are representative of what can be expected from a standard imaging scanner. It is quite clear that the surface near the true correlation peak is well behaved and appears to be quadratic in the *lx, lz* space. A polynomial fit to this (smooth) surface is given by:

$$q(l_x, l_z) = a{l_x}^2 + b{l_z}^2 + cl_x l_z + dl_x + el_z + f, \tag{21}$$

where l_x and l_z represent lateral and axial lags, respectively, and q is the magnitude of the 2-D, complex cross correlation in the vicinity of the true peak. It is possible to solve for the polynomial coefficients by minimizing the square error:

$$J(\theta) = \sum_{i=1}^{N} \left(q(l_{x_i}, l_{z_i}) - |\gamma_{12}(l_{x_i}, l_{z_i})|\right)^2, \tag{22}$$

where θ = [*a, b, c, d, e, f*]' and *N* is number of points on the grid (in this case *N* = 9).

[0135] This amounts to solving the over-determined system of equations:

$$\hat{\mathbf{q}} = \mathbf{A}\theta \tag{23}$$

$$\begin{bmatrix} |\gamma_{12}(l_{x_1}, l_{z_1})| \\ |\gamma_{12}(l_{x_2}, l_{z_2})| \\ \vdots \\ |\gamma_{12}(l_{x_N}, l_{z_N})| \end{bmatrix} = \begin{bmatrix} l_{x_1}^2 & l_{z_1}^2 & l_{x_1}l_{z_1} & l_{x_1} & l_{z_1} & 1 \\ l_{x_2}^2 & l_{z_2}^2 & l_{x_2}l_{z_2} & l_{x_2} & l_{z_2} & 1 \\ \vdots & \vdots & \vdots & \vdots & \vdots & \vdots \\ l_{x_N}^2 & l_{z_N}^2 & l_{x_N}l_{z_N} & l_{x_N} & l_{z_N} & 1 \end{bmatrix} \begin{bmatrix} a \\ b \\ c \\ d \\ e \\ f \end{bmatrix}. \tag{24}$$

[0136] This results in:

$$J(\theta) = (\hat{\mathbf{q}} - \mathbf{A}\theta)'(\hat{\mathbf{q}} - \mathbf{A}\theta) \tag{25}$$

$$= \hat{\mathbf{q}}'\hat{\mathbf{q}} - 2\hat{\mathbf{q}}\mathbf{A}\theta + \theta'\mathbf{A}'\mathbf{A}\theta. \tag{26}$$

[0137] By taking the gradient of this quadratic function with respect to the real vector θ and equating to zero, we obtain the solution:

$$\hat{\theta} = (\mathbf{A}'\mathbf{A})^{-1}\mathbf{A}'\hat{\mathbf{q}}, \qquad (27)$$

which is valid when the matrix **A** is well conditioned. If this is not the case, then a regularized solution (e.g., using singular value decomposition) is sought [17]. Once the coefficients θ are obtained, it is a simple matter to obtain l_{xmax} and l_{zmax} by analytically evaluating the gradients:

$$\frac{\partial q}{\partial l_x} = 2al_x + cl_z + d, \qquad (28)$$

$$\frac{\partial q}{\partial l_z} = cl_x + 2bl_z + e, \qquad (29)$$

and solving the matrix equation:

$$\begin{bmatrix} l_{x_{\max}} \\ l_{z_{\max}} \end{bmatrix} = \begin{bmatrix} 2a & c \\ c & 2b \end{bmatrix}^{-1} \begin{bmatrix} -d \\ -e \end{bmatrix}. \qquad (30)$$

[0138] However, this solution may amount to a form of interpolation based on magnitude only, which may result in unacceptably high levels of bias and variance in the estimation of the true correlation peak, especially in the axial direction. This is due to the almost flat nature of the surface described by q in the axial direction (axial extent of only ± 1 lag samples). However, q typically has a distinct peak in the lateral direction, and the derivative in this direction yields a reliable estimate of the peak. It is known that the analytic nature of ultrasonic echo signal allows for high subsample accuracy in axial shift estimation by using complex cross correlation without interpolation. An improved solution may be obtained if the lateral estimate from surface fitting solution described by (30) with the axial estimate obtained from the analytic RF data.

[0139] Accounting for phase information in 2-D can be done easily by using (13) as a constraint in conjunction with an appropriate cost function (e.g., using the Lagrange multiplier method). To do this, we recognize that the polynomial fit function given in (21) is itself a quadratic cost function in l_x and l_z. That is, one can rewrite (21) in the form:

$$\begin{aligned} q(l_x - dx_0, l_z - dz_0) &= \mathbf{l}'\mathbf{R}\mathbf{l}, \\ &= \mathbf{l}' \begin{bmatrix} a & \frac{c}{2} \\ \frac{c}{2} & b \end{bmatrix} \mathbf{l}, \end{aligned} \qquad (31)$$

[0140] where dx_0 and dz_0 are the coordinates of the center of the 3 X 3 grid in the vicinity of the true peak and $\mathbf{l} = [l_x\text{-}dx_0, l_z\text{-}dz_0]'$. The elements of R are obtained from the solution to least squares problem in (23). This can be shown by expanding the translated vector form in (31) and comparing with the coefficients of l^2_x, l^2_z and $l_x l_z$ in (21). The optimization problem is to find the subsample shift vector $\delta\mathbf{l} = [\delta_x, \delta_z]'$ (note that $\mathbf{l}_{max} = [dx_0, dz_0]' + [\delta_x, \delta_z]'$) that minimizes (31) subject to the constraints:

- $\mathbf{m}'\mathbf{m} = 1$, which implies $m_x = M_{xz}/\sqrt{M_{xz}^2 + M_{zx}^2}$ and $m_z = M_{zx}/\sqrt{M_{xz}^2 + M_{zx}^2}$
- $\delta\mathbf{l}'\mathbf{m} = \delta_x m_x + \delta_z m_z = 0$.

[0141] The first constraint is just a normalization that is typically used in eigenvalue problems. The second constraint restricts the solution vector to be orthogonal to the zerophase line at the true peak (13). The elements of **m** are obtained from the center frequency values in (6) and (7).

[0142] The constraints above allow us to define a new cost function in terms of the Lagrange multipliers, λ and μ:

$$J(\delta \mathrm{l}) = \delta \mathrm{l}' \mathbf{R} \delta \mathrm{l} - \lambda (\delta \mathrm{l}' \delta \mathrm{l}) + \mu \delta \mathrm{l}' \mathrm{m}. \qquad (32)$$

[0143] The solution to this problem can be obtained by taking the gradient of J with respect to δl:

$$\frac{\partial J}{\partial \delta \mathrm{l}} = 2\mathbf{R}\delta \mathrm{l} - 2\lambda \delta \mathrm{l} + \mu \mathrm{m}. \qquad (33)$$

[0144] Multiplying by m' and solving for μ:

$$\mu = -2\mathrm{m}'\mathbf{R}\delta \mathrm{l} - 2\lambda \mathrm{m}'\delta \mathrm{l} \qquad (34)$$

$$= -2\mathrm{m}'\mathbf{R}\delta \mathrm{l}, \qquad (35)$$

where the orthogonality constraint was used to drop the second term in (34). Substituting μ back in (33), we obtain the eigenvalue problem:

$$\begin{aligned} &2\mathbf{R}\delta \mathrm{l} - 2\lambda \delta \mathrm{l} - 2\mathrm{m}'\mathbf{R}\delta \mathrm{l} = 0 \\ &\Rightarrow (\mathbf{I} - \mathrm{mm}')\,\mathbf{R}\delta \mathrm{l} = \lambda \delta \mathrm{l}. \end{aligned} \qquad (36)$$

[0145] The solution to this eigenvalue problem is the eigenvector associated with the maximum eigenvalue of the matrix (I -mm')R. The Lagrange multiplier, λ, is the eigenvalue, which appropriately scales the eigenvector to give the true lag (at the true maximum). The projection matrix, (I -mm'), serves to align the solution obtained based on the magnitude-only method to be orthogonal to the observed slope of the zero-phase contour. Thus the coupling between the phase and magnitude characteristics for finding the true peak of the 2-D cross correlation is complete.

[0146] Various steps, routines, or processes may be implemented with the exemplary speckle tracking methods described herein (such as those described in Ebbini (2006)), that further assist in providing useful image data or enhancement of image data. For example, when performing speckle tracking of speckle regions in the region in which at least one portion of a blood vessel is located, if the speckle region (i.e., window or speckle cell) being tracked is partially within the vessel wall defining the at least one portion of the blood vessel and partially outside of the vessel wall (e.g., lying partially in the blood within the vessel or lying partially outside of the boundaries of the vessel wall), the speckle tracking process may be difficult to carry out or result in data that is inaccurate (e.g., difficult to cross correlate, etc.). As such, at least in one embodiment, once a vascular characteristic is identified or determined (e.g., the identification of one or more boundaries (or portions thereof) of the vessel based on speckle tracking), the vascular characteristic may be used in performing the speckle tracking method.

[0147] According to the invention, one or more vessel wall boundaries are be identified based on the speckle tracking of one or more speckle regions. Once such boundaries are identified, they can be used in the speckle tracking process. In one or more embodiments, for example, a characteristic of the one or more speckle regions (e.g., location, size, shape, etc.) may be modified based on the at least one identified vascular characteristic (e.g., such as the identification of vessel wall boundaries).

[0148] According to the invention, the location of at least one of the one or more speckle regions being tracked is modified (e.g., or any other characteristic of one or more speckle regions, such as size, or shape, may be modified) based on the one or more vessel wall boundaries identified such that the speckle region being tracked is entirely within or outside of the vessel wall. In other words, if the speckle tracking process determines that a speckle region or window being tracked is partially within the vessel wall defining the at least one portion of the blood vessel and partially outside of the vessel wall (e.g., lying partially in the blood within the vessel or lying partially outside of the boundaries of the vessel wall), then the speckle region location is modified or otherwise adjusted such the speckle region is entirely located within the vessel wall or outside of the vessel wall. Further, the size or shape (e.g., narrowness or width or length) of

the speckle region tracked may be modified during the speckle tracking such that the speckle region is entirely located within the vessel wall or outside of the vessel wall, or provides quality estimates, e.g., of displacement. In other words the speckle region is modified such that it falls entirely outside the vessel wall, entirely within the vessel wall, or entirely within the blood, based on the one or more boundaries determined for the vessel (e.g., by prior speckle tracking and generation of strain and/or shear strain image data for the region in which the at least one portion of the vessel is located).

[0149] For example, generally, tracking windows are designed to optimize or achieve a tradeoff between spatial resolution (e.g., generally improved by reducing the window size) and reducing the variance of the displacement estimates (e.g., generally, by increasing the window size). For example, in one embodiment, for a uniform speckle region, the signal-to-noise (SNR) of the echo data, together with the transducer bandwidth, are the primary factors in selecting the window size. Furthermore, in the absence of severe deformation, windows are designed to be approximately square, i.e., approximately the same axial and lateral dimensions. Near the vessel wall, especially on the lumen side, many assumptions may be violated. High frame rate imaging (e.g., M2D mode imaging) is provided to mitigate some of these effects, but there may also be a need to account directly for deformations within the tracking window (e.g., part of the window being in the vessel and part in the blood leading to deformation issues). In such cases, one may apply adaptive window size and shape design or selection algorithms that will produce optimal estimates (e.g., best possible displacement estimate). The 2D phase-coupled algorithm provides feedback on the quality of the estimates (e.g., figures of merit). These figures of merit may be used in characterizing the quality of the estimate obtained, for example, using different windows with the same height, but different width and vice versa. As such, it is possible to run these windows in parallel and implement a voting scheme that selects the estimates with the highest figures of merit and reject or weigh down (e.g., apply a lower weighting factor) the estimates with lower figures of merit.

[0150] Still further, vessel wall echo reverberations may corrupt pulse-echo data received from the blood. As such, in one or more embodiments of speckle tracking of one or more speckle regions within the blood, the speckle tracking may remove echo components in the pulse-echo data due to reflection at the vessel wall when performing such speckle tracking of the pulse-echo data from the one or more speckle regions in the blood (e.g., using a dereverberation filter).

[0151] In other words, as described herein, various speckle tracking methods (e.g., two-dimensional speckle tracking methods) can be used to image tissue motion and deformations in the vicinity of blood vessels (e.g., for use in detecting and staging of vascular disease). However, in one or more embodiments, vessel wall echo reverberations may overwhelm the echoes (scattering) from the blood and result in loss of flow information in large regions within the vessel. One embodiment that may be used to correct for such reverberations includes use of a time-varying dereverberation inverse filter for echo data within the vessel (e.g., echo data from the blood). The design for such a filter may be influenced by the fact that the reverberation pattern varies significantly with the pulsatory motion of the vessel wall. Minute changes in the location/orientation of the vessel wall with respect to the imaging beam result in measurable changes in the speckle-specular echo mixture at the vessel wall and the observed periodicities in the reverberation pattern within the vessel. Therefore, a time-varying inverse filter may be used to remove the reverberation components appropriately during the heart cycle.

[0152] Speckle tracking (e.g., two-dimensional speckle tracking) can be used for the analysis of tissue motion and deformation, especially in vascular imaging applications. In addition to the direct measurements and/or characterization of the vessel dynamics, such speckle tracking may provide tissue displacement fields and underlying anatomical information suitable for important challenge areas such as computational fluid dynamics.

[0153] For example, as described herein, simultaneous estimation of tissue motion/deformation and blood flow vector velocity in a blood vessel (e.g., the human carotid artery) using pulse-echo diagnostic ultrasound can be performed (e.g., using phase-coupled two-dimensional speckle tracking which achieves subsample displacement estimation accuracy in both axial and lateral directions together with a high frame rate (e.g., 325 frames per second) M2D imaging mode both lateral flow velocity and wall motion can be estimated simultaneously thus providing pressure (through vessel diameter) and flow (through vector velocity)). Such measurements can provide the basis for hemodynamic computations that may be used in the assessment of vessel wall compliance, an important indicator of the health of the vessel as described herein. Further, as described herein, axial and lateral displacement fields are well-behaved and allow for strain and shear strain calculations in both tissue and blood. Together with anatomical image information, these velocity/strain fields may provide input for computational fluid dynamic models, which may allow for inverse calculations suitable for the assessment of the health of the vasculature and surrounding tissue (e.g. detection and staging of atherosclerosis).

[0154] One possible limitation of two-dimensional speckle tracking methods based on pulse-echo ultrasound is the reverberation components associated with strong specular reflectors. Reverberation produces clutter signal components that mix with back scattering components from regions distal to the specular reflector. This is significant in blood vessels where the scattering from blood is typically 30 - 40 dB below the specular reflection from the vessel wall. For applications where both the tissue motion and blood velocity vectors are important, however, the clutter due to reverberation from the region within the vessel walls should be minimized. An algorithm for dereverberation of pulse-echo ultrasound data to restore echoes from the blood scattering region prior to two-dimensional speckle tracking may be used to address such reverberations. Due to the changes in the scattering characteristics of the vessel wall during the different phases

of the heart cycle, it is observed that the reverberation signal components are non-stationary, which indicates that a time-varying inverse filter for dereverberation may be needed. One possible filter design approach may utilize short-range correlation for the echo signal from the wall and the long-range correlation of the echo signal from the proximal wall and the vessel region. Periodicities in the correlation functions are attributed to the vessel wall architecture and multilayer tissue structure resulting in distinct specular components (e.g. adventia).

[0155] The following provides one or more implementations of dereverberation or examples testing the same. Such specific implementations or examples are not to be taken as being limiting to the present disclosure.

Exemplary Dereverberation Filtering Information

Data Acquisition for the example Dereverberation Filtering

[0156] A Sonix RP (Ultrasonix, Canada) ultrasound scanner loaded with a program used for M2D pulse-echo data collection. Collected data is then streamlined to a controller PC through Gigabit Ethernet for real-time data processing. The data processing computer can easily handle the intensive computations required by high resolution (both spatial and temporal) speckle tracking and separable 2D post filtering by utilizing a many core GPU (nVIDIA, Santa Clara, CA). A linear array probe (LA14-5/38) was used to acquire all data of this example. The center frequency of the transmit pulse on the probe was 7.5 MHz.

Received Signal Model

[0157] A received signal model for pulse-echo beamformed ultrasound data obtained from a typical scanner and typical vascular probe such as those described above is provided. The echo data forming one image line is given by

$$x_r(t,l) = x_c(t,l) + x_i(t,l) \qquad (1)$$

where $x_c(t; l)$ represents the coherent echo component from depth $z = c/t$ in image line l and $x_i(t; l)$ is the incoherent echo component from the same location. At the vessel wall, the coherent component is largely due to specular reflection from the multi-layered vessel and supporting structure. For simplicity, assume a single layer in a homogeneous medium and a narrowband model:

$$x_c(t,l) = R_{tw}\,p\left(t - \frac{2z_0}{c}\right) + \sum_{k=1}^{\infty} \alpha_k\, p\left(t - \frac{2z_0}{c} - \frac{2kd_w}{c}\right) \qquad (2)$$

where $p(t) = a(t)e^{j(\omega_0 t + \theta(t))}$ is the analytic transmitted ultrasound pulse, R_{tw} is the reflection coefficient, and d_w is the vessel wall thickness. In (2), R_{tw} represents the tissue-wall reflection coefficient and a_k is a function of the wall-tissue reflection and transmission coefficients. The reflection coefficients are typically small (e.g. < 10%) and the series in (2) is practically 2 to 4 terms for each layer. Unfortunately, the reverberation terms interfere with the echo components from the blood in the vessel. Despite their rapid decay, their amplitude remains high enough to mask the echoes from the blood in a region that extends several millimeters inside the vessel. A dereverberation filter can be used to unmask the echoes from the blood and allow the two-dimensional speckle tracking to estimate vector velocity inside the vessel.

Inverse Filter Design for Echo Dereverberation

[0158] The correlation function of the coherent echo component exhibits secondary peaks at $\tau_k = 2kdw/c$. The amplitude of these peaks diminishes exponentially with k (due to multiple reflection within the wall). These secondary peaks can be estimated from the autocorrelation function of the echo data after baseband conversion. Results from actual vascular imaging experiments suggest that a Gaussian mixture model (GMM) may be most appropriate for modeling the probability density function (pdf) of the clean echo data. The GMM is also motivated by a number of hypotheses on the scattering by blood (e.g. due to flow or red blood cell aggregation). An infinite impulse response (IIR) model is assumed for the dereverberation inverse filter

$$y[n] = x[n] - \sum_{k=1}^{N} a_k y[n-k] \qquad (3)$$

[0159] The coefficients, $\{a_k\}_{k=1}^{N}$ can be obtained by maximizing the log-likelihood with respect to the GMMs in the flow channel:

$$\mathscr{L} = \frac{1}{N_y} \sum_{n=n_0}^{n_0+N_y-1} \log\left(\sum_{i=1}^{N_g} \frac{w_i}{\sqrt{2\pi\sigma_i^2}} \exp\left(-\frac{(y[n]-\mu_i)^2}{2\sigma_i^2} \right) \right), \qquad (4)$$

where N_g is the number of Gaussian densities in the GMM (each represented by $\{w_i;\mu_i, \sigma_i\}$) and N_y is the length of output test sequence. The parameters of the IIR inverse filter can be obtained by maximizing $\mathscr{L}$ in (4) by partial derivatives with respect to $\{a_k\}_{k=1}^{N-1}$,

$$\frac{\partial \mathscr{L}}{\partial a_k} = \frac{1}{N_y} \sum_{n=n_0}^{n_0+N_y-1} \sum_{i=1}^{N_g} \frac{\mathscr{E}_{i,n}}{\mathscr{E}_n} \frac{(y[n]-\mu_i)y[n-k]}{\sigma_i^2} \qquad (5)$$

where $\varepsilon_{i,n}$ and ε_n are the ith term inside the inner summation in (4) and the inner summation, respectively. The parameters of the filter can be obtained iteratively through

$$a_k[m+1] = a_k[m] + \delta \frac{\partial \mathscr{L}}{\partial a_k[m]} \qquad (6)$$

where m is the iteration index and d is chosen sufficiently small to allow for fine convergence (at the expense of convergence speed). In at least one embodiment, (5) can be simplified if the GMM is dominated by one distribution, which is often the case. At any rate, an empirical values of δ =0:01 result in convergence within 10 iterations or less.

[0160] Model-order Selection: The parameter N in (3) can be determined from the identification of secondary peaks in the autocorrelation function of the complex envelope of the echo data from the proximal vessel wall and from the vessel including the proximal wall. Periodicities in these correlation functions are identifiable with the wall (and supporting-tissue) architecture, which is primarily responsible for reverberation within the vessel. For the carotid artery of an typical human subject, the order varies depending on the phase of the cardiac cycle with a range of 20 - 45 (lower orders when the vessel wall is maximally stretched). A maximum value, N_{max} on the model order could be set from the observation of the periodicities throughout the heart cycle.

Reverberation-free Training Data

[0161] Obtaining reverberation-free echo data can be accomplished by tilting the imaging transducer to avoid specular reflections from the vessel wall (after identifying the vessel wall). In practice, a very small tilt is sufficient to significantly remove the specular echo and maintain a good view of the vessel. Color flow or power Doppler mode can be used to define the flow region for extracting the training echo data. Once this is achieved, the imaging transducer is returned to a position where the vessel boundaries can be best defined from specular reflections. It is also possible to get reverberation-free data from corrupted views by carefully selecting regions where the reverberation components are not present.

[0162] For example, a blood vessel with 6-mm diameter may provide 2 mm region of reverberation-free echo data at its distal end. One can use the latter approach to identify the GMM during a typical heart cycle. Based on actual echo data from a human subject, the value of N_g in (4) is typically 3 to 4, all with zero mean.

Time-varying Filter Design Algorithm

[0163] Based on the above derivation and facts about the data acquisition model for beamformed echo data from typical vascular imaging ultrasound, the following filter design steps are provided. For image line 1 and image frame p,

Step 0 Detect the proximal vessel wall from complex envelope data.

Step 1 Determine the IIR model order, N, from the short range and long-range correlation functions.

Step 2 Determine the GMM parameters from the reverberation free segment of the vessel echo data.

Step 3 Determine the filter coefficients using the maximum likelihood algorithm (Equations 4 - 6).

Step 4 Apply the IIR filter to vessel data with appropriate initial conditions to avoid breaks in the echo data.

Step 5 Compute long-range correlation function on y[n]. If reverberation still detectable, While $N < N_{max}$ GoTo Step 3. Otherwise Stop.

Results and Discussion regarding Example:

[0164] Data Collection - The Sonix RP was used to collect M2D mode data from imaging the right carotid artery of a healthy volunteer. Real-time beamformed RF data was collected at a frame rate of 325 fps and processed off-line to produce images similar to those shown in Figures 16A-16B, which shows lateral (Figure 16A) and axial displacements (Figure 16B) of the carotid artery coded (in color or gray scale) and overlaid on the B-mode gray scale images. The displacement fields were estimated using the phase coupled two-dimensional speckle tracking algorithm described in Ebbini 2006.

[0165] Approximately 1.9 seconds (642 frames) of data was acquired capturing more than three heart cycles to allow for modeling the dynamics of echoes and reverberation from the vessel, primarily due to the proximal wall. Spatio-temporal maps of the echoes from the vessel (proximal wall through the vessel, but excluding the distal wall) are shown in Figure 17A. The image shows the envelope of the RF data from one image line (approximately at the center of the images). This is referred to as M-mode ultrasound and it allows for the analysis of wall motion in cardiac and vascular imaging application.

[0166] Figure 17B shows an M-mode image of the echoes from the proximal wall only during the acquisition period. The image illustrates the dynamics of the wall echoes during the heart cycle. For example, for the first few lines ($0 < t < 0{:}1$s), the wall represents a purely specular reflector. On the other hand, the wall echo appears less organized when the wall undergoes expansion due to pressure changes in the vessel. Examining the envelope in the vessel shown in Figure 17A, one can see a strong reverberation pattern down to about 4 mm into the vessel. This pattern masks any scattering from the blood and makes it difficult, if not impossible, to estimate the flow velocity vectors in a large region within the vessel.

[0167] Figures 18A-18B show spatio-temporal maps of normalized correlation function of the complex envelope from the vessel including the proximal wall (Figure 18A - a long range correlation) and proximal wall only (Figures 18B - a short range correlation) corresponding to the M-mode images shown in Figures 17A-17B. One can see the strong secondary peaks at $\approx \pm 0{:}8$ mm when the vessel wall is not stretched and behaves as a specular reflector. On the other hand, this peak is diminished and the main lobe of the correlation function is broadened when the vessel wall is stretched. This result demonstrates that a time-varying dereverberation filter will be beneficial.

[0168] Figures 19A-19D illustrate the performance of the dereverberation filters obtained through the proposed maximum likelihood algorithm. Using short-range and long-range correlation data, the filter order was determined to be 21 for two frames (Frame 1 at $t = 0.003$ s and Frame 100 at $t = 0.31$ sec). The GMM models were estimated from the vessel data near the distal wall using $N_g = 3$. $N_y = 50$ was used in both cases and $\delta = 0{:}005$. Convergence was achieved in 7 and 9 iterations for Frame 1 and Frame 100 data, respectively. The magnitude response of both filters demonstrate inverse filtering and dereverberation characteristics; signal bandwidth 2 - 6 MHz is inverted and ripple throughout. Figures 19A-19D represent the dereverberation filters and vessel data with and without filtering for Filter Frame 1 (Figures 19A-19B) and Filter Frame 100 (Figures 19C-19D) (the filtered signals generally being closer to 0 line axis than the original).

[0169] Results from vascular imaging experiment from a healthy volunteer demonstrate the feasibility of dereverberation of echo data from blood vessels using time-varying inverse dereverberation filters to account for the time-varying nature of the reverberation components during the heart cycle. Such filtering may for more accurate vector velocity estimation in the vessel using speckle tracking (e.g., two-dimensional speckle tracking) methods. The exemplary algorithm is robust and computationally efficient and requires minimal training making it well-suited for real-time ultrasound

imaging applications.

[0170] The following provides one or more implementations of vascular imaging and characterization of vessel wall dynamics or examples testing the same, such as generally described herein. Such specific implementations or examples are not to be taken as being limiting to the present disclosure.

[0171] Generally, a method for simultaneous imaging of tissue motion and flow with subsample accuracy in both axial and lateral directions is illustrated. The method utilizes a phase-coupled 2D speckle tracking approach, which employs the true 2D complex cross correlation to find sub-pixel displacements in both axial and lateral directions. The imaging sequence on a Sonix RP scanner has been modified to allow high frame rate 2D data collection in a limited field of view covering the region of interest (M2D-mode). Together with the robust 2D speckle tracking method, M2D imaging allows for capturing the full dynamics of the flow and wall/tissue motion, even when the flow is primarily in the lateral direction (with respect to the imaging beam). The fine vector displacement estimates in both axial and lateral directions are shown to allow for smooth and contiguous strain and shear strain calculations with minimal filtering. The quality of the displacement and strain fields is demonstrated by experimental results from a flow phantom (ATS Model 524) and *in vivo* images of the carotid artery in a healthy volunteer. The results demonstrate simultaneous imaging of the vector flow field and the wall/tissue motion and the corresponding strains at high spatial and temporal sampling. This may provide an essential tool in modeling the fluid-solid interactions between the blood and blood vessel.

Materials and Methods for an Exemplary Imaging Method

[0172] Phase-Coupled 2D Speckle Tracking - The phase-coupled 2D speckle tracking algorithm used is described in Ebbini 2006 and also at least partially described herein. The speckle tracking method is based on the gradients of the magnitude and phase of 2D complex correlation in a search region. This approach couples the phase and magnitude gradients near the correlation peak to determine its coordinates with subsample accuracy in both axial and lateral directions. This is achieved with a minimum level of lateral interpolation determined from the angles between the magnitude and phase gradient vectors on the sampled (laterally interpolated) 2D cross-correlation grid. One result behind this algorithm is that the magnitude gradient vectors' final approach to the true peak is orthogonal to the zero-phase contour. This leads to a 2D robust projection on the zero-phase contour that results in subsample accuracy at interpolation levels well below those needed using previously proposed methods. It is shown that estimated 2D vector displacement fields obtained using the phase-coupled technique display a full range of values covering the dynamic range without evidence of quantization. In comparison, a previously published method using 1D phase-projection after lateral interpolation produces severely quantized lateral displacement fields (at the same levels of interpolation as the 2D, phase-coupled method).

[0173] Data Acquisition - A Sonix RP (Ultrasonix, Canada) ultrasound scanner loaded with a program used for high frame-rate M2D pulse-echo data collection is used. Collected data is then streamlined to a controller PC through Gigabit Ethernet for real-time data processing. The data processing computer can easily handle the intensive computations required by high resolution (both spatial and temporal) speckle tracking and separable 2D post filtering by utilizing a many core GPU (nVIDIA, Santa Clara, CA). A linear array probe (LA14-5/38) was used to acquire all data shown in this paper. The center frequency of the transmit pulse on the probe was 7.5 MHz.

[0174] Experiments using the ATS Model 524 flow phantom and a Cole-Parmer MasterFlex roller pump were conducted to illustrate the displacement tracking in axial and lateral directions. M2D data was collected using the Sonix RP scanner at a frame rate of 111 fps. Images of a 4-mm flow channel in the ATS phantom were collected under controlled fluid flow with an appropriate speed setting of the MasterFlex pump to mimic typical blood flow rates (*e.g.* 336 ml/min) in carotid arteries. Cellulose microspheres were diluted in water to produce linear scattering from the flow channel during data collection (pure water was also imaged as a control to determine the channel boundaries as a ground truth).

[0175] Strain Computation - Strain and shear strain calculations were performed using MATLAB's gradient command on the axial and lateral displacement fields obtained using the 2D speckle tracking algorithm. The strain and shear strain computations are followed by a simple Gaussian lowpass filter with size of 3×3 and standard deviation of 1, i.e. minimal post filtering of the strain and shear strain fields.

Results and Discussion Regarding the Exemplary Imaging Method

Experimental Phantom Result

[0176] The 4-mm flow channel was imaged using the LA14-5 probe with the channel axis perpendicular to the beam axis, i.e. lateral flow. Typical examples of the resulting strain and shear strain fields are shown in Figures 8A-8B and Figures 9A-9B. Figures 8A-8B show axial strain and axial shear strain of the 4-mm flow channel longitudinal walls, respectively. Figures 9A-9B show lateral strain and lateral shear strain of the 4-mm flow channel longitudinal walls, respectively. One can see the smoothness of the strain fields which demonstrates the well-behaved nature of the

displacement fields. At the same time, one can appreciate the clear demarcation between the channel and the surrounding tissue-mimicking material.

[0177] The dynamics of the estimated vector flow field are illustrated by the result in Figure 10 which shows a plot of the periodic channel diameter (dashed lines) (obtained from the axial component at the channel walls computed from the tracked channel wall displacement) and the corresponding average lateral flow velocity in the channel (solid lines) for several cycles of pump operation (i.e., within the 4 mm flow channel in the ATS phantom). The result shows clearly the quasi-periodic nature of the observed flow velocity and the phase relationship between the diameter (pressure in the channel) and flow. Note that the small negative component in the flow velocity occurs right after the diameter reaches its maximum value (i.e. minimum pressure in the channel). This "back up" of the fluid in the channel was easily observed in B-mode movies, but the wall motion was much more subtle (< 150mm) and was only seen in the axial displacement field.

[0178] The dynamic behavior of the lateral flow along the axis of the imaging beam (at a lateral distance of -3.2 mm) is illustrated by Figure 11. One can see the smooth, well-behaved nature of the lateral displacement fields consistent with the quasi-periodic pattern shown in Figure 10. It is noted that the results shown in Figure 11 are minimally processed, i.e., the continuity and the high SNR of the vector displacement estimation in the fluid and the surrounding tissue is a direct consequence of the proper application of the phase-coupled 2D speckle tracking method.

In Vivo Experiment

[0179] A segment of the carotid artery of a healthy volunteer was imaged using the LA14-5 probe at 111 fps. As in the phantom case, the axial and lateral displacement fields were contiguous throughout the region of interest and allowed for the computation of the strain and shear strain fields shown in Figures 12A-12B and Figures 13A-13B. Figures 12A-12B show axial strain and axial shear strain of the carotid artery longitudinal vessel walls, respectively. Figures 13A-13B show lateral strain and lateral shear strain of the carotid artery longitudinal vessel walls, respectively. One can see the clear demarcation between the vessel and the wall/perivascular tissue in the axial strain and lateral shear strain images. Also, the pulsation effect can be appreciated from the axial shear strain and lateral strain images. These results demonstrate reliable estimation of the vector motion fields (axial and lateral) and their utility in obtaining realistic strain and shear strain fields.

[0180] Finally, we show a cross sectional view of the strain fields around the carotid artery of a healthy volunteer. The strains and shear strains in both axial and lateral directions are shown in Figures 14A-14B and Figures 15A-15B, respectively. Figures 14A-14B show axial strain and axial shear strain of the carotid artery cross-sectional vessel walls, respectively. Figures 15A-15B show lateral strain and lateral shear strain of the carotid artery cross-sectional vessel walls, respectively. Examining Figures 14A-14B one can observe that the motion in the axial direction produced a strain in the axial direction at the wall (Figure 14A) and a shear component to the lateral direction (Figure 14B). The direction of the strains in this case depicts an expanding vessel. Similarly, the motion in the lateral direction produced a strain in the lateral direction (Figure 15A) and a shear component to the axial direction as in (Figure 15B). Movies of the strain and shear strain fields have showed the dynamics of wall movement clearly (such not presentable in this application). In addition to the wall dynamics, the strain images provide a tool for identifying the boundaries of the vessel in both axial and lateral directions. The latter is generally difficult to determine from B-mode images.

[0181] As a result of the example, a method for imaging the displacement and strain fields in the vicinity of flow channels has been demonstrated experimentally in a flow phantom and *in vivo* imaging of the carotid artery of healthy volunteer. The results show that, at sufficiently high frame rates, speckle tracking methods produce well-behaved displacement estimates of both the tissue motion and flow in the channel. These displacement fields are well suited for strain and shear strain calculations with minimum filtering. Further, it has been demonstrated that time waveforms of flow velocity and pressure to follow the periodic motion of the roller pump in the phantom experiments. Furthermore, the axial wall displacements (indicative of pressure) and average lateral flow velocity in the channel have a clear phase relationship. This indicates that the method used may be useful in obtaining the full dynamic motion fields suitable for use in solid-fluid interface modeling of vascular mechanics.

[0182] This disclosure has been provided with reference to illustrative embodiments and is not meant to be construed in a limiting sense. As described previously, one skilled in the art will recognize that other various illustrative applications may use the techniques as described herein to take advantage of the beneficial characteristics of the apparatus and methods described herein. Various modifications of the illustrative embodiments, as well as additional embodiments of the disclosure, will be apparent upon reference to this description.

Claims

1. An imaging method carried out by using ultrasound transducers (22) and a processing apparatus (12) comprising:

providing ultrasound pulse-echo data (18) of a region in which at least one portion of a blood vessel (50) is located, wherein the pulse-echo data (18) comprises pulse-echo data at a frame rate of at least 100 frames per second, such that measured displacement of the vessel wall (52) defining the at least one portion of the blood vessel (50) and measured average blood flow through the at least one portion of the blood vessel (50) have a quasi-periodic profile over time to allow motion tracking of both the vessel wall (52) and the blood flow simultaneously;
applying speckle tracking (34) to the pulse-echo data to generate strain and shear strain image data for the region in which the at least one portion of the vessel (50) is located, wherein the speckle tracking comprises using multi-dimensional correlation of the pulse-echo data (18) of one or more speckle regions undergoing deformation in the region in which the at least one portion of a blood vessel (50) is located, wherein the multi-dimensional correlation comprises determining a cross-correlation peak for the sampled pulse-echo data based on phase and magnitude gradients of the cross-correlated pulse-echo data (18); and
identifying at least one vessel wall boundary of the region in which at least one portion of a blood vessel (50) is located based on the strain and shear strain image data, and
characterized in that the speckle tracking further comprises modifying a characteristic, such as location, size or shape of at least one of the one or more speckle regions being tracked based on the one or more vessel wall boundaries identified such that the at least one speckle region is entirely within or outside of the vessel wall (50).

2. The method of claim 1, wherein identifying one or more vessel wall boundaries comprises identifying vessel wall boundaries around the entire blood vessel (50).

3. The method of any of claims 1-2, wherein identifying at least one vascular characteristic comprises measuring tissue property within the one or more vessel wall boundaries, or
identifying one or more portions of a plaque architecture adjacent the one or more vessel wall boundaries, or
calculating one or more hemodynamic measurements based on both the motion tracking motion of the vessel wall and the blood flow simultaneously, or
any combination thereof.

4. The method of any of claims 1-3, wherein using multi-dimensional correlation of sampled pulse-echo data of one or more speckle regions comprises using two-dimensional correlation of sampled pulse-echo data of one or more speckle regions.

5. The method of claim 1-4, wherein determining the cross-correlation peak comprises:

coarsely searching the magnitude of the sampled pulse-echo data in a lateral and axial direction to locate a vicinity of the cross-correlation peak within the cross-correlated sampled pulse-echo data;
determining, within the vicinity of the cross-correlation peak, at least two opposing gradient vectors in proximity to the cross-correlation peak;
determining, within the vicinity of the cross-correlation peak, a zero-phase line of the cross-correlated sampled pulse-echo data; and
using the at least two opposing gradient vectors in proximity to the cross-correlation peak and the zero-phase line to estimate the cross-correlation peak.

6. The method of any of claims 1-5, wherein generating strain and shear strain image data for the region in which the at least one portion of the vessel is located using two-dimensional speckle tracking comprises generating at least one of axial strain and axial shear strain image data and/or lateral strain and lateral shear strain image data.

7. The method of any of claims 1-6, wherein providing ultrasound pulse-echo data of a region in which at least one portion of a blood vessel (50) is located comprises using coded excitation.

8. The method of any of claims 1-7, wherein the method further comprises applying a dereverberation filter to the pulse-echo data from one or more speckle regions in the blood to remove echo components in the pulse-echo data due to reflection at the vessel wall (52) when performing speckle tracking of the pulse-echo data from the one or more speckle regions in the blood.

9. A system for vascular imaging (10), comprising:

one or more ultrasound transducers (22), wherein the one or more transducers (22) are configured to deliver

ultrasound energy to a vascular region resulting in pulse-echo data (18) therefrom; and
means for controlling the capture of pulse-echo data at a frame rate of at least 100 frames per second, such that measured displacement of a vessel wall (52) defining at least one portion of a blood vessel (50) in the vascular region and measured average blood flow through the at least one portion of the blood vessel (50) have a quasi-periodic profile over time to allow motion tracking of both the vessel wall (52) and the blood flow simultaneously;
means for applying speckle tracking (34) to the pulse-echo data to generate strain and shear strain image data for the region in which the at least one portion of the vessel (50) is located, wherein the speckle tracking comprises using multi-dimensional correlation of the pulse-echo data (18) of one or more speckle regions undergoing deformation in the region in which the at least one portion of a blood vessel (50) is located, wherein the multi-dimensional correlation comprises determining a cross-correlation peak for the sampled pulse-echo data based on phase and magnitude gradients of the cross-correlated pulse-echo data (18); and
means for identifying at least one vessel wall boundary of the vascular region in which at least one portion of a blood vessel (50) is located based on the strain and shear strain image data,
characterized by means for modifying a characteristic, such as location, size or shape of at least one of the one or more speckle regions being tracked based on the one or more vessel wall boundaries identified such that the at least one speckle region is entirely within or outside of the vessel wall (50) .

10. The system of claim 9, wherein the system further includes therapy means (20) for delivering therapy to a patient based on the identification of the at least one vascular characteristic of the region in which at least one portion of a blood vessel (50) is located.

11. The system of claim 10, wherein the therapy means (20) comprises a system operable to use ultrasonic energy to deliver therapy based on the identification of the at least one vascular characteristic of the region in which at least one portion of a blood vessel (50) is located.

12. The system of any of claims 9-11, wherein the therapy means (20) comprises at least one transducer configured to transmit and receive ultrasonic energy, wherein the at least one transducer is operable to provide ultrasonic energy to deliver therapy based on the identification of the at least one vascular characteristic of the region in which at least one portion of a blood vessel (50) is located and the at least one transducer is operable for use in obtaining the pulse-echo data to generate image data.

13. The system of any of claims 9-12, comprising a processing apparatus (12) employed to carry out the exemplary imaging methods according to any of claims 1 to 8.

Patentansprüche

1. Ein Bildgebungsverfahren, durchgeführt unter Verwendung von Ultraschallköpfen (22) und einem Verarbeitungsgerät (12), umfassend:

Erstellen von Ultraschall-Puls-Echo-Daten (18) einer Region, in der sich wenigstens ein Teilbereich eines Blutgefäßes (50) befindet, wobei die Puls-Echo-Daten (18) Puls-Echo-Daten mit einer Bildfrequenz von wenigstens 100 Bildern pro Sekunde umfassen, in einer Weise, dass die gemessene Dislokation der Gefäßwand (52), welche den wenigstens einen Teilbereich des Blutgefäßes (50) definiert, und die gemessene mittlere Blutströmung durch den wenigstens einen Teilbereich des Blutgefäßes (50) zeitlich gesehen ein quasi-periodisches Profil aufweisen, um eine gleichzeitige Verfolgung der Bewegung der Gefäßwand (52) und der Blutströmung zu ermöglichen;
Anwenden von Speckle Tracking (34) auf die Puls-Echo-Daten, um Strain- und Shear-Strain- bzw. Scherverformungs-Bilddaten der Region, in welcher sich der wenigstens eine Teilbereich des Gefäßes (50) befindet, zu generieren, wobei Speckle Tracking das Verwenden von einer mehrdimensionalen Korrelation der Puls-Echo-Daten (18) von einer oder mehreren Speckle-Regionen, welche eine Deformation in der Region eingehen, in der der wenigstens eine Teilbereich eines Blutgefäßes (50) sich befindet, umfasst, wobei die mehrdimensionale Korrelation das Bestimmen eines Kreuzkorrelationssignals für die aufgenommenen Puls-Echo-Daten basierend auf Phasen- und Größengradienten der kreuzkorrellierten Puls-Echo-Daten (18)umfasst; und
Identifizieren wenigstens einer Gefäßwandgrenze der Region, in welcher sich wenigstens ein Teilbereich eines Blutgefäßes (50) befindet, und zwar basierend auf den Strain- und Shear-Strain-Bilddaten, und
dadurch gekennzeichnet, dass das Speckle Tracking ferner das Modifizieren einer Eigenschaft wie etwa des

Ortes, der Größe oder der Gestalt der wenigstens einen oder der einen oder mehreren Speckle-Regionen, die basierend auf der einen oder mehreren identifizierten Gefäßwandgrenzen verfolgt werden, in einer Weise umfasst, dass sich die wenigstens eine Speckle-Region vollständig innerhalb oder außerhalb der Gefäßwand (50) befindet.

2. Das Verfahren gemäß Anspruch 1, wobei das Identifizieren der einen oder mehreren Gefäßwandgrenzen das Identifizieren der Gefäßwandgrenzen rund um das gesamte Blutgefäß (50) umfasst.

3. Das Verfahren gemäß einem der Ansprüche 1 - 2, wobei das Identifizieren wenigstens einer vaskularen Eigenschaft das Messen der Gewebeeigenschaft innerhalb der einen oder mehreren Gefäßwandgrenzen umfasst,
das Identifizieren eines oder mehrerer Teilbereiche eines an die eine oder an mehrere Gefäßwandgrenzen angrenzenden Plaque-Aufbaus umfasst,
das Berechnen einer oder mehrerer hämodynamischer Messgrößen basierend sowohl auf der Bewegung der Bewegungsverfolgung der Gefäßwand als auch gleichzeitig auf dem Blutstrom, oder
einer Kombination davon.

4. Das Verfahren gemäß einem der Ansprüche 1 - 3, wobei das Verwenden von mehrdimensionaler Korrelation der aufgenommenen Puls-Echo-Daten der einen oder mehreren Speckle-Regionen das Verwenden einer zweidimensionalen Korrelation der aufgenommenen Puls-Echo-Daten der einen oder mehreren Speckle-Regionen umfasst.

5. Das Verfahren gemäß einem der Ansprüche 1 - 4, wobei das Bestimmen des Kreuzkorrelationssignals umfasst:

grobes Suchen der Größe der aufgenommenen Puls-Echo-Daten in einer lateralen und axialen Richtung, um die Nähe des Kreuzkorrelationssignals innerhalb der kreuzkorrelierten aufgenommenen Puls-Echo-Daten zu lokalisieren;
Bestimmen von wenigstens zwei gegenüberliegenden Gradientenvektoren in der Umgebung zu dem Kreuzkorrelationssignal, und zwar innerhalb der Umgebung des Kreuzkorrelationssignals;
Bestimmen einer Nullphasenlinie der kreuzkorrelierten aufgenommen Puls-Echo-Daten, und zwar innerhalb der Umgebung des Kreuzkorrelationssignals; und
Verwenden von wenigstens zwei gegenüberliegenden Gradientenvektoren in der Nähe des kreuzkorrelierten Signals und der Nullphasenlinie, um das Kreuzkorrelationssignal abzuschätzen.

6. Das Verfahren gemäß einem der Ansprüche 1 - 5, wobei das Erzeugen von Strain- und Shear-Strain-Bilddaten für die Region, in der sich der wenigstens eine Teilbereich des Gefäßes befindet, unter Verwendung von zweidimensionalem Speckle-Tracking das Erzeugen wenigstens eines aus axialen Strain- und axialen Shear-Strain-Bilddaten und/oder lateralen Strain- und lateralen Shear-Strain-Bilddaten umfasst.

7. Das Verfahren gemäß einem der Ansprüche 1 - 6, wobei das Erstellen von Ultraschall-Puls-Echo-Daten einer Region, in der sich wenigstens ein Teilbereich eines Blutgefäßes (50) befindet, die Verwendung von kodierter Anregung umfasst.

8. Das Verfahren gemäß einem der Ansprüche 1 - 7, wobei das Verfahren ferner die Anwendung eines Hallunterdrückungsfilters ("*dereverberation filter*") auf die Puls-Echo-Daten aus einer oder mehreren Speckle-Regionen in dem Blut umfasst, um die Echokomponenten in den Puls-Echo-Daten aufgrund der Reflexion an der Gefäßwand (52) während der Durchführung des Speckle Trackings der Puls-Echo-Daten aus den einen oder mehreren Speckle-Regionen in dem Blut zu entfernen.

9. Ein System zur vaskulären Bildgebung (10), umfassend:

einen oder mehrere Ultraschallköpfe (22), wobei der eine oder die mehreren Ultraschallköpfe (22) derart ausgestaltet sind, dass sie Ultraschallenergie an eine vaskuläre Region abgeben, wobei sich Puls-Echo-Daten (18) daraus ergeben; und
Einrichtungen zur Steuerung der Erfassung von Puls-Echo-Daten mit einer Bildfrequenz von wenigstens 100 Bildern pro Sekunde, und zwar in einer Weise, dass die gemessene Dislokation der Gefäßwand (52), welche den wenigstens einen Teilbereich des Blutgefäßes (50) in der vaskulären Region definiert, und die gemessene mittlere Blutströmung durch den wenigstens einen Teilbereich des Blutgefäßes (50) zeitlich gesehen ein quasiperiodisches Profil aufweisen, um eine gleichzeitige Verfolgung der Bewegung der Gefäßwand (52) und der Blutströmung zu ermöglichen;

Einrichtungen zur Anwendung von Speckle Tracking (34) auf die Puls-Echo-Daten, um Strain- und Shear-Strain- bzw. Scherverformungs-Bilddaten der Region, in welcher sich der wenigstens eine Teilbereich des Gefäßes (50) befindet, zu generieren, wobei Speckle Tracking das Verwenden einer mehrdimensionalen Korrelation der Puls-Echo-Daten (18) von einer oder mehreren Speckle-Regionen, welche eine Deformation in der Region eingehen, in der der wenigstens eine Teilbereich eines Blutgefäßes (50) sich befindet, umfasst, wobei die mehrdimensionale Korrelation das Bestimmen eines Kreuzkorrelationssignals für die aufgenommenen Puls-Echo-Daten basierend auf Phasen- und Größengradienten der kreuzkorrellierten Puls-Echo-Daten (18) umfasst; und

Einrichtungen zur Identifizierung wenigstens einer Gefäßwandgrenze der vaskulären Region, in welcher sich wenigstens ein Teilbereich eines Blutgefäßes (50) befindet, und zwar basierend auf den Strain- und Shear-Strain-Bilddaten, und

gekennzeichnet durch Einrichtungen für eine Modifizierung einer Eigenschaft wie etwa des Ortes, der Größe oder der Gestalt der wenigstens einen oder der einen oder mehreren Speckle-Regionen, die basierend auf der einen oder mehreren identifizierten Gefäßwandgrenzen verfolgt werden, so dass sich die wenigstens eine Speckle-Region vollständig innerhalb oder außerhalb der Gefäßwand (50) befindet.

10. Das System gemäß Anspruch 9, wobei das System ferner eine Therapieeinrichtung (20) für die Durchführung einer Therapie an einem Patienten umfasst, basierend auf der Identifizierung der wenigstens einen vaskularen Eigenschaft der Region, in welcher sich der wenigstens eine Teilbereich eines Blutgefäßes (50) befindet.

11. Das System gemäß Anspruch 10, wobei die Therapieeinrichtung (20) ein System umfasst, das zur Verwendung von Ultraschallenergie für die Durchführung einer Therapie, basierend auf der Identifizierung der wenigstens einen vaskularen Eigenschaft der Region, in welcher sich der wenigstens eine Teilbereich eines Blutgefäßes (50) befindet, funktionsbereit ist.

12. Das System gemäß einem der Ansprüche 9 - 11, wobei die Therapieeinrichtung (20) wenigstens einen Schallkopf umfasst, der zur Aussendung und zum Empfang der Ultraschallenergie angepasst ist, wobei der wenigstens eine Schallkopf zur Bereitstellung von Ultraschallenergie für die Durchführung einer Therapie, basierend auf der Identifizierung der wenigstens einen vaskularen Eigenschaft der Region, in welcher sich der wenigstens eine Teilbereich eines Blutgefäßes (50) befindet, funktionsbereit ist und der wenigstens eine Schallkopf für die Aufnahme der Puls-Echo-Daten zur Erzeugung von Bilddaten funktionsbereit ist.

13. Das System gemäß einem der Ansprüche 9 - 12, umfassend ein Verarbeitungsgerät (12), das zur Durchführung der exemplarischen Bildgebungsverfahren gemäß einem der Ansprüche 1 bis 8 verwendet wird.

Revendications

1. Procédé d'imagerie effectué par utilisation de transducteurs ultrasonores (22) et d'un appareil de traitement (12) comprenant :

fournir des données d'écho d'impulsion ultrasonore (18) d'une région dans laquelle au moins une partie d'un vaisseau sanguin (50) est située, les données d'écho d'impulsion (18) comprenant des données d'écho d'impulsion à une fréquence d'image d'au moins 100 images par seconde, de telle sorte qu'un déplacement mesuré de la paroi de vaisseau (52) définissant ladite au moins une partie du vaisseau sanguin (50) et le flux sanguin moyen mesuré à travers ladite au moins une partie du vaisseau sanguin (50) ont un profil quasi-périodique au cours du temps pour permettre un suivi de mouvement à la fois de la paroi de vaisseau (52) et du flux sanguin simultanément ;

appliquer un suivi de speckle (34) aux données d'écho d'impulsion pour générer des données d'image de déformation et de déformation de cisaillement pour la région dans laquelle ladite au moins une partie du vaisseau (50) est située, le suivi de speckle comprenant l'utilisation d'une corrélation multi-dimensionnelle des données d'écho d'impulsion (18) d'une ou plusieurs régions à speckle subissant une déformation dans la région dans laquelle ladite au moins une partie d'un vaisseau sanguin (50) est située, la corrélation multi-dimensionnelle comprenant la détermination d'un pic d'intercorrélation pour les données d'écho d'impulsion échantillonnées sur la base de gradients de phase et d'amplitude des données d'écho d'impulsion intercorrélées (18) ; et

identifier au moins une limite de paroi de vaisseau de la région dans laquelle au moins une partie d'un vaisseau sanguin (50) est située sur la base des données d'image de déformation et de déformation de cisaillement, et **caractérisé par le fait que** le suivi de speckle comprend en outre la modification d'une caractéristique, telle

que l'emplacement, la dimension ou la forme d'au moins l'une de la ou des régions à speckle qui sont suivies sur la base de la ou des limites de paroi de vaisseau identifiées de telle sorte que ladite au moins une région à speckle est entièrement à l'intérieur ou à l'extérieur de la paroi de vaisseau (50).

2. Procédé selon la revendication 1, dans lequel l'identification d'une ou plusieurs limites de paroi de vaisseau comprend l'identification des limites de paroi de vaisseau autour du vaisseau sanguin entier (50).

3. Procédé selon l'une quelconque des revendications 1 et 2, dans lequel l'identification d'au moins une caractéristique vasculaire comprend la mesure d'une propriété de tissu à l'intérieur de la ou des limites de paroi de vaisseau, ou l'identification d'une ou plusieurs parties d'une architecture de plaque adjacente à la ou aux limites de paroi de vaisseau, ou
le calcul d'une ou plusieurs mesures hémodynamiques sur la base à la fois du mouvement de suivi de mouvement de la paroi de vaisseau et du flux sanguin simultanément, ou
toute combinaison de ceux-ci.

4. Procédé selon l'une quelconque des revendications 1 à 3, dans lequel l'utilisation d'une corrélation multi-dimensionnelle de données d'écho d'impulsion échantillonnées d'une ou plusieurs régions à speckle comprend l'utilisation de la corrélation bidimensionnelle de données d'écho d'impulsion échantillonnées d'une ou plusieurs régions à speckle.

5. Procédé selon l'une des revendications 1 à 4, dans lequel la détermination du pic d'intercorrélation comprend :

rechercher de manière grossière l'amplitude des données d'écho d'impulsion échantillonnées dans une direction latérale et axiale pour localiser un voisinage du pic d'intercorrélation à l'intérieur des données d'écho d'impulsion échantillonnées intercorrélées ;
déterminer, à l'intérieur du voisinage du pic d'intercorrélation, au moins deux vecteurs de gradient opposés à proximité du pic d'intercorrélation ;
déterminer, à l'intérieur du voisinage du pic d'intercorrélation, une ligne de phase nulle des données d'écho d'impulsion échantillonnées intercorrélées ; et
utiliser lesdits au moins deux vecteurs de gradient opposés à proximité du pic d'intercorrélation et de la ligne de phase nulle pour estimer le pic d'intercorrélation.

6. Procédé selon l'une quelconque des revendications 1 à 5, dans lequel la génération de données d'image de déformation et de déformation de cisaillement pour la région dans laquelle ladite au moins une partie du vaisseau est située à l'aide du suivi de speckle bidimensionnel comprend la génération d'au moins l'une de données d'image de déformation axiale et de déformation de cisaillement axiale et/ou de données d'image de déformation latérale et de déformation de cisaillement latérale.

7. Procédé selon l'une quelconque des revendications 1 à 6, dans lequel la fourniture de données d'écho d'impulsion ultrasonore d'une région dans laquelle au moins une partie d'un vaisseau sanguin (50) est située comprend l'utilisation d'une excitation codée.

8. Procédé selon l'une quelconque des revendications 1 à 7, dans lequel le procédé comprend en outre l'application d'un filtre de déréverbération aux données d'écho d'impulsion à partir d'une ou plusieurs régions à speckle dans le sang pour retirer des composantes d'écho dans les données d'écho d'impulsion dues à une réflexion au niveau de la paroi de vaisseau (52) lors de la réalisation d'un suivi de speckle des données d'écho d'impulsion à partir de la ou des régions à speckle dans le sang.

9. Système pour l'imagerie vasculaire (10), comprenant :

un ou plusieurs transducteurs ultrasonores (22), le ou les transducteurs (22) étant configurés pour délivrer une énergie ultrasonore à une région vasculaire, conduisant à des données d'écho d'impulsion (18) à partir de celle-ci ; et
des moyens pour contrôler la capture de données d'écho d'impulsion à une fréquence d'image d'au moins 100 images par seconde, de telle sorte qu'un déplacement mesuré d'une paroi de vaisseau (52) définissant au moins une partie d'un vaisseau sanguin (50) dans la région vasculaire et un flux sanguin moyen mesuré à travers ladite au moins une partie du vaisseau sanguin (50) ont un profil quasi-périodique au cours du temps pour permettre un suivi de mouvement à la fois de la paroi de vaisseau (52) et du flux sanguin simultanément ;

des moyens pour appliquer un suivi de speckle (34) aux données d'écho d'impulsion pour générer des données d'image de déformation et de déformation de cisaillement pour la région dans laquelle ladite au moins une partie du vaisseau (50) est située, le suivi de speckle comprenant l'utilisation d'une corrélation multi-dimensionnelle des données d'écho d'impulsion (18) d'une ou plusieurs régions à speckle subissant une déformation dans la région dans laquelle ladite au moins une partie d'un vaisseau sanguin (50) est située, la corrélation multi-dimensionnelle comprenant la détermination d'un pic d'intercorrélation pour les données d'écho d'impulsion échantillonnées sur la base de gradients de phase et d'amplitude des données d'écho d'impulsion intercorrélées (18) ; et

des moyens pour identifier au moins une limite de paroi de vaisseau de la région vasculaire dans laquelle au moins une partie d'un vaisseau sanguin (50) est située sur la base des données d'image de déformation et de déformation de cisaillement,

caractérisé par des moyens pour modifier une caractéristique, telle qu'un emplacement, une dimension ou une forme d'au moins l'une de la ou des régions à speckle qui sont suivies sur la base de la ou des limites de paroi de vaisseau identifiées de telle sorte que ladite au moins une région à speckle est entièrement à l'intérieur ou à l'extérieur de la paroi de vaisseau (50).

10. Système selon la revendication 9, dans lequel le système comprend en outre des moyens de thérapie (20) pour délivrer une thérapie à un patient sur la base de l'identification de ladite au moins une caractéristique vasculaire de la région dans laquelle au moins une partie d'un vaisseau sanguin (50) est située.

11. Système selon la revendication 10, dans lequel les moyens de thérapie (20) comprennent un système actionnable pour utiliser l'énergie ultrasonore pour délivrer une thérapie sur la base de l'identification de ladite au moins une caractéristique vasculaire de la région dans laquelle au moins une partie d'un vaisseau sanguin (50) est située.

12. Système selon l'une quelconque des revendications 9 à 11, dans lequel les moyens de thérapie (20) comprennent au moins un transducteur configuré pour émettre et recevoir une énergie ultrasonore, ledit au moins un transducteur étant actionnable pour fournir une énergie ultrasonore pour délivrer une thérapie sur la base de l'identification de ladite au moins une caractéristique vasculaire de la région dans laquelle au moins une partie d'un vaisseau sanguin (50) est située et ledit au moins un transducteur étant actionnable pour une utilisation dans l'obtention des données d'écho d'impulsion pour générer des données d'image.

13. Système selon l'une quelconque des revendications 9 à 12, comprenant un appareil de traitement (12) employé pour effectuer les procédés d'imagerie à titre d'exemples selon l'une quelconque des revendications 1 à 8.

Fig. 1

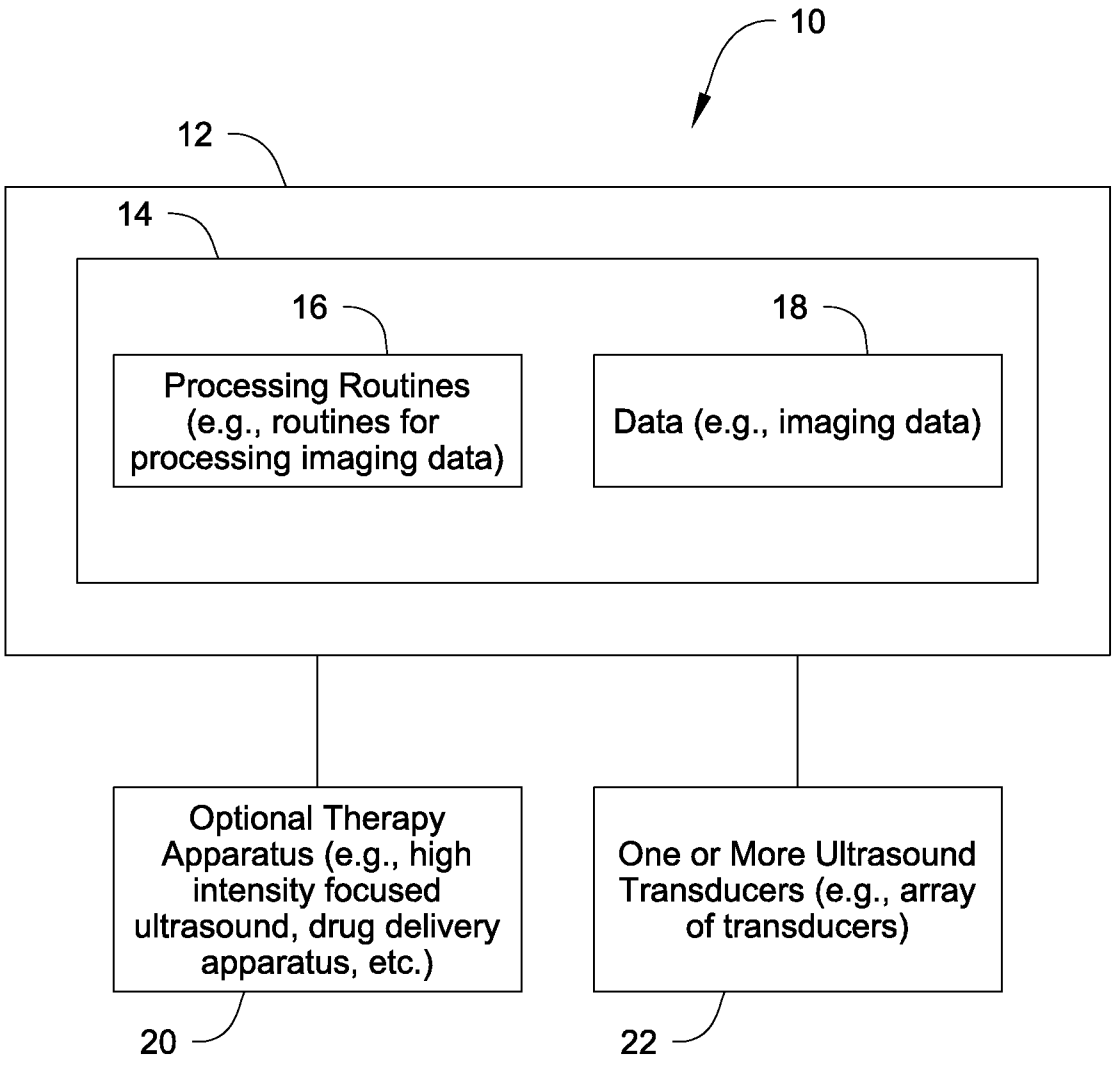
10
12
14
16
Processing Routines (e.g., routines for processing imaging data)
18
Data (e.g., imaging data)
Optional Therapy Apparatus (e.g., high intensity focused ultrasound, drug delivery apparatus, etc.)
One or More Ultrasound Transducers (e.g., array of transducers)
20
22

Fig. 2

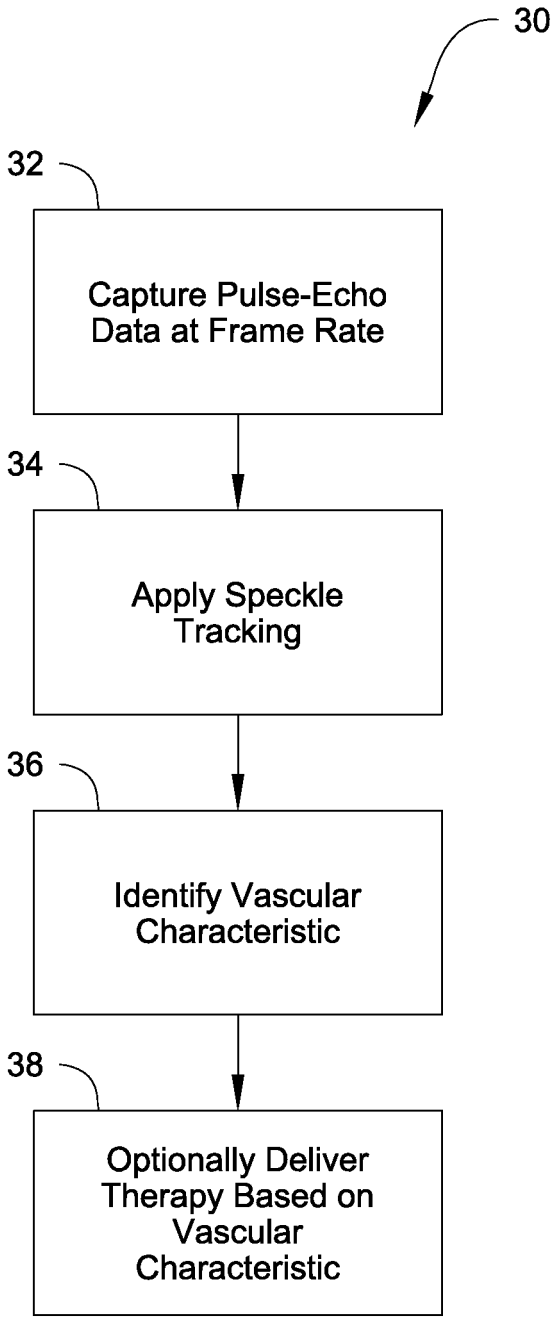
30
32
Capture Pulse-Echo Data at Frame Rate
34
Apply Speckle Tracking
36
Identify Vascular Characteristic
38
Optionally Deliver Therapy Based on Vascular Characteristic

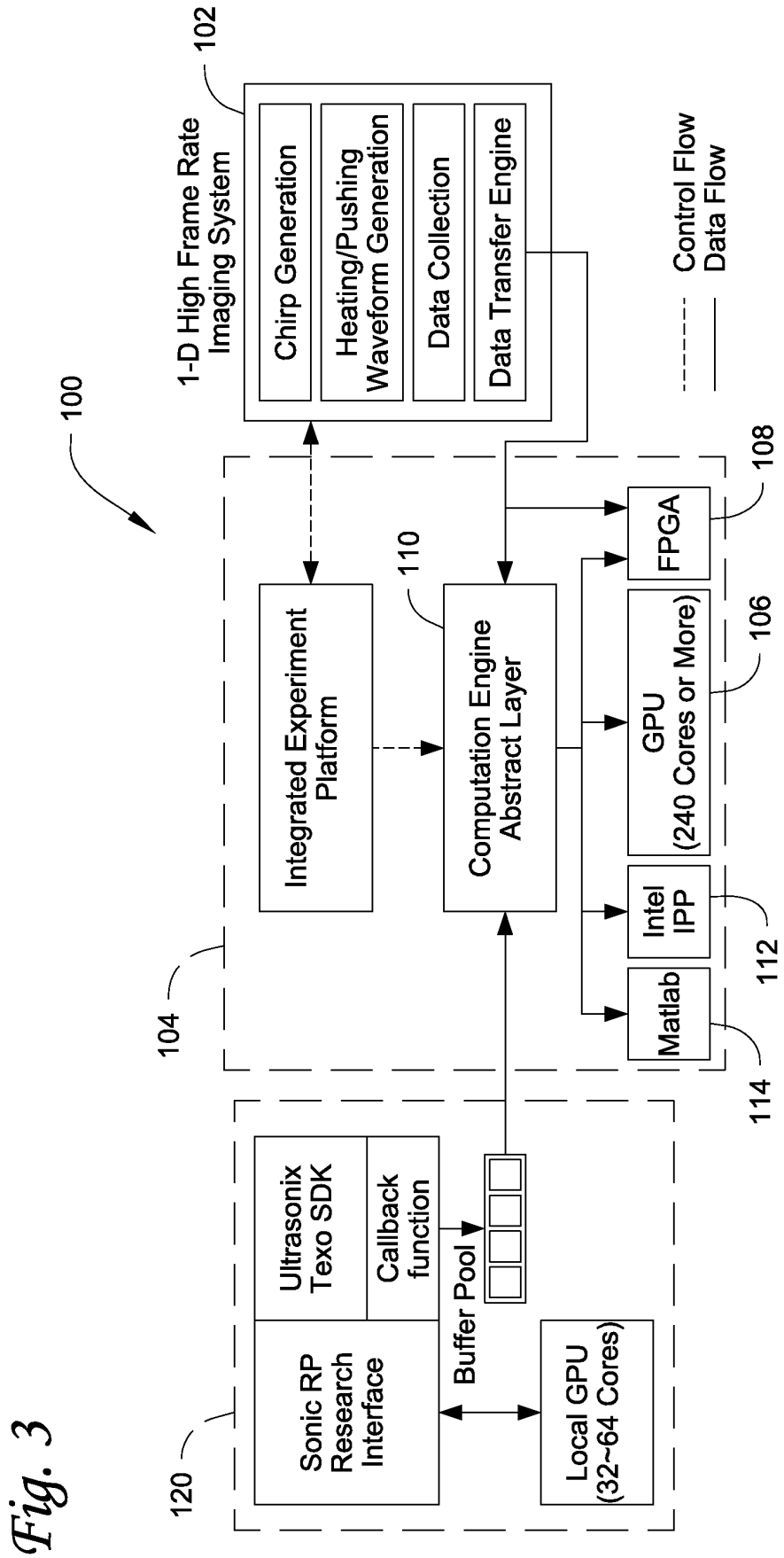
100
102
1-D High Frame Rate Imaging System
Chirp Generation
Heating/Pushing Waveform Generation
Data Collection
Data Transfer Engine
Control Flow
Data Flow
104
Integrated Experiment Platform
110
Computation Engine Abstract Layer
108
FPGA
106
GPU (240 Cores or More)
112
Intel IPP
114
Matlab
120
Sonic RP Research Interface
Ultrasonix Texo SDK
Callback function
Buffer Pool
Local GPU (32~64 Cores)

Fig. 3

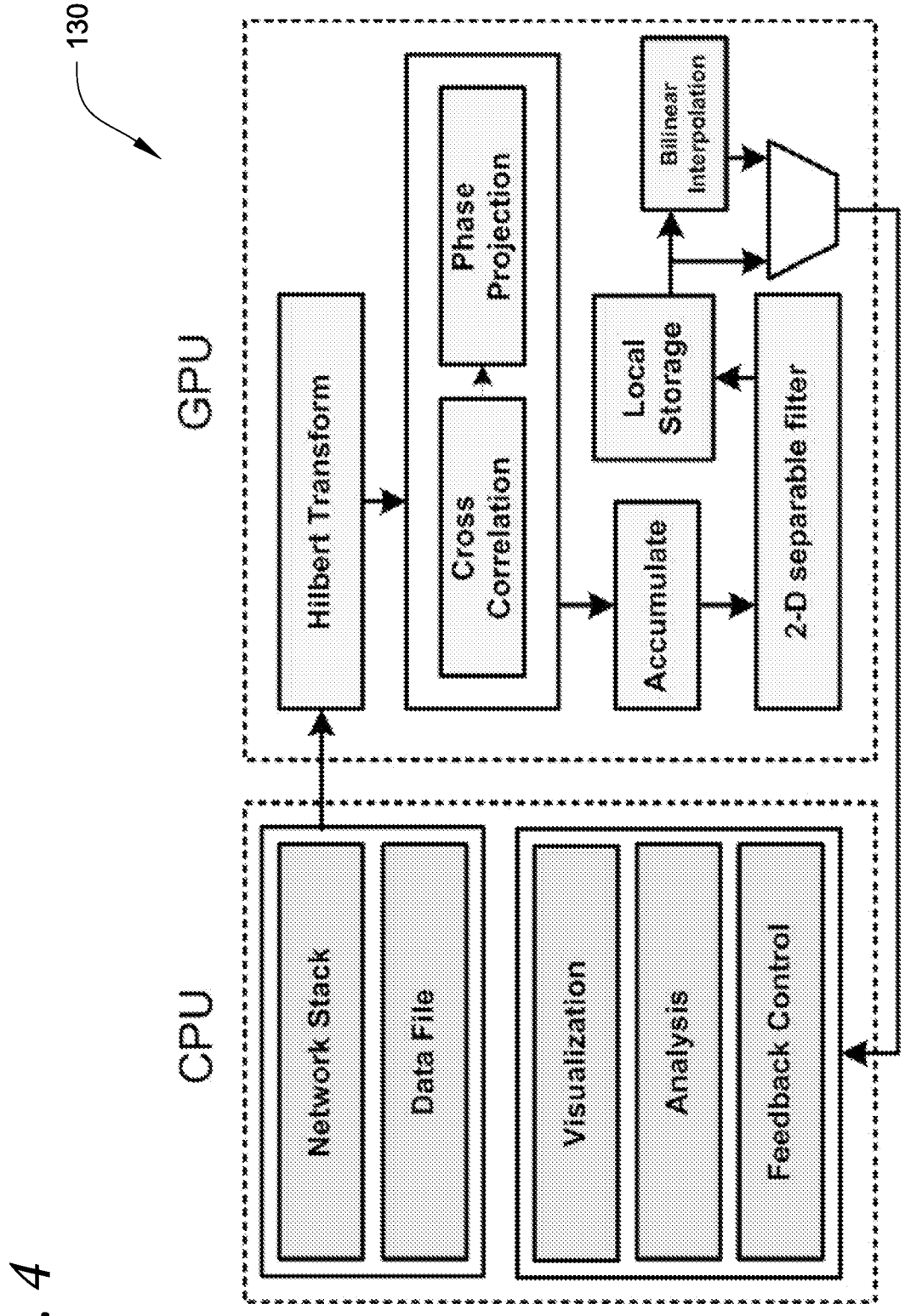
130
GPU
Hilbert Transform
Phase Projection
Cross Correlation
Local Storage
Bilinear Interpolation
Accumulate
2-D separable filter
CPU
Network Stack
Data File
Visualization
Analysis
Feedback Control

Fig. 4

Fig. 5A

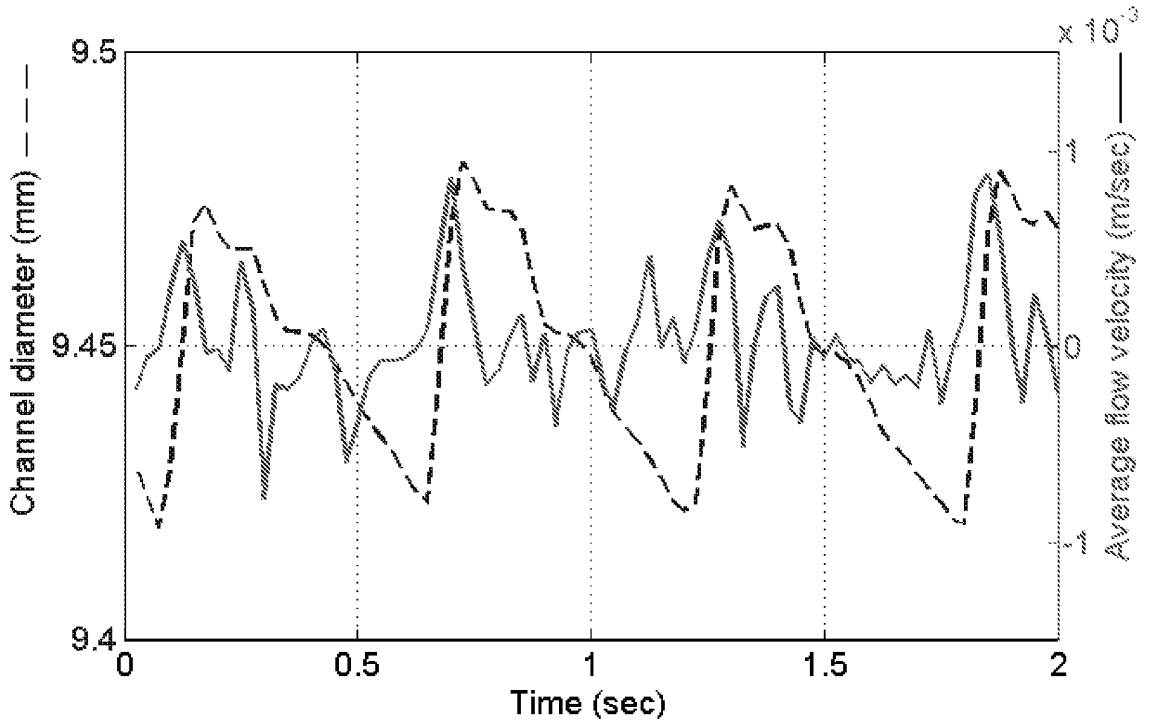
Channel diameter (mm) — — —
Average flow velocity (m/sec) ——
x 10^-3
9.5
9.45
9.4
1
0
-1
0
0.5
1
1.5
2
Time (sec)

Fig. 5B

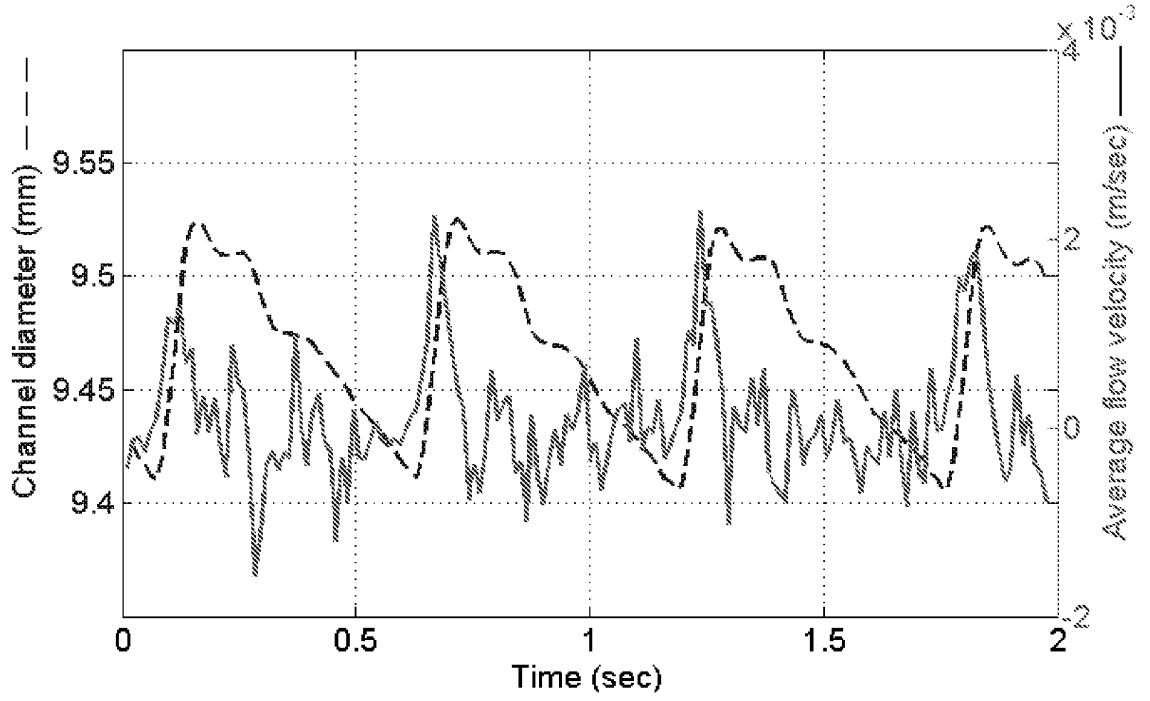
Channel diameter (mm) — — —
Average flow velocity (m/sec) ——
x 10^-3
9.55
9.5
9.45
9.4
4
2
0
-2
0
0.5
1
1.5
2
Time (sec)

Fig. 5C

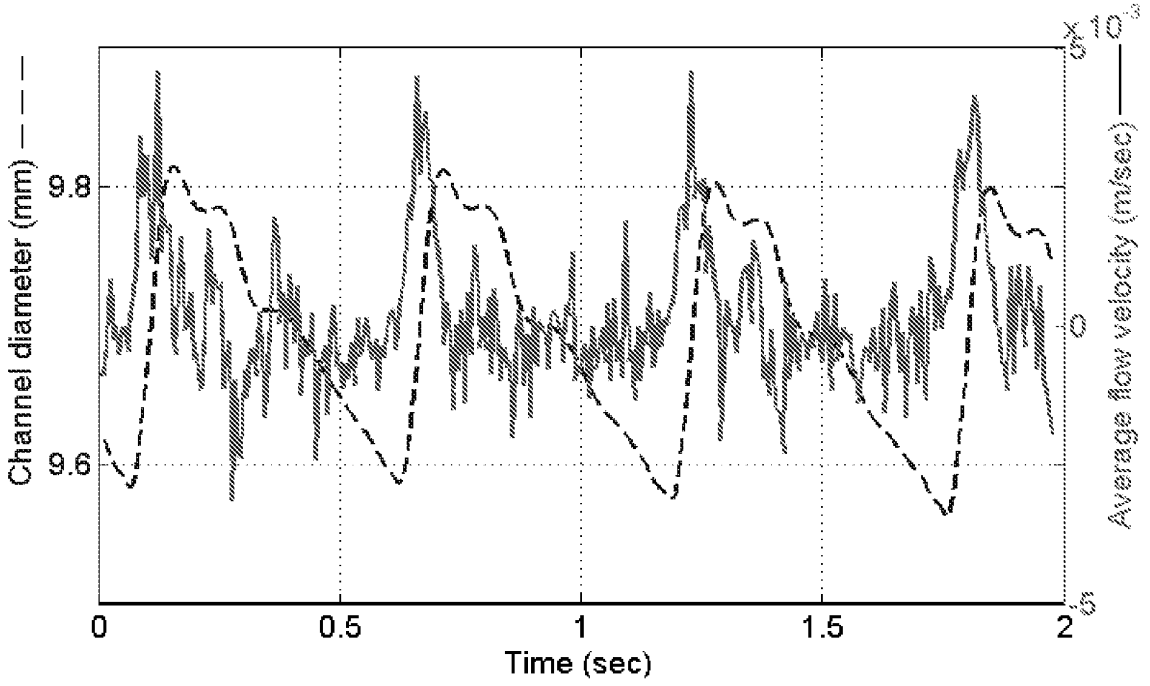
Channel diameter (mm) — — —
9.8
9.6
0
0.5
1
1.5
2
Time (sec)
Average flow velocity (m/sec) ——
0

Fig. 5D

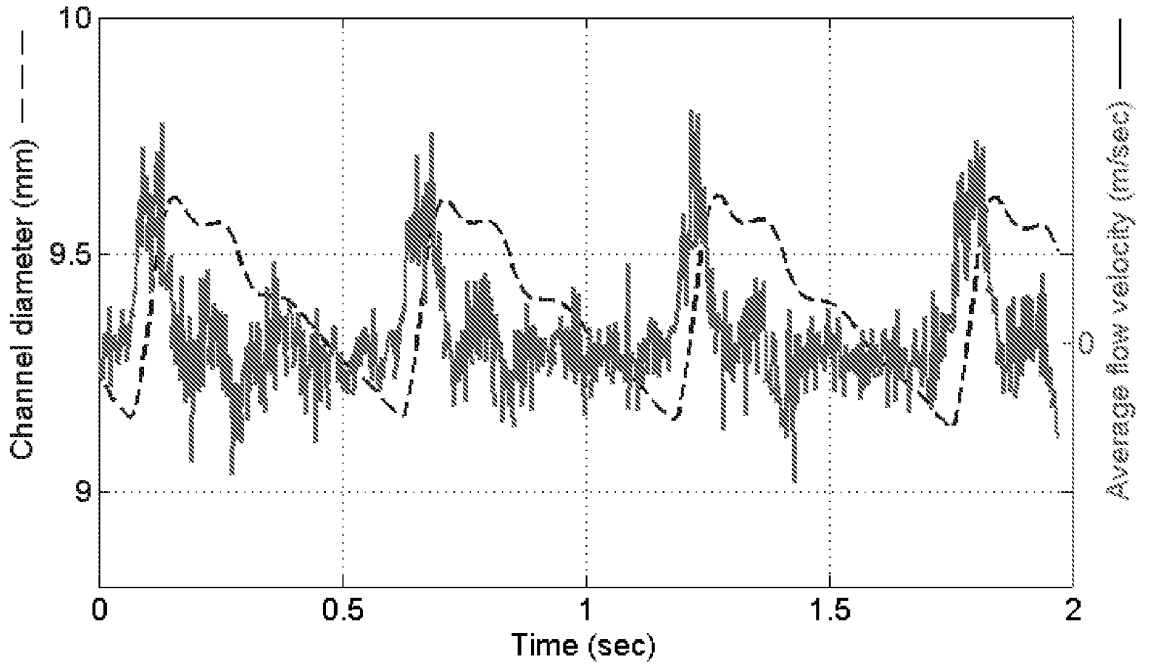
Channel diameter (mm) — — —
10
9.5
9
0
0.5
1
1.5
2
Time (sec)
Average flow velocity (m/sec) ——
0

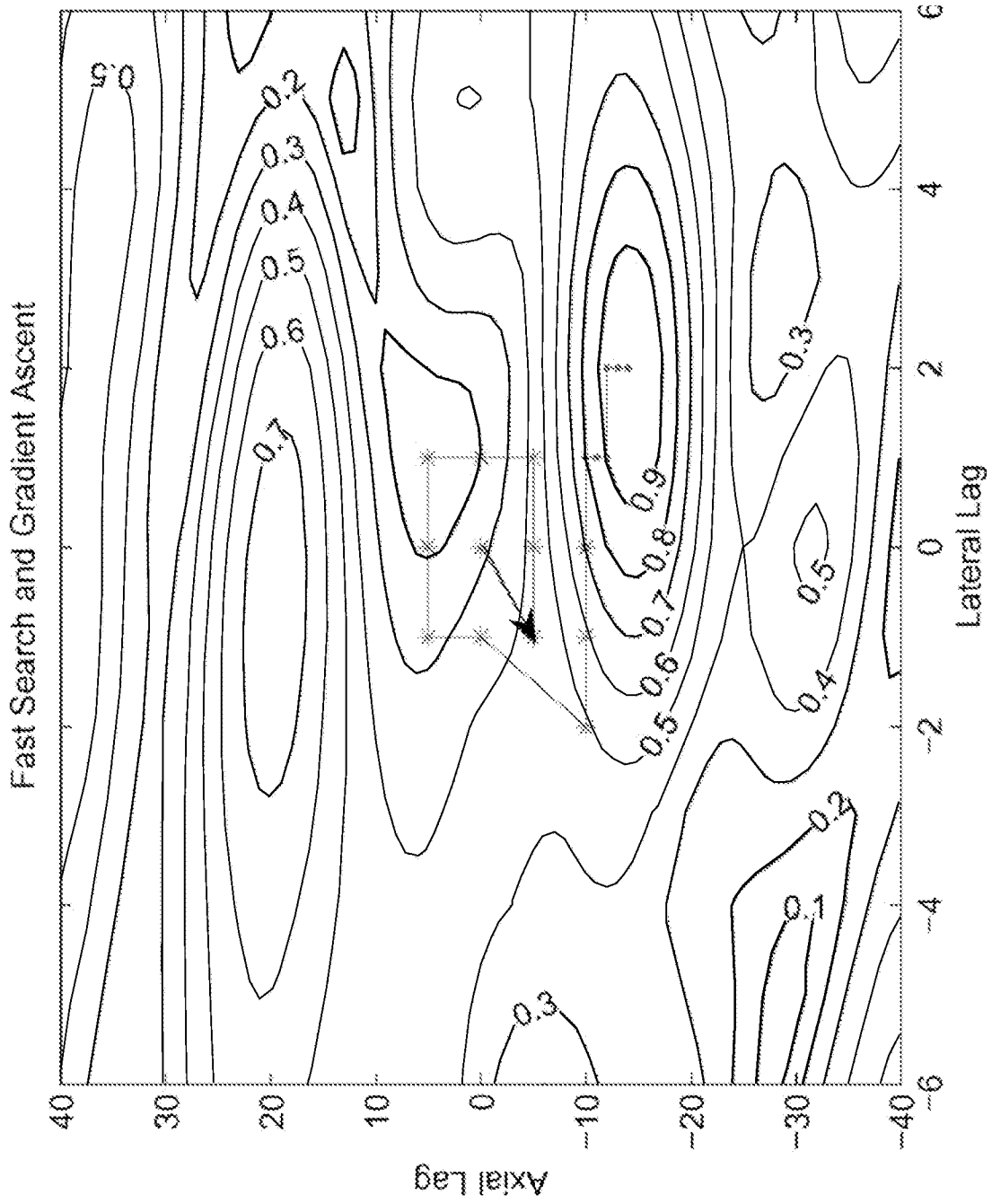
Fast Search and Gradient Ascent
Axial Lag
Lateral Lag
40
30
20
10
0
−10
−20
−30
−40
6
4
2
0
−2
−4
−6
0.5
0.2
0.3
0.4
0.5
0.6
0.7
0.9
0.8
0.7
0.6
0.5
0.4
0.3
0.2
0.1
0.3

Fig. 6A

Fig. 6B

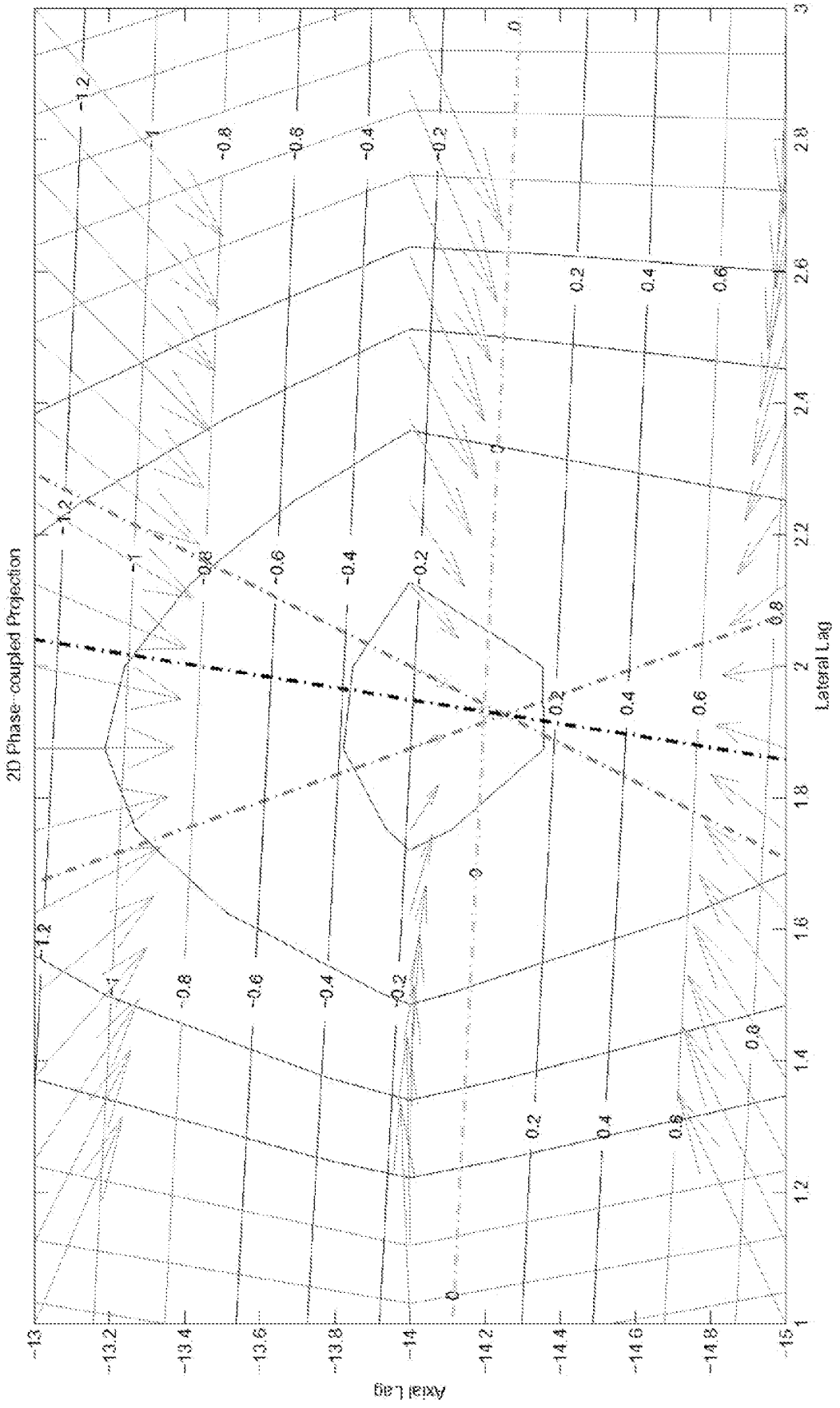

Fig. 7

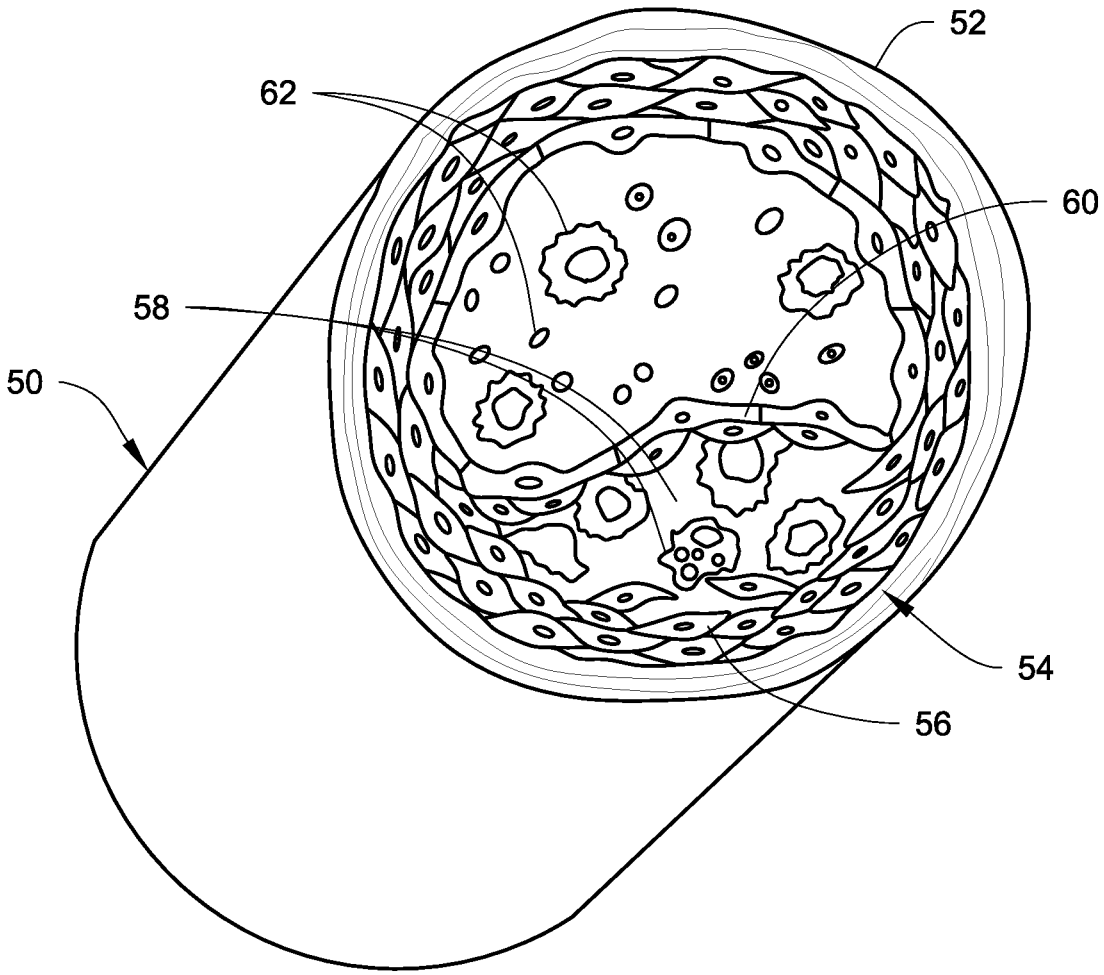

Fig. 8A

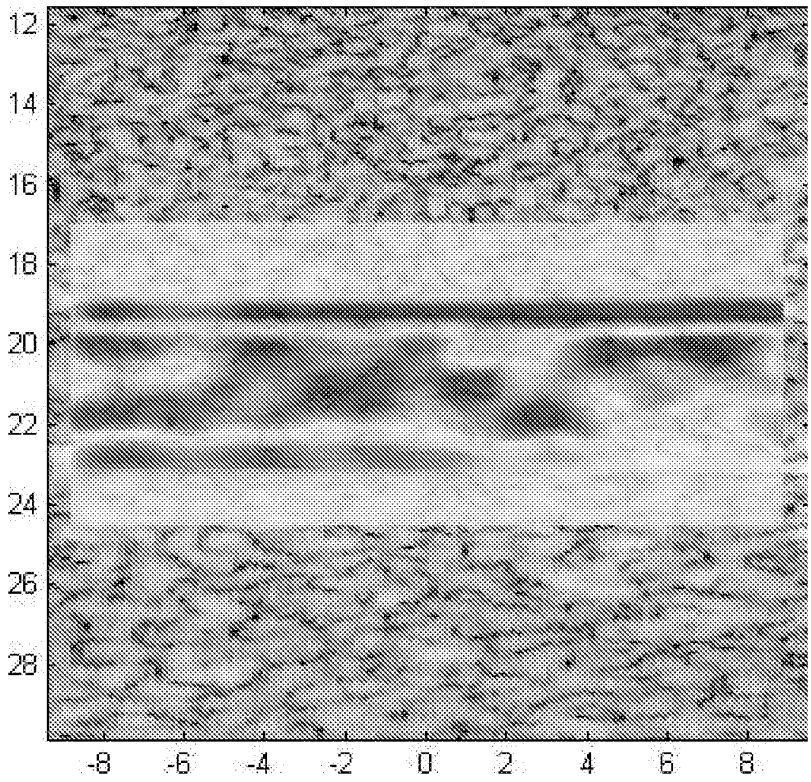
12
14
16
18
20
22
24
26
28
-8
-6
-4
-2
0
2
4
6
8

Fig. 8B

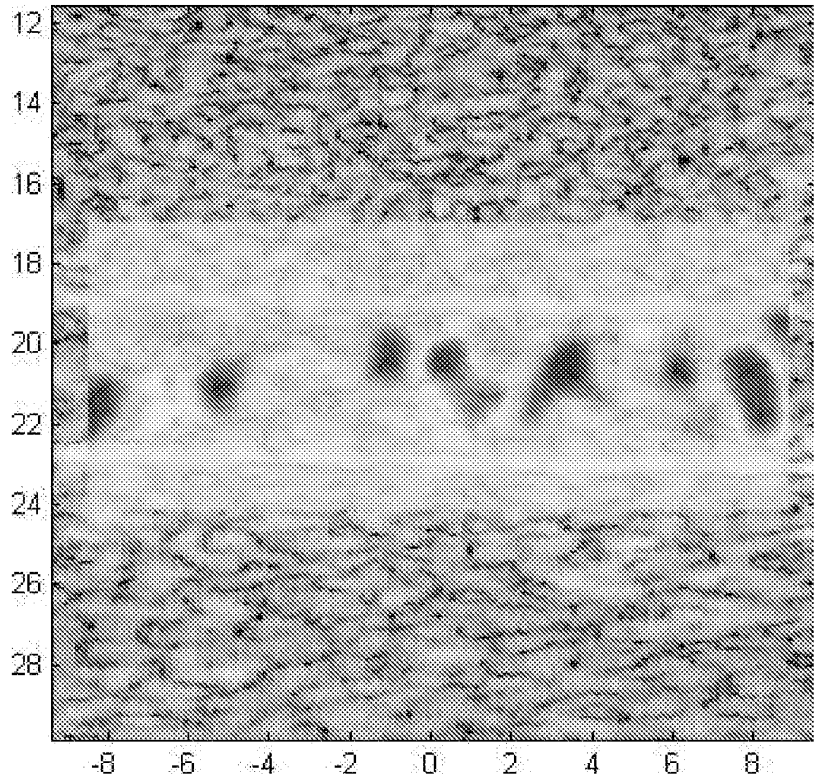
12
14
16
18
20
22
24
26
28
-8
-6
-4
-2
0
2
4
6
8

Fig. 9A

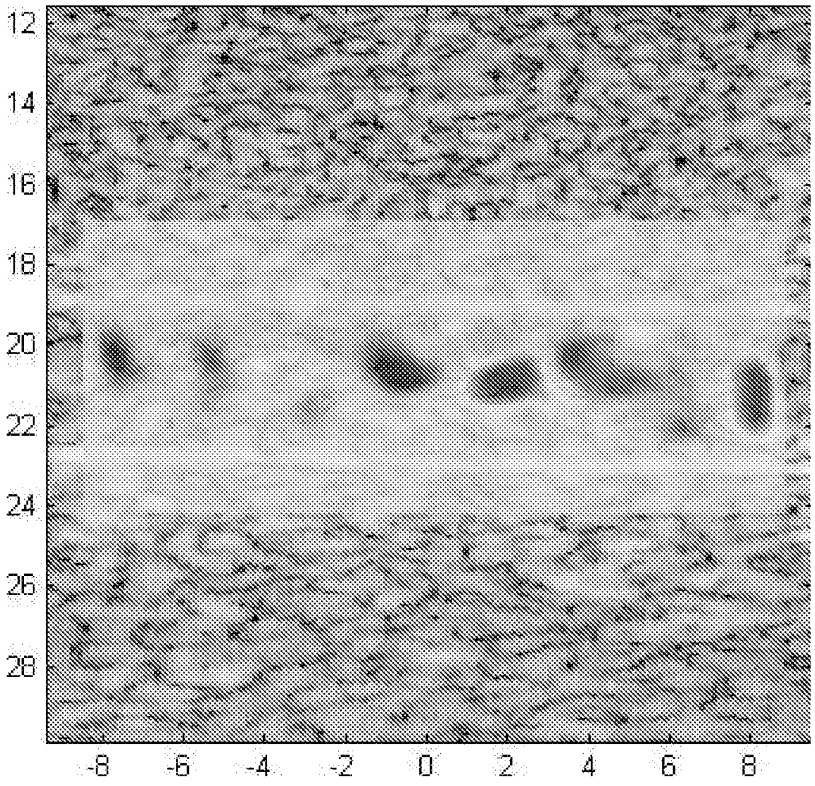
12
14
16
18
20
22
24
26
28
-8
-6
-4
-2
0
2
4
6
8

Fig. 9B

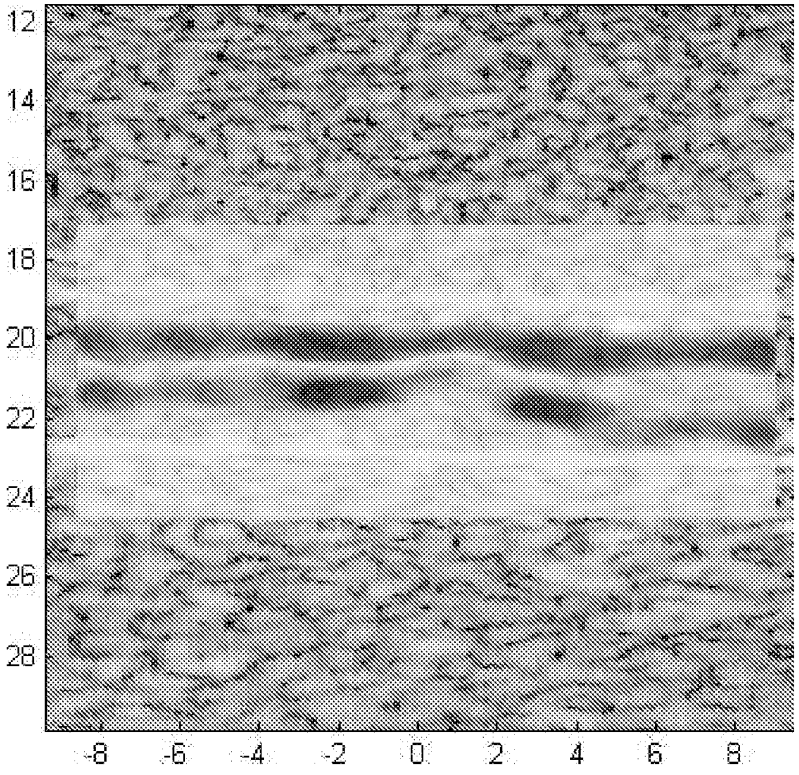
12
14
16
18
20
22
24
26
28
-8
-6
-4
-2
0
2
4
6
8

Fig. 10

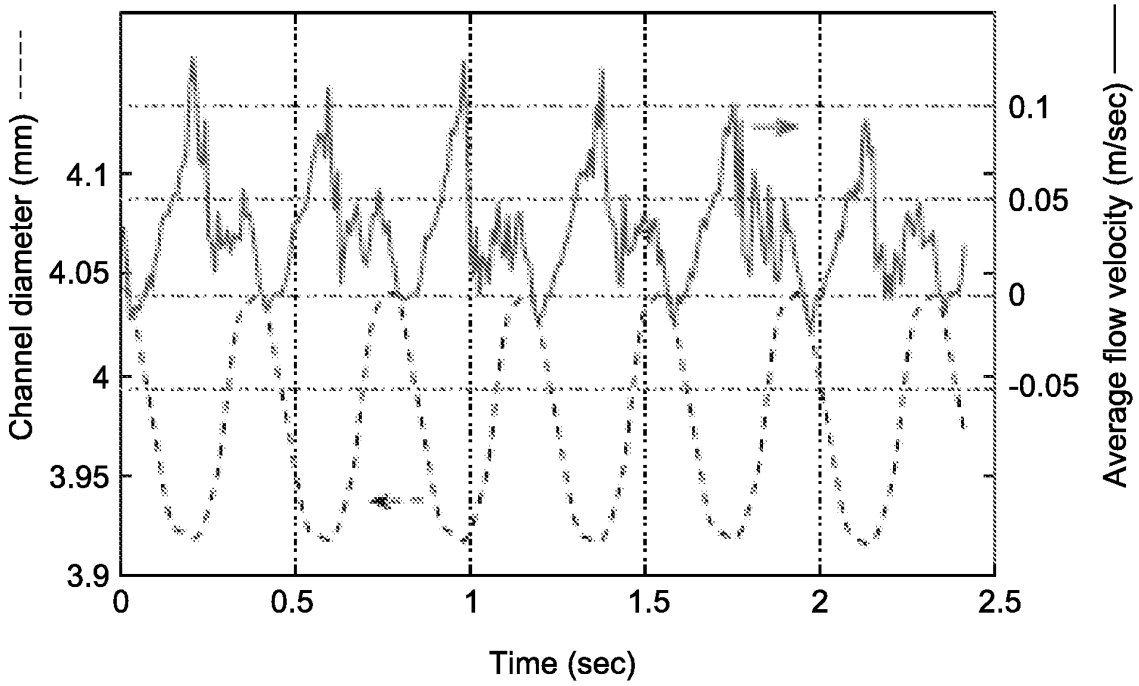
Channel diameter (mm)
Average flow velocity (m/sec)
Time (sec)
4.1
4.05
4
3.95
3.9
0.1
0.05
0
-0.05
0
0.5
1
1.5
2
2.5

Fig. 11

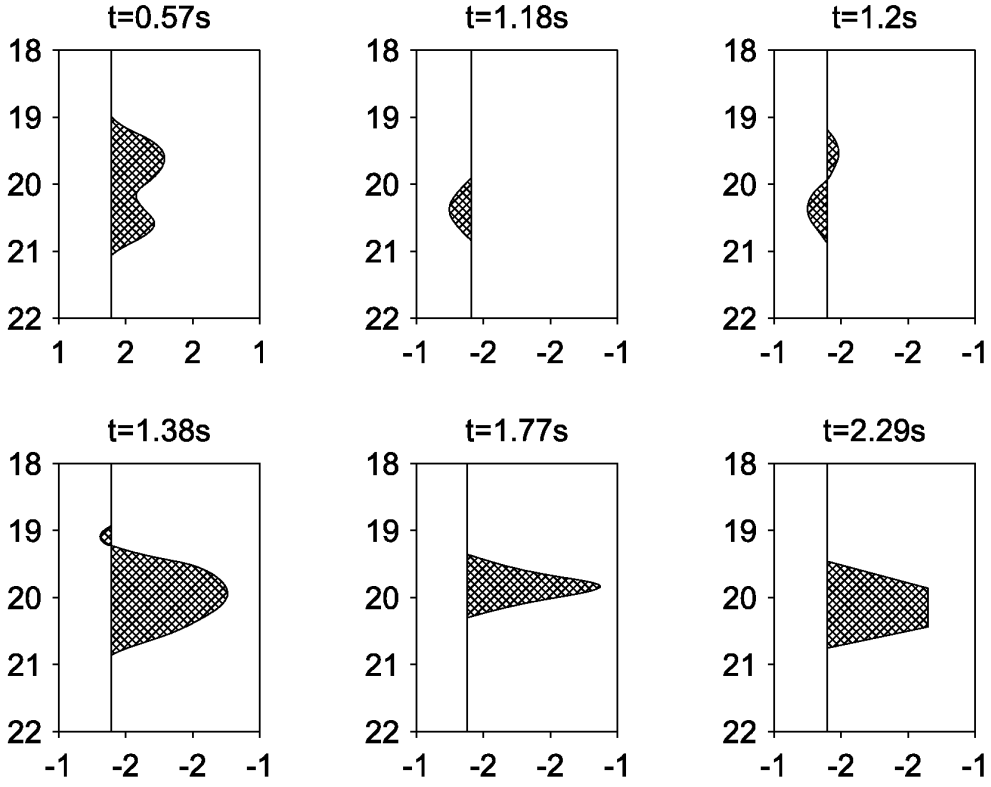
t=0.57s
t=1.18s
t=1.2s
t=1.38s
t=1.77s
t=2.29s
18
19
20
21
22
1
2
2
1
-1
-2
-2
-1

Fig. 12A

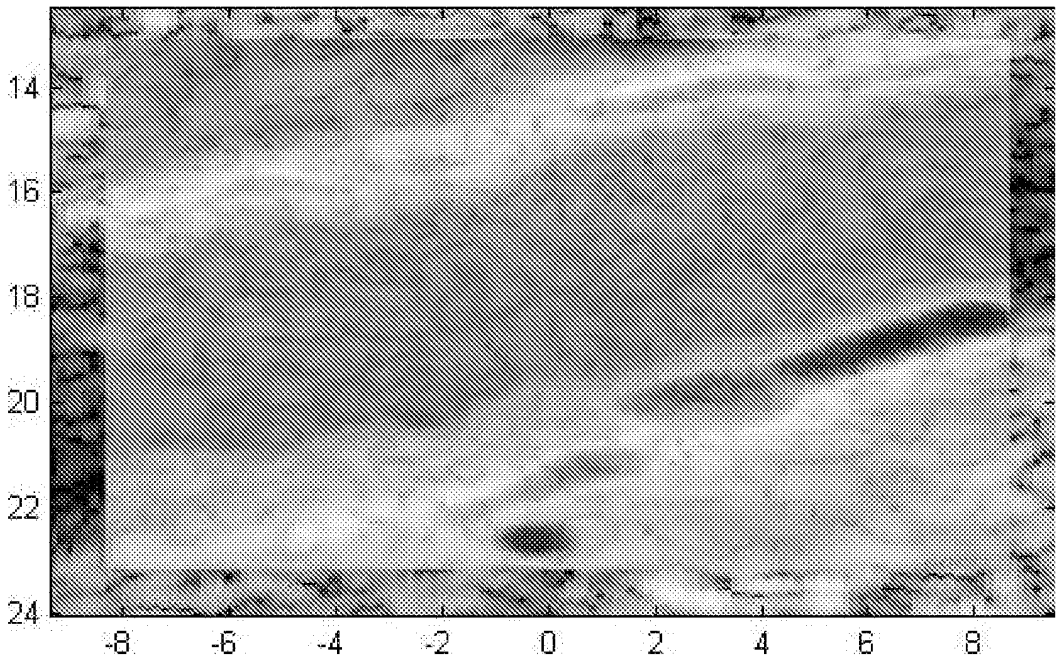

Fig. 12B

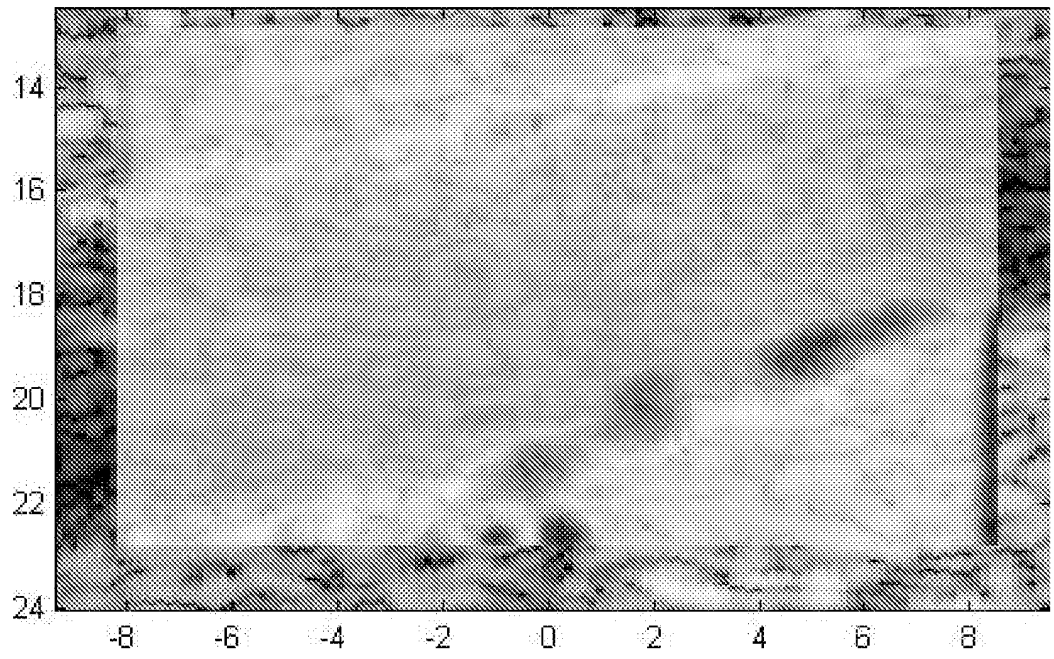

Fig. 13A

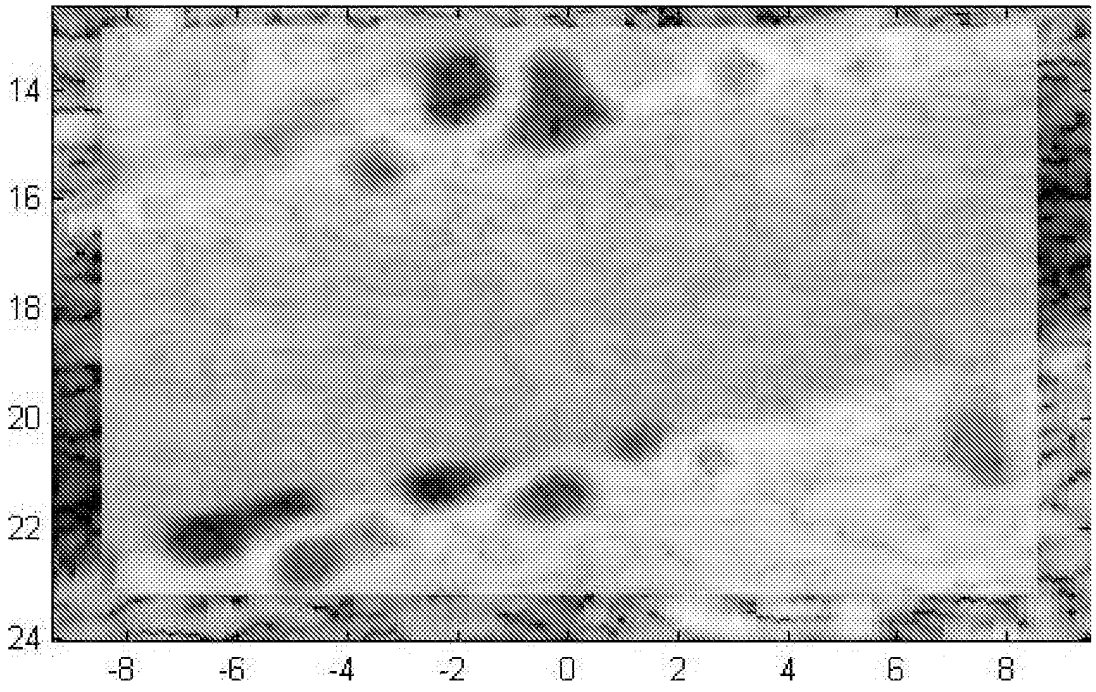

Fig. 13B

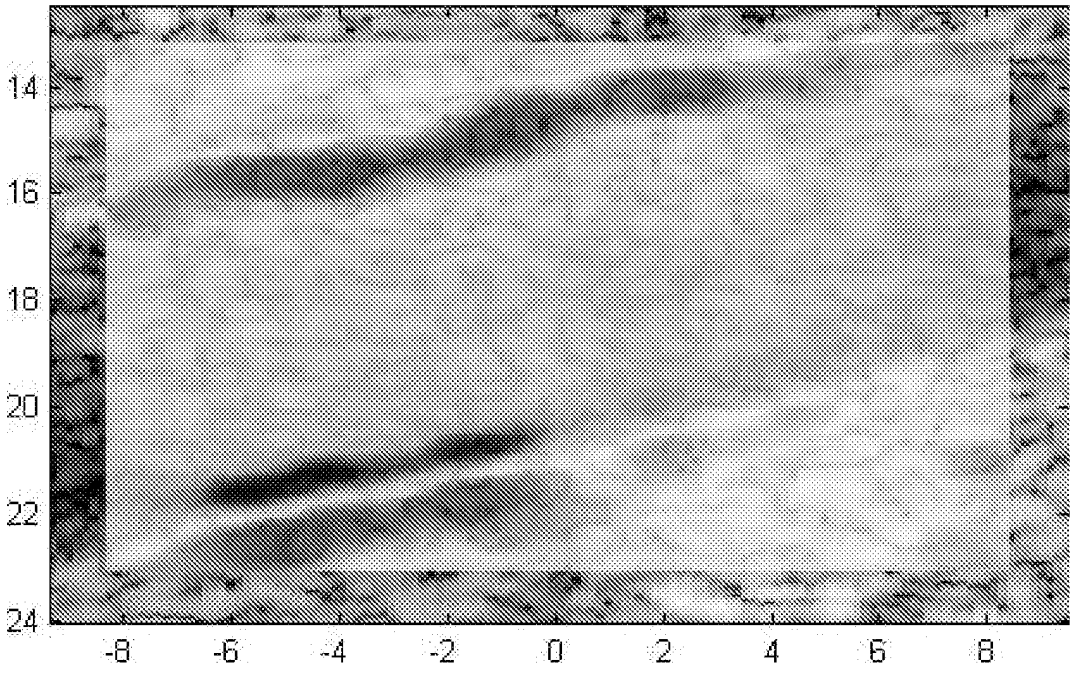

Fig. 14A

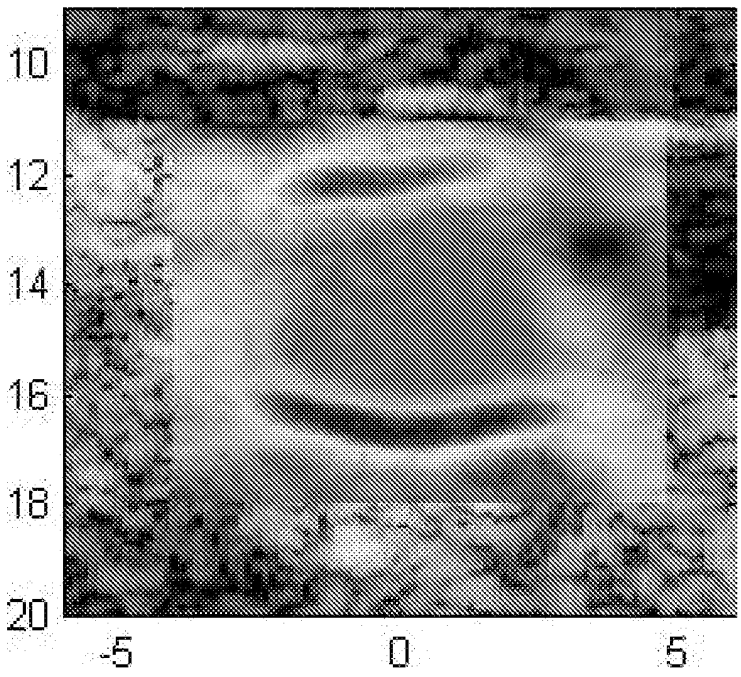

Fig. 14B

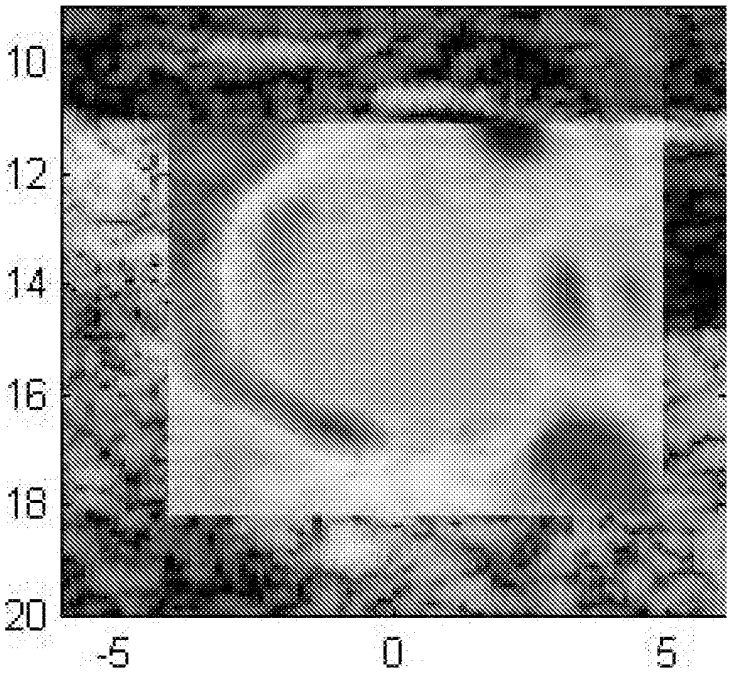

Fig. 15A

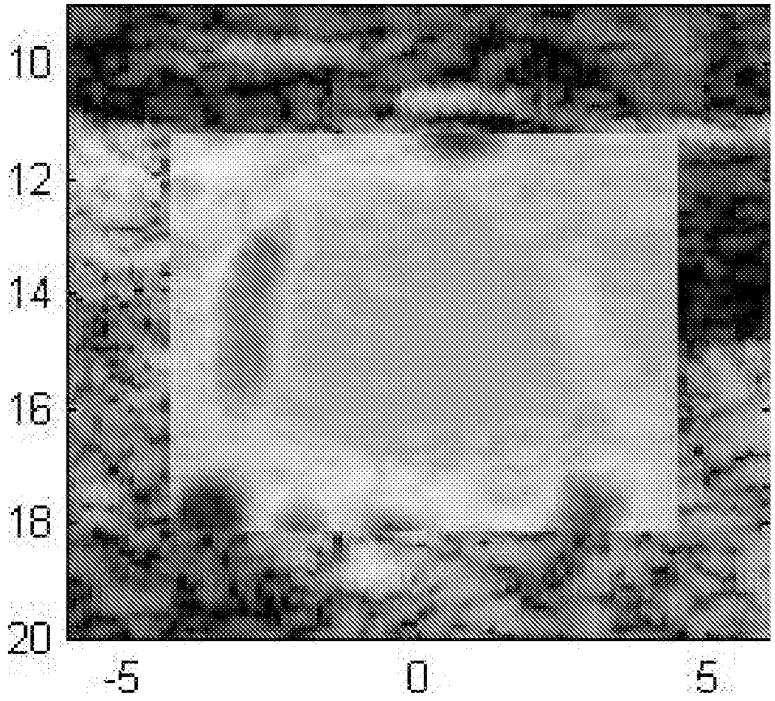

Fig. 15B

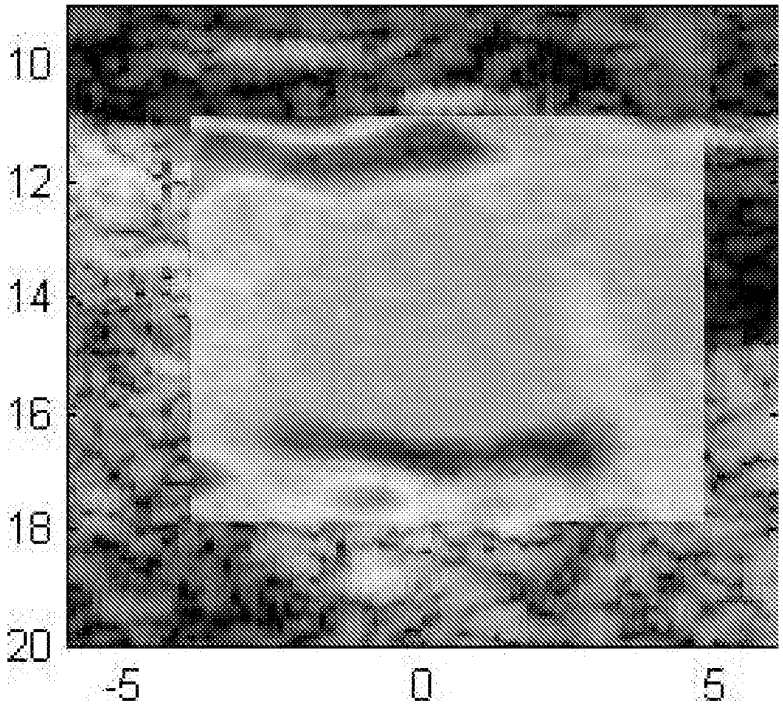

Fig. 16A

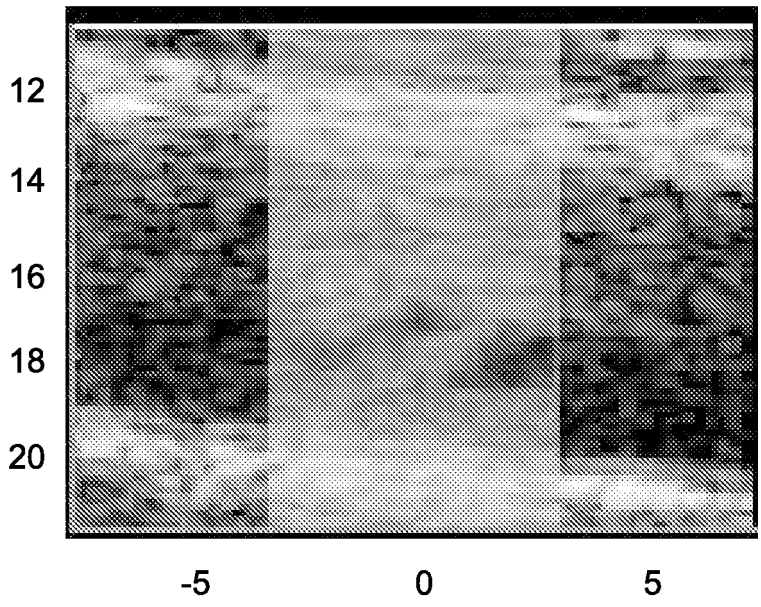

Fig. 16B

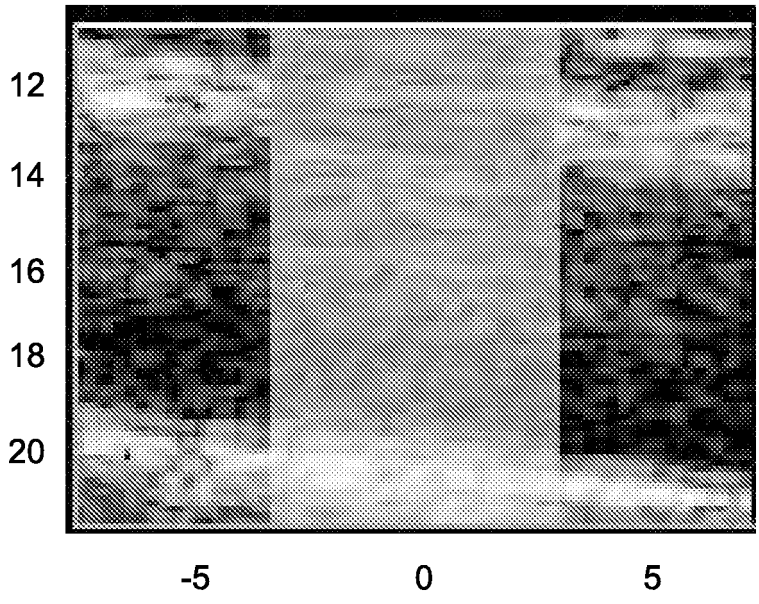

Fig. 17A

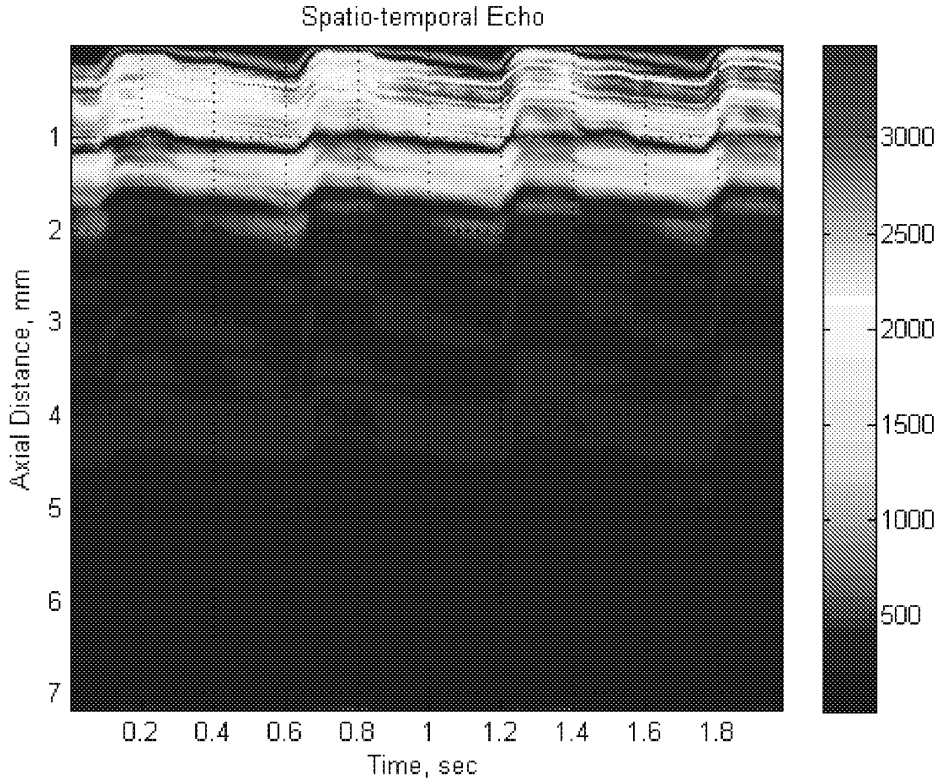

Fig. 17B

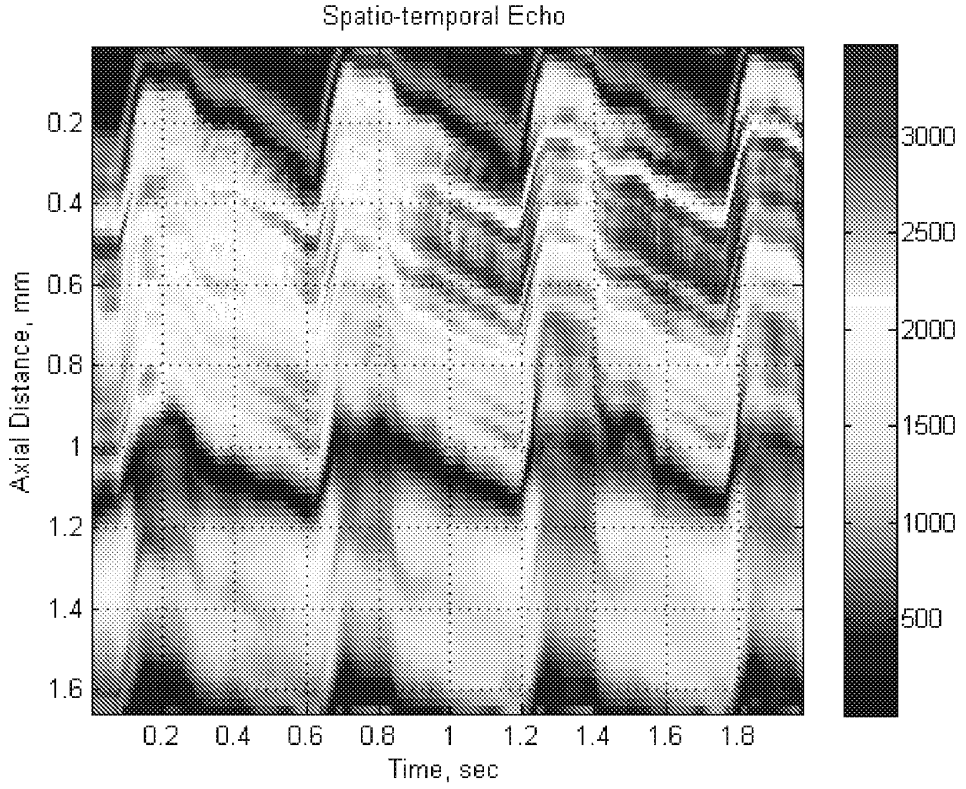

Fig. 18A

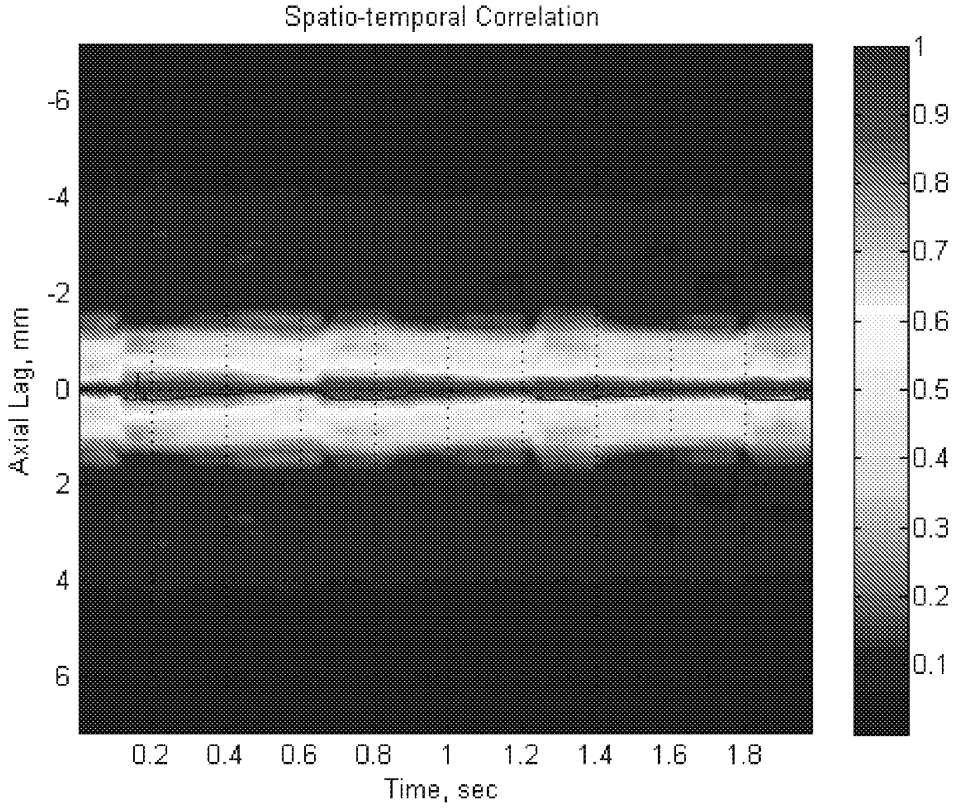

Fig. 18B

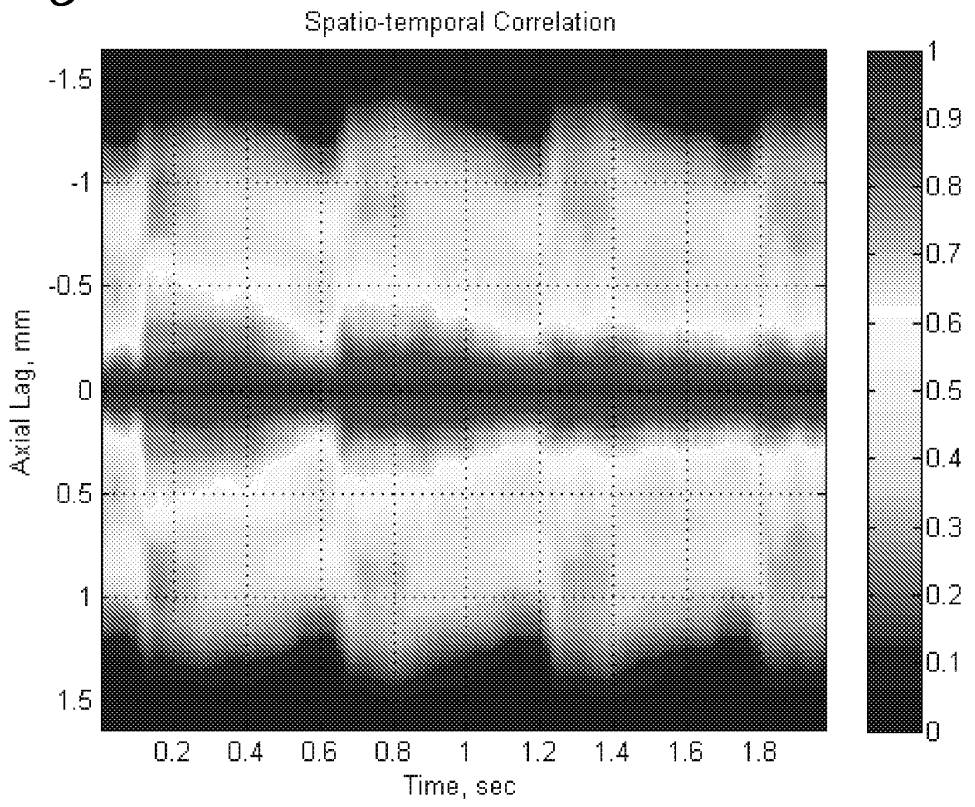

Fig. 19A

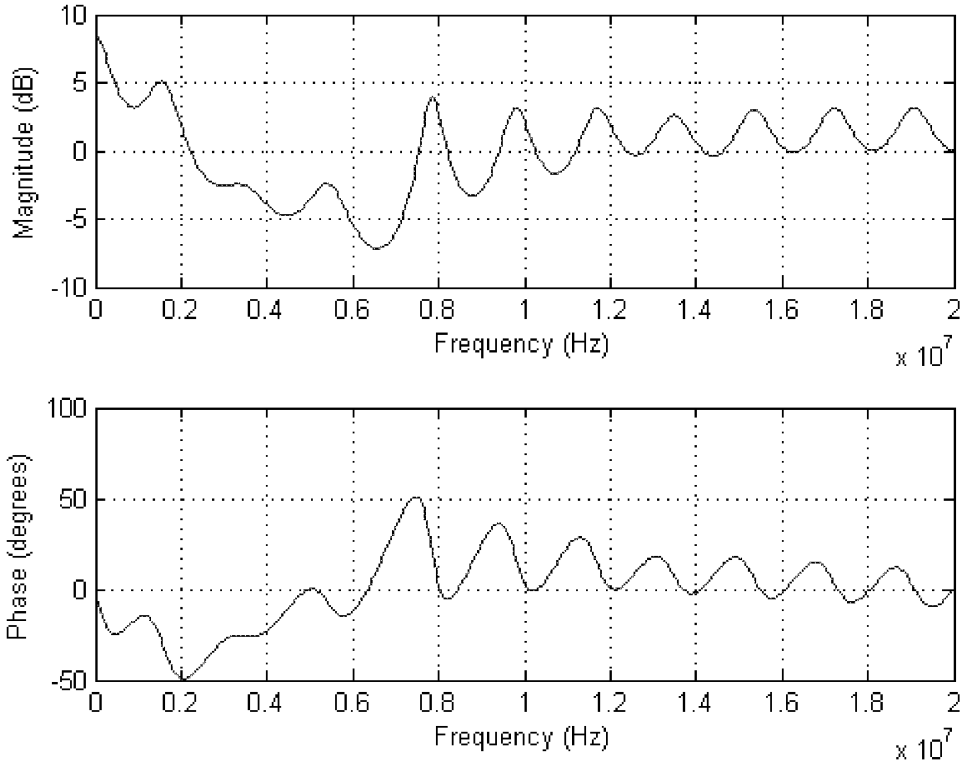

Fig. 19B

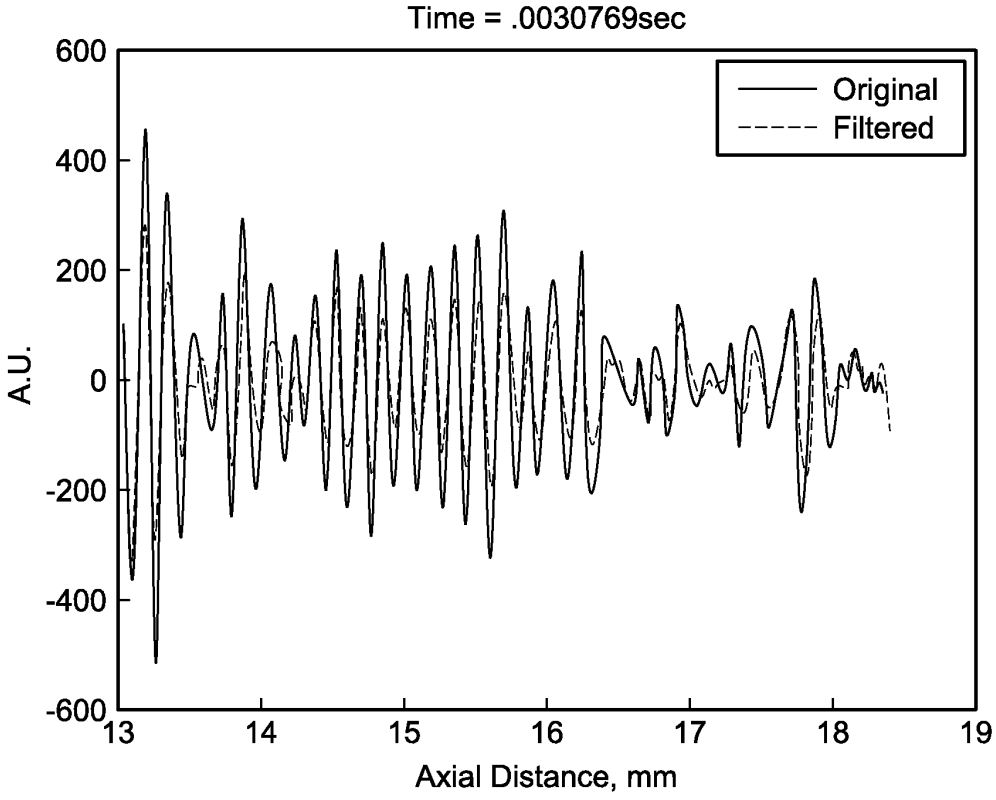

Fig. 19C

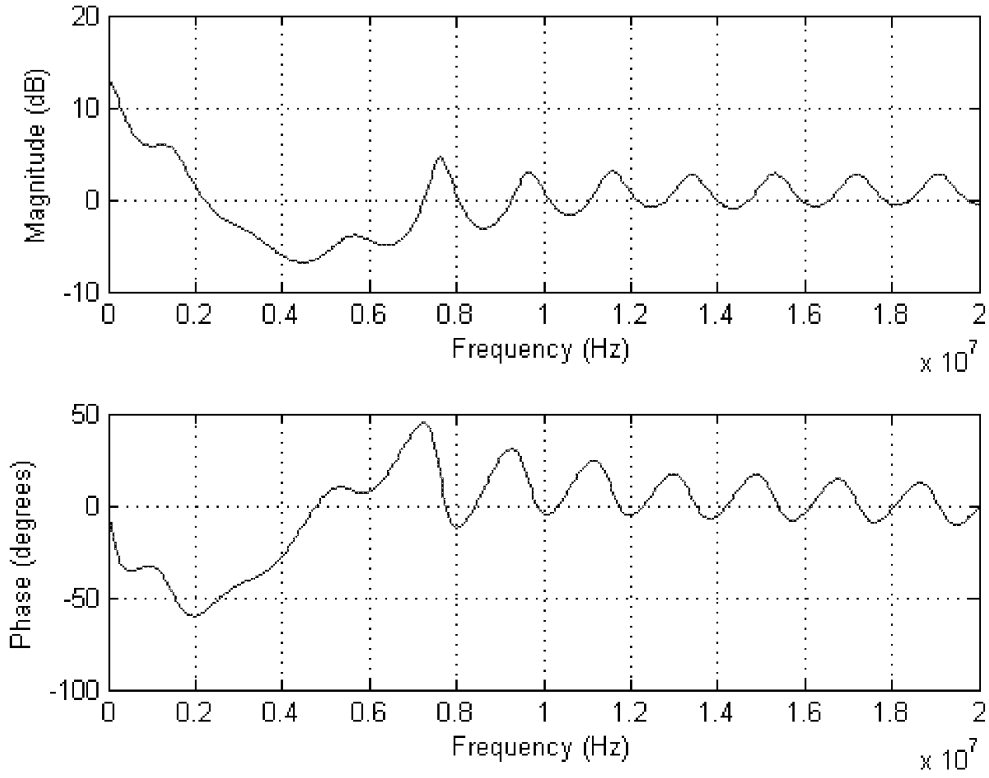

Fig. 19D

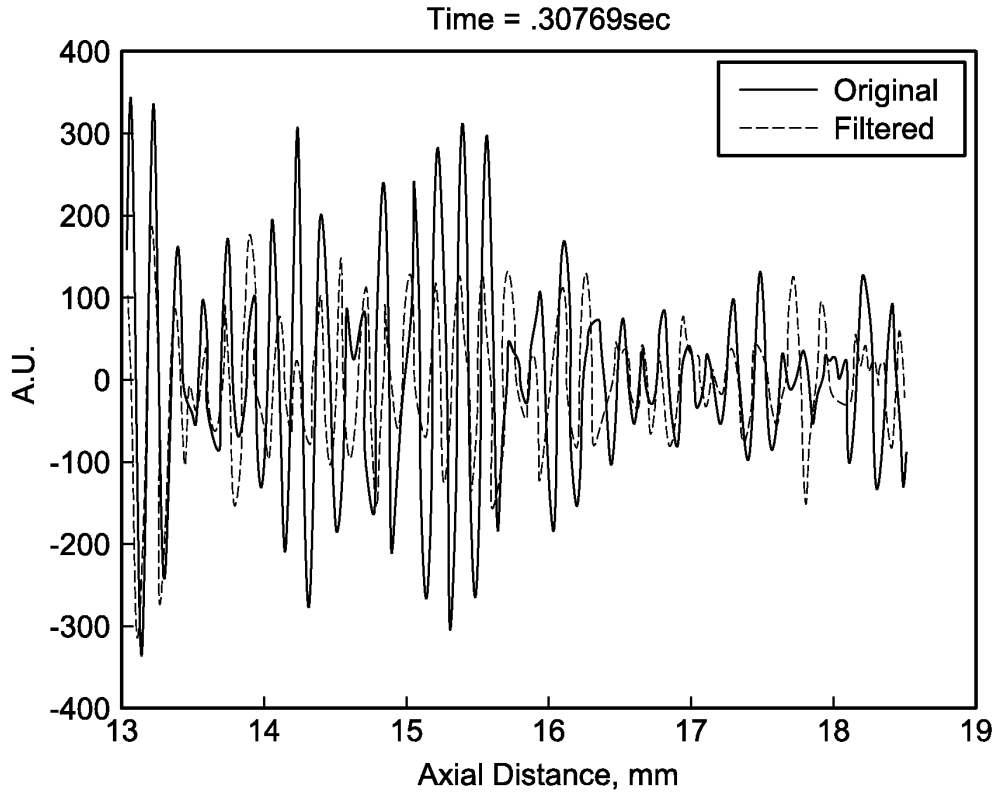

REFERENCES CITED IN THE DESCRIPTION

This list of references cited by the applicant is for the reader's convenience only. It does not form part of the European patent document. Even though great care has been taken in compiling the references, errors or omissions cannot be excluded and the EPO disclaims all liability in this regard.

Patent documents cited in the description

- WO 2008053457 A2 **[0005]**
- WO 2009002492 A **[0050] [0058]**
- US 61353096 A **[0055]**

Non-patent literature cited in the description

- 3D ultrasound measurement of change in carotid plaque volume - A tool for rapid evaluation of new therapies. *Stroke,* September 2005, vol. 36 (9), 1904-1909 **[0002]**
- **BLAKE et al.** A method to estimate wall shear rate with a clinical ultrasound scanner. *Ultrasound in Medicine and Biology,* May 2008, vol. 34 (5), 760-764 **[0003]**
- **TSOU et al.** Role of ultrasonic shear rate estimation errors in assessing inflammatory response and vascular risk. *Ultrasound in Medicine and Biology,* June 2008, vol. 34 (6), 963-972 **[0003]**
- **KARIMI et al.** Estimation of Nonlinear Mechanical Properties of Vascular Tissues via Elastography. *Cardiovascular Engineering,* December 2008, vol. 8 (4), 191-202 **[0003]**
- **WEITZEL et al.** High-Resolution Ultrasound Elasticity Imaging to Evaluate Dialysis Fistula Stenosis. *Seminars In Dialysis,* January 2009, vol. 22 (1), 84-89 **[0003]**
- **STEINMAN et al.** Flow imaging and computing: Large artery hemodynamics. *ANNALS OF BIOMEDICAL ENGINEERING,* December 2005, vol. 33 (12), 1704-1709 **[0004]**
- **FIGUEROA et al.** A computational framework for fluid-solid-growth modeling in cardiovascular simulations. *Computer Methods in Applied Mechanics and Engineering,* 2009, vol. 198 (45- 46), 3583-3602 **[0004]**
- **TAYLOR et al.** Open problems in computational vascular biomechanics: Hemodynamics and arterial wall mechanics. *Computer Methods in Applied Mechanics and Engineering,* 2009, vol. 198 (45-46), 3514-3523 **[0004]**
- **GRONNINSAETER et al.** *IEEE TRANSACTIONS ON ULTRASOUND ELECTRONICS, FERROELECTRICS AND FREQUENCY CONTROL,* 01 May 1996, vol. 43 (3), 359-369 **[0005]**
- **EBBINI et al.** Dual-Mode Ultrasound Phased Arrays for Image-Guided Surgery. *Ultrasound Imaging,* 2006, vol. 28, 65-82 **[0068]**
- **BALLARD et al.** Adaptive Transthoracic Refocusing of Dual-Mode Ultrasound Arrays. *IEEE Transactions on Biomedical Engineering,* January 2010, vol. 57 (1), 93-102 **[0068]**
- **WAN et al.** Imaging with Concave Large-Aperture Therapeutic Ultrasound Arrays Using Conventional Synthetic-Aperture Beamforming. *IEEE Transactions on Ultrasound, Ferroelectrics, and Frequency Control,* August 2008, vol. 55 (8), 1705-1718 **[0068]**
- **SIMON et al.** Two-Dimensional Temperature Estimation Using Diagnostic Ultrasound. *IEEE Transactions on Ultrasonics, Ferroelectronics, and Frequency Control,* July 1998, vol. 45 (4), 1088-1099 **[0084]**
- **SHEN et al.** A New Coded-Excitation Ultrasound Imaging System---Part I: Basic Principles. *IEEE Transactions on Ultrasonics, Ferroelectrics, and Frequency Control,* January 1996, vol. 43 (1), 131-140 **[0094]**
- **SHEN et al.** A New Coded-Excitation Ultrasound Imaging System---Part II: Operator Design. *IEEE Transactions on Ultrasonics, Ferroelectrics, and Frequency Control,* January 1996, vol. 43 (1), 141-148 **[0094]**
- **SHEN et al.** Filter-Based Coded-Excitation System for High-Speed Ultrasound Imaging. *IEEE Transactions on Medical Imaging,* December 1998, vol. 17 (6), 923-934 **[0094]**
- **LIU et al.** Real-Time 2-D Temperature Imaging Using Ultrasound. *IEEE Transactions on Biomedical Engineering,* January 2010, vol. 57 (1), 12-16 **[0098]**
- **E. S. EBBINI.** Phase-coupled two-dimensional speckle tracking algorithm. *IEEE Trans. Ultrason., Ferroelect., Freq. Contr.,* May 2006, vol. 53 (5), 972-990 **[0104]**

专利名称(译)	使用超声成像的血管表征		
公开(公告)号	EP2696771A2	公开(公告)日	2014-02-19
申请号	EP2012715304	申请日	2012-04-13
[标]申请(专利权)人(译)	明尼苏达大学		
申请(专利权)人(译)	明尼苏达大学校董会		
当前申请(专利权)人(译)	明尼苏达大学校董会		
[标]发明人	EBBINI EMAD S LIU DALONG WAN YAYUN CASPER ANDREW J		
发明人	EBBINI, EMAD S. LIU, DALONG WAN, YAYUN CASPER, ANDREW J.		
IPC分类号	A61B8/08 A61B8/06		
代理机构(译)	LATZEL，KLAUS		
优先权	61/475550 2011-04-14 US		
其他公开文献	EP2696771B8 EP2696771B1		
外部链接	Espacenet		

摘要(译)

超声方法和/或系统提供血管壁运动和血流的运动跟踪（例如，使用高帧率超声脉冲回波数据和斑点跟踪，可以同时跟踪壁运动和流动）。